

Volume 8, Issue 19 – e20240819 January – December – 2024

ISSN 2523-2428

Journal Civil Engineering



ECORFAN-Peru

Editor in Chief

Jaliri-Castellon, María Carla Konradis. PhD

Executive Director

Ramos-Escamilla, María. PhD

Editorial Director

Peralta-Castro, Enrique. MsC

Web Designer

Escamilla-Bouchan, Imelda. PhD

Web Designer

Luna-Soto, Vladimir. PhD

Editorial Assistant

Trejo-Ramos, Iván. BsC

Philologist

Ramos-Arancibia, Alejandra. BsC

Journal Civil Engineering, Volume 8, Issue 19: e20240819 January – December 2024, is a Continuous publication - Journal edited by ECORFAN-Peru. La Raza Av. 1047 No.-Santa Ana, Cusco Peru. Postcode: 11500. WEB: www.ecorfan.org/republicofperu, revista@ecorfan.org. Editor in Chief: Jaliri-Castellon, María Carla Konradis. PhD. ISSN: 2523-2428. Responsible for the last update of this issue of the ECORFAN Informatics Unit. Escamilla-Bouchán Imelda, Luna-Soto, Vladimir, updated December 31, 2024.

The views expressed by the authors do not necessarily reflect the views of the publisher.

Reproduction of all or part of the contents and images of the publication without the permission of the National Institute for the Defence of Competition and Protection of Intellectual Property is strictly prohibited.

Journal Civil Engineering

Definition of Journal

Scientific Objectives

Support the international scientific community in its written production Science, Technology and Innovation in the Field of Engineering and Technology, in Subdisciplines Bridge construction, development of environmental engineering, management in housing construction, hydraulic infrastructure, soil mechanics, sanitary engineering, road infrastructure.

ECORFAN-Mexico, S.C. is a Scientific and Technological Company in contribution to the Human Resource training focused on the continuity in the critical analysis of International Research and is attached to CONAHCYT-RENIECYT number 1702902, its commitment is to disseminate research and contributions of the International Scientific Community, academic institutions, agencies and entities of the public and private sectors and contribute to the linking of researchers who carry out scientific activities, technological developments and training of specialized human resources with governments, companies and social organizations.

Encourage the interlocation of the International Scientific Community with other Study Centers in Mexico and abroad and promote a wide incorporation of academics, specialists and researchers to the publication in Science Structures of Autonomous Universities - State Public Universities - Federal IES - Polytechnic Universities - Technological Universities - Federal Technological Institutes - Normal Schools - Decentralized Technological Institutes - Intercultural Universities - S & T Councils - CONAHCYT Research Centers.

Scope, Coverage and Audience

Journal Civil Engineering is a Journal edited by ECORFAN-Mexico, S.C. in its Holding with repository in Republic of Peru, is a scientific publication arbitrated and indexed with semester periods. It supports a wide range of contents that are evaluated by academic peers by the Double-Blind method, around subjects related to the theory and practice of Bridge construction, development of environmental engineering, management in housing construction, hydraulic infrastructure, soil mechanics, sanitary engineering, road infrastructure with diverse approaches and perspectives, that contribute to the diffusion of the development of Science Technology and Innovation that allow the arguments related to the decision making and influence in the formulation of international policies in the Field of Engineering and Technology. The editorial horizon of ECORFAN-Mexico® extends beyond the academy and integrates other segments of research and analysis outside the scope, if they meet the requirements of rigorous argumentative and scientific, as well as addressing issues of general and current interest of the International Scientific Society.

Editorial Board

Herrera - Diaz, Israel Enrique. PhD
Center of Research in Mathematics

Lara - Rosano, Felipe. PhD
Universidad de Aachen

Vega - Pineda, Javier. PhD
University of Texas

Vazquez - Martinez, Ernesto. PhD
University of Alberta

Rocha - Rangel, Enrique. PhD
Oak Ridge National Laboratory

Cendejas - Valdez, José Luis. PhD
Universidad Politécnica de Madrid

De La Rosa - Vargas, José Ismael. PhD
Universidad París XI

Hernández - Prieto, María De Lourdes. PhD
Universidad Gestalt

López - López, Aurelio. PhD
Syracuse University

Diaz - Ramirez, Arnoldo. PhD
Universidad Politécnica de Valencia

Arbitration Committee

Galaviz - Rodríguez, José Víctor. PhD
Universidad Popular Autónoma del Estado de Puebla

Morales - Ibarra, Rodolfo. PhD
Universidad Autónoma de Nuevo Leon

Romo - Gonzalez, Ana Eugenia. PhD
Universidad Popular Autónoma del Estado de Puebla

Salazar - Peralta, Araceli. PhD
Universidad Autónoma del Estado de México

Morillón - Gálvez, David. PhD
Universidad Nacional Autónoma de México

Alonso - Calpeño, Mariela J. PhD
Instituto Tecnológico Superior de Atlixco

Enciso - Contreras, Ernesto. PhD
Instituto Politécnico Nacional

Serrano - Arrellano, Juan. PhD
Universidad de Guanajuato

Núñez - González, Gerardo. PhD
Universidad Autónoma de Querétaro

Salazar - Peralta, Araceli. PhD
Universidad Autónoma del Estado de México

Vera - Serna, Pedro. PhD
Universidad Autónoma del Estado de Hidalgo

Assignment of Rights

The sending of an Article to Journal Civil Engineering emanates the commitment of the author not to submit it simultaneously to the consideration of other series publications for it must complement the Originality Format for its Article.

The authors sign the Authorization Format for their Article to be disseminated by means that ECORFAN-Mexico, S.C. In its Holding Republic of Peru considers pertinent for disclosure and diffusion of its Article its Rights of Work.

Declaration of Authorship

Indicate the Name of Author and Coauthors at most in the participation of the Article and indicate in extensive the Institutional Affiliation indicating the Department.

Identify the Name of Author and Coauthors at most with the CVU Scholarship Number-PNPC or SNI-CONAHCYT- Indicating the Researcher Level and their Google Scholar Profile to verify their Citation Level and H index.

Identify the Name of Author and Coauthors at most in the Science and Technology Profiles widely accepted by the International Scientific Community ORC ID - Researcher ID Thomson - arXiv Author ID - PubMed Author ID - Open ID respectively.

Indicate the contact for correspondence to the Author (Mail and Telephone) and indicate the Researcher who contributes as the first Author of the Article.

Plagiarism Detection

All Articles will be tested by plagiarism software PLAGSCAN if a plagiarism level is detected Positive will not be sent to arbitration and will be rescinded of the reception of the Article notifying the Authors responsible, claiming that academic plagiarism is criminalized in the Penal Code.

Arbitration Process

All Articles will be evaluated by academic peers by the Double-Blind method, the Arbitration Approval is a requirement for the Editorial Board to make a final decision that will be final in all cases. MARVID® is a derivative brand of ECORFAN® specialized in providing the expert evaluators all of them with Doctorate degree and distinction of International Researchers in the respective Councils of Science and Technology the counterpart of CONAHCYT for the chapters of America-Europe-Asia- Africa and Oceania. The identification of the authorship should only appear on a first removable page, in order to ensure that the Arbitration process is anonymous and covers the following stages: Identification of the Research Journal with its author occupation rate - Identification of Authors and Coauthors - Detection of plagiarism PLAGSCAN - Review of Formats of Authorization and Originality-Allocation to the Editorial Board- Allocation of the pair of Expert Arbitrators - Notification of Arbitration - Declaration of observations to the Author - Verification of Article Modified for Editing - Publication.

Instructions for Scientific, Technological and Innovation Publication

Knowledge Area

The works must be unpublished and refer to topics of Bridge construction, development of environmental engineering, management in housing construction, hydraulic infrastructure, soil mechanics, sanitary engineering, road infrastructure and other topics related to Engineering and Technology.

Presentation of Content

In the Issue 19, as first article we present *Physicochemical characterization of the material used in the manufacture of brick in an artisanal way* by Salazar-Peralta, Araceli, Bernal-Martínez, Lina Agustina, Pichardo-Salazar, José Alfredo and Pichardo-Salazar, Ulises, with adscription in Tecnológico de Estudios Superiores de Jocotitlán, Centro de Bachillerato Tecnológico Industrial y de Servicios No. 161 and Centro de Estudios Tecnológicos Industrial y de Servicios No. 23, as the next article we present, *Feasibility of dry canals in the Americas* by Castillo-Aguirre, Alfredo Humberto, Cruz-Gómez, Marco Antonio, Mejia-Perez, José Alfredo and Espinosa-Carrasco, María del Rosario, with adscription in Benemerita Universidad Autónoma de Puebla, as the next article we present, *Dynamic evaluation of composite roofs: thermal optimization with PCM under extreme climate conditions* by López Salazar, Samanta, Simá, E., Chagolla-Aranda, M. A. and Chávez-Chena, Y., with adscription in TecNM/CENIDET, as the next article we present, *Analysis of the behavior of the seafloor of the mouth of the Grijalva river, Tabasco in the years 2012, 2017 and 2021* by Aguilar-Ramírez, Ana María, Domínguez-González, Agustín, Utrera-Zárate, Alberto and Molina-Navarro, Antonio, with adscription in Instituto Oceanográfico del Golfo y Mar Caribe, as the next article we present, *Influence of particle size on soil consolidation processes* by Rojas, Eduardo, Reynoso, Eva Guadalupe and Arroyo, Hiram, with adscription in Universidad Autónoma de Querétaro and Universidad de Guanajuato, as the last article we present, *Strength analysis of structural concrete blocks with five mixture materials* by Álvarez-Arellano, Juan Antonio, Lastra-González, Isabel Christine, El-Hamzaoui, Youness and Álvarez-Bello Martínez, Rodrigo Daniel, with adscription in Universidad Autónoma del Carmen.

Content

Article	Page
Physicochemical characterization of the material used in the manufacture of brick in an artisanal way Salazar-Peralta, Araceli, Bernal-Martínez, Lina Agustina, Pichardo-Salazar, José Alfredo and Pichardo-Salazar, Ulises <i>Tecnológico Nacional de México. Tecnológico de Estudios Superiores de Jocotitlán</i> <i>Centro de Bachillerato Tecnológico Industrial y de Servicios No. 161</i> <i>Centro de Estudios Tecnológicos Industrial y de Servicios No. 23</i>	1-5
Feasibility of dry canals in the Americas Castillo-Aguirre, Alfredo Humberto, Cruz-Gómez, Marco Antonio, Mejia-Perez, José Alfredo and Espinosa-Carrasco, María del Rosario <i>Benemerita Universidad Autónoma de Puebla</i>	1-13
Dynamic evaluation of composite roofs: thermal optimization with PCM under extreme climate conditions López Salazar, Samanta, Simá, E., Chagolla-Aranda, M. A. and Chávez-Chena, Y. <i>TecNM/CENIDET</i>	1-14
Analysis of the behavior of the seafloor of the mouth of the Grijalva river, Tabasco in the years 2012, 2017 and 2021 Aguilar-Ramírez, Ana María, Domínguez-González, Agustín, Utrera-Zárate, Alberto and Molina-Navarro, Antonio <i>Instituto Oceanográfico del Golfo y Mar Caribe</i>	1-10
Influence of particle size on soil consolidation processes Rojas, Eduardo, Reynoso, Eva Guadalupe and Arroyo, Hiram <i>Universidad Autónoma de Querétaro</i> <i>Universidad de Guanajuato</i>	1-7
Strength analysis of structural concrete blocks with five mixture materials Álvarez-Arellano, Juan Antonio, Lastra-González, Isabel Christine, El-Hamzaoui, Youness and Álvarez-Bello Martínez, Rodrigo Daniel <i>Universidad Autónoma del Carmen</i>	1-11

Physicochemical characterization of the material used in the manufacture of brick in an artisanal way

Caracterización fisicoquímica del material empleado en la fabricación de tabique en forma artesanal

Salazar-Peralta, Araceli^a, Bernal-Martínez, Lina Agustina^b, Pichardo-Salazar, José Alfredo^c and Pichardo-Salazar, Ulises^d

^a ROR Tecnológico Nacional de México. Tecnológico de Estudios Superiores de Jocotitlán • ^{ORCID} 0000-0001-5861-3748
^b ROR Tecnológico Nacional de México. Tecnológico de Estudios Superiores de Jocotitlán • ^{ORCID} 0000-0002-4922-043X
^c ROR Dirección General de Educación Tecnológica Industrial. Centro de Bachillerato Tecnológico Industrial y de Servicios No. 161 • ^{ORCID} 0000-0002-8939-9921
^d ROR Dirección General de Educación Tecnológica Industrial. Centro de Estudios Tecnológicos Industrial y de Servicios no. 23 • ^{ORCID} 0000-0002-3758-2038

CONAHCYT classification:

Area: Engineering
Field: Technological sciences
Discipline: Material technology
Subdiscipline: Ceramic materials

^{DOI} <https://doi.org/10.35429/JCE.2024.8.19.1.5>

Article History:

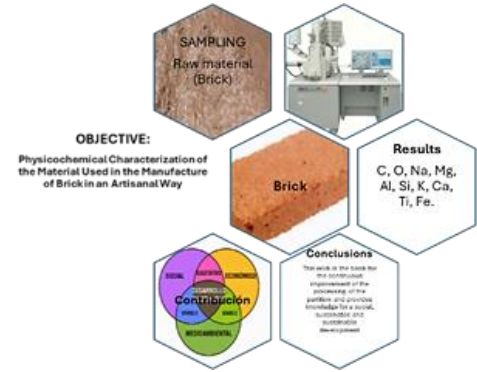
Received: January 19, 2024
Accepted: December 31, 2024



* ✉ [\[araceli.salazar@tesjo.edu.mx\]](mailto:araceli.salazar@tesjo.edu.mx)

Abstract

The manufacture of Brick in an artisanal way is a traditional activity carried out by the knowledge and experience transmitted from person to person, due to this there are no work instructions, nor data on the chemical composition of the raw material used, nor control of the process of manufacturing. The objective of this study was to physicochemically characterize the raw material for the manufacture of Brick. The elemental chemical composition found was the following. C, O, Na, Mg, Al, Si, K, Ca, Ti, Fe. Elements to which the mechanical properties of the Brick are attributed. The compressive strength of the Brick without heat treatment was 12 to 15 kg/cm², after heat treatment it was 24 to 45 kg/cm². Regarding morphology, particles from 4 to 301 μm were observed in the raw material. And in the Brick from 18 to 257 μm. It is concluded that the homogenization of the raw material, as well as the temperature control in the thermal treatment of the Brick allowed to obtain greater resistance to compression, since the Peruvian Standard ITINTEC 331.017. And Standard NMX-C-404-1997 establishes 60N/cm². and 24kg/cm² minimum respectively.



Artisanal brick, Raw material, Compression resistance

Resumen

La fabricación de tabique en forma artesanal es una actividad tradicional realizada por el conocimiento y experiencia transmitido de persona a persona, debido a ello no se cuenta con instrucciones de trabajo, ni datos sobre la composición química de la materia prima utilizada, ni control del proceso de fabricación. El objetivo de este estudio fue caracterizar fisicoquímicamente la materia prima para la fabricación de tabique. La composición química elemental encontrada fue la siguiente. C, O, Na, Mg, Al, Si, K, Ca, Ti, Fe. Elementos a los cuales se le atribuye las propiedades mecánicas del tabique. La resistencia a la compresión del tabique sin tratamiento térmico fue 12 a 15kg/cm², después del tratamiento térmico fue de 24 a 45 kg/cm². En cuanto a la morfología se observaron partículas de 4 a 301 μm en la materia prima y en el tabique de 18 a 257 μm. Se concluye que la homogenización de la materia prima, así como el control de temperatura en el tratamiento térmico del tabique permitió obtener mayor resistencia a la compresión, ya que la Norma Peruana ITINTEC 331.017. Y la Norma NMX-C-404-1997, establecen 60N/cm². y 24kg/cm² mínimo respectivamente.



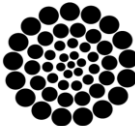
Tabique artesanal, Materia prima, Resistencia a la compresión

Citation: Salazar-Peralta, Araceli, Bernal-Martínez, Lina Agustina, Pichardo-Salazar, José Alfredo and Pichardo-Salazar, Ulises. [2024]. Physicochemical characterization of the material used in the manufacture of brick in an artisanal way. Journal Civil Engineering. 8[19]-1-5: e10819105.



ISSN 2523-2428/© 2009 The Author[s]. Published by ECORFAN-Mexico, S.C. for its Holding Republic of Peru on behalf of Journal Civil Engineering. This is an open access article under the CC BY-NC-ND license [\[http://creativecommons.org/licenses/by-nc-nd/4.0/\]](http://creativecommons.org/licenses/by-nc-nd/4.0/)

Peer Review under the responsibility of the Scientific Committee MARVID® - in contribution to the scientific, technological and innovation Peer Review Process by training Human Resources for the continuity in the Critical Analysis of International Research.



RENIECYT
Registro Nacional de Instituciones y
Empresas Científicas y Tecnológicas

1702902

CONAHCYT

Introduction

A brick is a ceramic piece, generally orthohedral, obtained by molding, drying and firing at high temperatures of a clay paste, whose dimensions are usually 24 x 11.5 x 6 cm. It is used in masonry, for the construction of walls, houses, industries, etc. It is estimated that the first bricks were created around the year 6,000 BC. (Tell Mureybet and Ali Kosh).

The brick is unalterable to humidity and has, as a fired material, a very useful network of capillary ducts. Its capacity to retain moisture and its thermal inertia are great. One of its characteristics is to absorb moisture from the environment with higher water vapor pressure, transfer it through its capillary network and dissipate it in the environment with lower pressure. The brick wall “breathes” until it is dry. For this reason, it is appropriate for constructions intended for wet processes, as long as the breathing of the brick is not obstructed. The thermal conductivity of the brick is moderate^{II, VI, VII}.

It is important that the conductivity is proportional to the conductivity of the water vapor. This means that in each section of a brick wall, as the temperature drops, the water vapor pressure decreases, therefore condensation does not occur. If a wall is not prevented from “breathing” its cold side remains dry^{III, IV, V}.

The Olmecs (1200 BC), for the construction of La Venta (Villahermosa, Tabasco) used red and yellow clay block walls also joined with clay^{III}.

The Mayans made large and impressive buildings and large cities since the middle preclassic period. The most notable monuments are the pyramids that they built in their religious centers, next to the palaces of their rulers. All stone for the Mayan structures appears to have been taken from local quarries; It was often limestone that, recently quarried, remained soft enough to be worked with stone tools, and only hardened after a time, losing its natural moisture. In addition to the structural use of limestone, they used crushed, burned and beaten limestone that had properties similar to cement and was widely used both for plaster finishes and for joining stones; In the Valley of Mexico (in the preclassic period, 700 BC) masonry was already used for various purposes^{III}.

The purpose of this study was to characterize the raw material, as well as its processing for the production of the partition, since it is an important aspect on which its compression resistance will depend.

This study is addressed in the following sections:

- Introduction.
- Methodology.
- Results.
- Acknowledgment.
- Conclusions.
- References.

Methodology

Samples of the tepetate, mud and soil from the site were taken for elemental chemical and morphological characterization with a JEOL JSM-5900LV scanning electron microscope. Table 1 and figures 1, 2, 3, 4, 5, 6.

The raw material was mixed in the following proportions:

- Sandy tepetate (25%).
- Tepetate (25%).
- Mud (red soap) 25%.
- Land of the place 25%.

The materials were sifted in a mason's hoard.

The materials were kneaded with 20% water.

The mixture was made with a hoe until homogeneous consistency to be placed in the mold.

The mold was sandblasted.

The mold was filled with the dough.

The material protruding from the mold was trimmed with the tool called a trimmer.

The partition was removed from the mold and placed face up in rows on the floor.

It was left to dry on the floor for 4 days.

The partition was dried in the sun for a month during the rainy season. (In the dry season it is enough for 15 days).

The partition was placed in the oven to cook for 30 hours.

The morphology of the septum was characterized Figure 4.

The compressive strength of the septum was verified (Table 2).

Results

As can be seen in table 1. The three types of soil used to mix the raw material to be used in the manufacture of the partition have the same chemical elements: Carbon (C), Oxygen (O), Sodium (Na) , Magnesium (Mg), Aluminum (Al), Silicon (Si), Potassium (K), Calcium (Ca), Titanium (Ti), Iron (Fe), only the one with the highest content of all of them is mud.

The tepetate of origin from San Lorenzo Cuauhtenco, presented a particle size of 50 to 300 μm , a very variable size due to the agglomeration of particles, which form conglomerates (Figure 1).

The mud from San Lorenzo Cuauhtenco had a particle size of 75 to 150 μm . Just as in the previous case, it presents conglomerates, due to a heterogeneous mixing operation (Figure 2).

Regarding the soil of San Bartolomé Tlaltelulco, particles between 5 to 90 μm were found (Figure 3).

The finished product (partition) had a particle size of 15 to 250 μm , which gives it different porosities throughout the partition, which can influence its compressive strength (Figure 4).

As can be seen in the three types of soil, different morphologies of the particles were found, ovoid characteristics typical of clays, partially folded edges characteristic of potassium feldspars, as well as spherical shapes.

The chemical element silicon denotes the presence of quartz (SiO_2).

Box 1

Table 1

Elemental composition of the raw material

Chemical Element	Mix of Snack and Sandy Tepetate %	Clay %	Land of the Place %	Brick%
C	19.53	29	24.4	21.42
O	40	38	40	40.68
Na	1.15	1.1	0.95	0.96
Mg	0.24	0.21	0.15	0.31
Al	10	7.6	8.23	8.64
Si	21.61	17.5	19.4	20
K	0.79	0.79	0.83	0.90
Ca	2.1	1.44	1.21	1.35
Ti	0.48	0.38	0.40	0.46
Fe	4.22	4.21	4.5	5.32

Source: Own elaboration

Box 2

Table 2

Compression resistance of brick

Brick	Compression Resistance (No Baking) (dried in the sun)	Compression Resistance (Baked)
1	10 kg/cm^2	20 kg/cm^2
2	12 kg/cm^2	31 kg/cm^2
3	12 kg/cm^2	20 kg/cm^2
4	10 kg/cm^2	30 kg/cm^2
5	11 kg/cm^2	36 kg/cm^2
6	13 kg/cm^2	40 kg/cm^2

Source: Own elaboration

Box 3

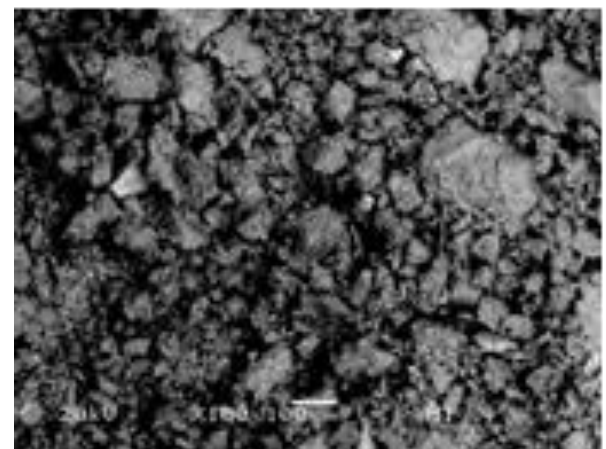
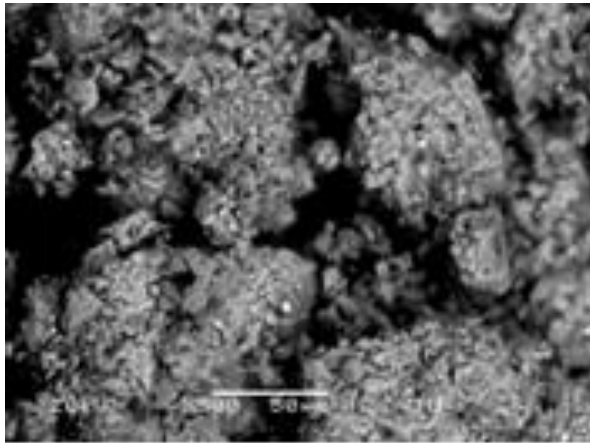


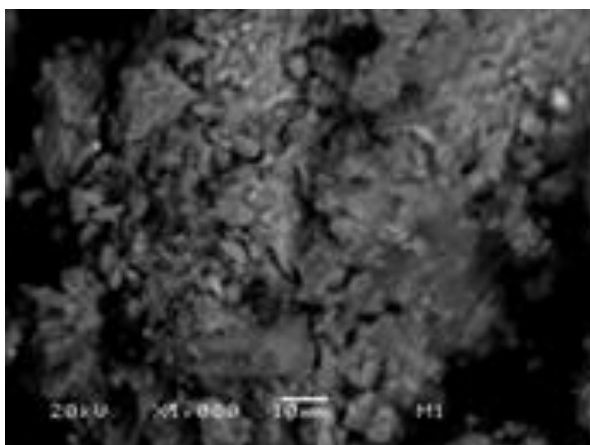
Figure 1

Morphology of the mix of snack and sandy temperate to 100X magnification

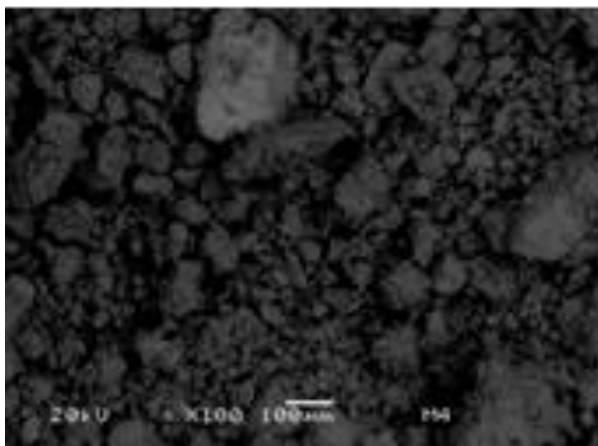
Source: Own elaboration

Box 4**Figure 2**

Morphology of Clay to 100X magnification

*Source: Own elaboration***Box 5****Figure 3**

Morphology of the land of San Bartolomé Tlaltelulco to 100X magnification

*Source: Own elaboration***Box 6****Figure 4**

Morphology of the Brick to 100X magnification

*Source: Own elaboration***Acknowledgments**

To Jehovah God for life and health, without which the study would not be possible. To the National Technology of Mexico to which the Higher Studies Technology of Jocotitlán belongs for the scientific and moral support. To the General Direction of Industrial Technological Education, to which the Industrial and Services Technological High School Center No. 161 belongs, and the Center for Industrial and Services Technological Studies No. 23, which prepare students with the bases to pursue higher education.

To the National Institute of Nuclear Research in memory of Dra. Rosa Hilda Chávez. To the artisans of San Bartolomé Tlaltelulco for allowing us to take data on their process and samples of raw materials and partitions to carry out the study. To all my collaborators for their scientific and technological support.

Conclusions

The results obtained allowed us to propose a series of morphological characteristics of the raw material used in the manufacture of the San Bartolomé Tlaltelulco Brick, as well as to determine the presence of chemical elements typical of quartz, feldspars and clays. The particle size observed microscopically allows us to conclude that there is a lot of variation, which contributes to the compressive strength of the septum, which tends to the minimum value established by the applicable Regulations. It is suggested to homogenize the mixing of the raw material during the brick manufacturing process, to control the particle size. Additionally, it is recommended to keep a record of the oven temperature for heat treatment, to increase the compressive strength of the product.

Conflict of interest

The authors declare no interest conflict. They have no known competing financial interests or personal relationships that could have appeared to influence the article reported in this article

Authors' Contribution

This is a collaborative work in which all the following authors:

Araceli Salazar Peralta, Lina Agustina Bernal Martínez, José Alfredo Pichardo Salazar, and Ulises Pichardo Salazar, contributed in teamwork in the following activities: taking of samples, methodology to be used, writing and revision of the article.

Availability of data and materials

The availability of the material was achieved with the contribution of the artisans of San Bartolomé Tlaltelulco, as for the measurement equipment for the tests was made with the collaboration of the laboratories of the ININ, as well as the Tecnológico de Estudios Superiores de Jocotitlán.

Funding

The research did not receive any funding.

References

Antecedents

- I. Fernando, Bárbara Z., [Materiales y Procedimientos de Construcción](#), México 1955.
- II. Plazola, Cisneros Alfredo, [Normas y Costos de Construcción](#), editorial.
- III. Juárez, Badillo, [Mecánica de suelos](#). Editorial Limusa, México, 1980, Tomo 1.

Basic

- IV. ITINTEC 331.017 [Norma Técnica Peruana 1976](#).
- V. NMX-C-038-ONNCCE- 2004 [Determinación de las dimensiones de ladrillos, tabiques, bloques y tabicones para la construcción](#). Icono de web global DOF - Diario Oficial de la Federación.
- VI. NMX- C-404- ONNCCE- 1997 [Especificaciones y métodos de prueba](#)
- VII. NMX-C-036-ONNCCE- 2004. [Resistencia a la compresión-método de prueba](#). Icono de web global DOF - Diario Oficial de la Federación.



VIII. Silva Acevedo, G.; Deleón Argüello, J.A. (2009), “[Determinación de los parámetros de diseño a compresión de mampostería de tabique de barro rojo recocido asentados con mortero cemento-calhidra-arena 1:2:10](#)”, Tesis de Licenciatura, Facultad de Ingeniería, Universidad Autónoma de Chiapas.

IX. Gaceta oficial del Distrito Federal. (2004), “[Normas Técnicas Complementarias para Diseño y Construcción de Estructuras de Mampostería](#)”, Gobierno del Distrito. Portal de Transparencia de la CDMX.

Feasibility of dry canals in the Americas

Factibilidad de canales secos en el continente Americano

Castillo-Aguirre, Alfredo Humberto^a, Cruz-Gómez, Marco Antonio^b, Mejia-Perez, José Alfredo^c and Espinosa-Carrasco, María del Rosario^d

- ^a  Benemerita Universidad Autónoma de Puebla •  KQF-3856-2024 •  0009-0007-1564-2611 •  2030591
- ^b  Benemerita Universidad Autónoma de Puebla •  S-3098-2018 •  0000-0003-1091-8133 •  349626
- ^c  Benemerita Universidad Autónoma de Puebla •  G-3354-2019 •  0000-0002-4090-8828 •  473808
- ^d  Benemerita Universidad Autónoma de Puebla •  AAP-2965-2020 •  0000-0002-5094-2800 •  1018747

CONAHCYT classification:

Area: Engineering
Field: Engineering
Discipline: Naval Engineering
Subdiscipline: Port engineering

 <https://doi.org/10.35429/JCE.2024.8.19.1.13>

Article History:

Received: January 30, 2024
Accepted: December 31, 2024

*  [\[castilloalfredog@gmail.com\]](mailto:castilloalfredog@gmail.com)

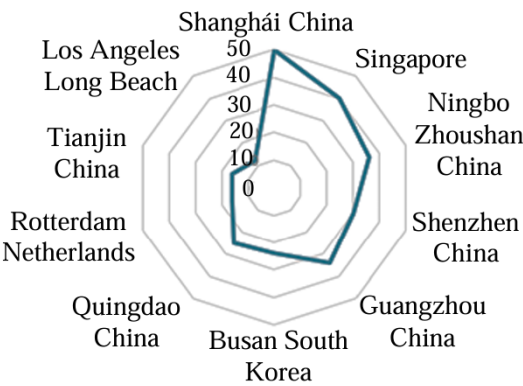


Abstract

The future of global maritime trade is being guided by the Triad generating uncontrollable infrastructure expansion. The objective of this research was to analyze the feasibility of dry canals in the American continent as sustainable development projects with fine relief from the Panama Canal. On the other hand, the success of a dry port depends on the preferences for use as a port route over its competitors. However, dry ports that are not competitive will be locally supplied. A mixed analysis was carried out to identify the feasibility criteria for dry canals, based on the quantification and estimation of statistical control variables, decision making, geopolitics and modernization. The characterization of data obtained from requirements so that a dry port can act as a detonator of sustainable and sustainable development in a cutting-edge environment. The identification of parameters of island-type port systems will be the subject of future work.

Objetives	Methodology	Contribution
The objective of this research was to analyze the feasibility of dry canals in the American continent as sustainable development projects with fine relief from the Panama Canal..	A mixed analysis was carried out to identify the feasibility criteria for dry canals, based on the quantification and estimation of statistical control variables, decision making, geopolitics and modernization.	The characterization of data obtained from requirements so that a dry port can act as a detonator of sustainable and sustainable development in a cutting-edge environment.

Triad Traffic in Millions of TEUs 2023



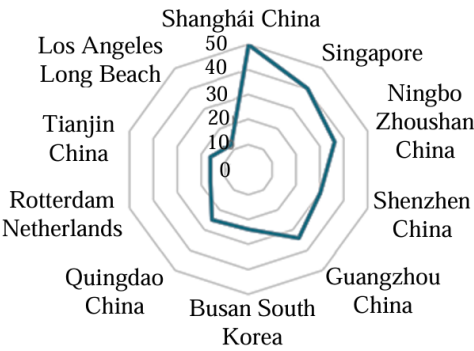
Dry port, inner port, Trunk port

Resumen

El futuro del comercio global marítimo está siendo guiado por la Triada generando una expansión de infraestructura incontrolable. El objetivo de esta investigación fue analizar la factibilidad de canales secos en el continente Americano como proyectos de desarrollo sustentable con fines desahogo del canal de Panamá. Por otro lado, El éxito de un puerto seco depende de las preferencias de utilización como ruta portuaria sobre sus competidores. Sin embargo, los puertos secos que no son competitivos serán de abastecimiento local. Un análisis mixto fue realizado para identificar los criterios de factibilidad de canales secos, basado en la cuantificación y estimación de variables de control estadísticas, toma de decisiones, geopolíticas y modernización. La caracterización de datos obtenidos de requerimientos para que un puerto seco pueda actuar como detonador de desarrollo sustentable y sostenible en un entorno vanguardista. La identificación de parámetros de sistemas portuarios tipo isla será motivo de trabajos futuros.

Objetivos	Metodología	Contribución
El objetivo de esta investigación fue analizar la factibilidad de canales secos en el continente Americano como proyectos de desarrollo sustentable con fines desahogo del canal de Panamá.	Un análisis mixto fue realizado para identificar los criterios de factibilidad de canales secos, basado en la cuantificación y estimación de variables de control estadísticas, toma de decisiones, geopolíticas y modernización.	La caracterización de datos obtenidos de requerimientos para que un puerto seco pueda actuar como detonador de desarrollo sustentable y sostenible en un entorno vanguardista.

Triad Traffic in Millions of TEUs 2023



Puerto seco, puerto interior, Puertos troncales

Citation: Castillo-Aguirre, Alfredo Humberto, Cruz-Gómez, Marco Antonio, Mejia-Perez, José Alfredo and Espinosa-Carrasco, María del Rosario. [2024]. Feasibility of dry canals in the Americas. Journal Civil Engineering. 8[19]-1-13: e20819113.



Introduction

Seaports are a spatial system that function as networks of logistics platforms that control cargo flows in supply chains that contribute to industrial development and global trade.

Ports interact with other nodes directly and indirectly, such as neighboring and overseas seaports, intermodal terminals and inland logistics platforms of different levels of connectivity. These form networks of sequential chains of transport flows, where the output of one node is the input of another (Bernacki, et. al. 2024).

Ports are nodes in a competitive system of complementary transactional networks. These use advantages such as location, cost and productivity to attract or retain service and shipping traffic. A range of ports may be located along the same coast and share inherent geographical, economic and functional characteristics (Li et al., 2024).

The Atlantic Ocean links South American ports, including those in Brazil, Argentina and Chile, with prominent European ports in countries such as Spain, Portugal, the United Kingdom and the Netherlands. The waterways on this route are the South Atlantic Ocean and the North Atlantic Ocean, relying on efficient logistics and infrastructure for reliable cargo flow and accurate supply chain management.

Supply chain logistics can be disrupted by primary choke points. These are crucial points in global trade. If they are interrupted, there are limited and unprofitable maritime transport alternatives. These bottlenecks are the Panama Canal, Suez Canal and the Strait of Malacca, key in world trade.

A clear example was the blockade of the Suez Canal in 2021, where this depends on the access granted to the Red Sea through the Bab el-Manded Strait. Secondary bottlenecks are those that connect to maritime dead ends with substantial resources and commercial potential, such as the Strait of Hormuz, which allows access to the Persian Gulf, and the Bosphorus Strait, which grants access to the Black Sea.

The Oresund Strait is the only access to the Baltic Sea and Russia's main ports. Closing these bottlenecks would force the use of alternative land routes that are unlikely to have the capacity to handle maritime load volumes. (Bartosiewicz et al., 2024, Bernacki, et. al. 2024 and Mechai & Wicaksono, 2024).

The aims of this research was to analyze the feasibility of dry canals in the American continent as sustainable development projects for the relief of the Panama Canal. The characterization of data obtained from requirements so that a dry port can act as a detonator of sustainable and sustainable development in a cutting-edge environment.

The evolution of maritime trade routes places all port systems that provide supply chain services in a committed competition to cover the parameters required by the port infrastructure trends of sustainable development, in an avant-garde environment, but How to achieve the success of a dry port? This depends on the preference for use as a port route over its competitors. The global port chain is migrating from a government sector to a private company sector, which makes it a transnational private capital company that is governed to a certain extent by the laws of the country of settlement and international laws, but business strategies and company laws are governed by the private company, as well as the profits among its shareholders. The feasibility of a dry port for any Latin American country must take into consideration that the top of the profit pyramid is occupied by the transnational, not the government of the country or the region of settlement.

The identification of parameters of island-type port systems will be the subject of future work.

International port trade

International trade occurs within economic trading blocs such as NAFTA in North America, the EU Single Market in Europe, ASEAN in Southeast Asia, MERCOSUR in South America, and ECOWAS in West Africa. (WTO) and the initiatives of organizations such as UNCTAD or the World Bank.

The most important transpacific and transatlantic trade flows are between Asia and North America (especially the United States), between Europe and North America, and between Europe and Asia. The sea routes pass critical points such as the Strait of Malacca (30%), the Suez Canal (15%), the Strait of Gibraltar and the Panama Canal (5%). These bottlenecks the transatlantic, transpacific and Asia-Europe routes. Shipping lines tend to organize their services to connect dominant trade flows directly and less dominant trade flows indirectly through transshipments (De Santa Marta, 2020) and (Mechai & Wicaksono, 2024).

International trade is centered on three exporting powers called the Triad made up of China-Singapore-Korea, with around 255 million TEUs, followed by the Netherlands with approximately 16 million TEUs and the United States with 13 million TEUs annually reported during 2023, you can see figure 3 (Li, L., et. al., 2024).

Box 1

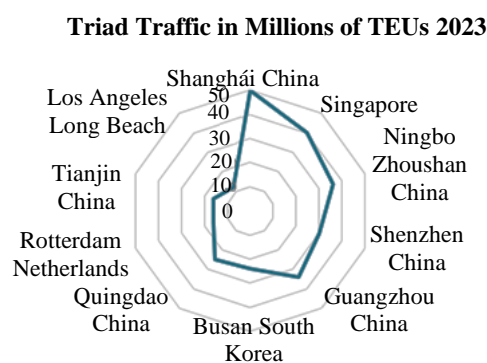


Figure 3

International trade of the Triad in 2023

Throughout the world during 2022, the existence of 348 ports, with a mobility of around 500 million TEU's, were censused and reported in the Global Ranking of Container Ports. On the other hand, the Rankin of the American Continent of Ports reports the 33 ports with the highest activity with around 95.2 million TEU's, which represents that the American Continent imports 40% of the triad's global exports, of which North America imports 65.5% and 34.5% is distributed in Latin America. See table 1, (Cidell, 2024).

The successive stages of port development is called the port hierarchy, which ranges from small ports serving a niche market to large gateway ports serving a vast area made up of a wide range of economic activities. This does not imply that small ports have limited importance for the economies they serve, because although they are not a means of generating economic resources for the passage of container ships that greatly impact the Gross Domestic Product of a Nation, however, it can present advantages such as having a means of access to global markets with its port infrastructure that allows them to import and export to satisfy the economies of the nation, turning them into a port system with national competition.

A multiport is identified by the location relationship with nearby areas of identical hinterland traffic, criteria for grouping adjacent container ports in the same gateway region competing for the same port calls in the networks, and the hinterland connectivity profile. On the other hand, feeder ports or interior nodes can cooperate and coordinate by grouping transportation flows and land for development. Provides economic activities, manufacturing and logistics. These follow a macroeconomic and microeconomic analyst perspective, forming port clusters that offer scale, scope and environmental advantages, linked to the physical flows of cargo through intermodal transport (short sea shipping, barge or railway). Just as "ecologies of scale" due to their spatial concentration can face accessibility challenges (congestion) and higher costs of the surrounding land. (Li et al., 2024).

Specialized maritime transport

International trade and Maritime Transport Services covers cargo markets such as: Bulk; solid, liquid, and gaseous, Rolled Cargo; Ro-Ro, Containers; general, and refrigerated, Oversized and Passenger.

Container ships have evolved logarithmically in tandem with the growth of the global market transported by this means. World trade advances logarithmically with increases per decade of around 35%.

The world's largest container ships reported until 2023 is 1st. MSC Irina, (2023, Liberia) with capacity 24, 346 TEU, length 400 m and beam 61 m. 2nd. MSC Loreto, (2023, Liberia) with capacity 24, 300 TEU, length 399.99 m and beam 61.3 m. 3rd. MSC Tessa, (2022, Liberia) with capacity 24, 116 TEU, length 399.99 and beam 61.56. 4th. Evergreen Ever A lot (2022), with a maximum capacity of 23,964 TEU, length 399.99 m and beam 61.50 m. 5th. HMM Algeciras (2020). Maximum TEU: 23,964. Length 400 m, beam 61 m and depth 33.20 m. maximum height point container ship 50 m. 6th. HMM Oslo (2020). Maximum TEU: 23,820, length 399.9 m and beam 61.5 m. 7th MSC Gülsün (2019). Maximum TEU: 23,756. 8th. MSC Mina (2019). Maximum TEU: 23,656 9no. CMA CGM Jacques Saadé (2020). Maximum TEU: 23, 112. 10th. OOCL Hong Kong (2017). Maximum TEU: 21,413.

During 2016, the modernization of the Panama Canal incorporated locks 427 m long, 55 m wide and 18.3 m deep in the port area. The depth of the locks is 25.9 m, because they contain fresh water and the draft of the ships depends on the density of the water, directly related to salinity and temperature. The Neopanamax vessels suitable for transit through the new locks are 49 m wide by 366 m long, draft of 15.2 m and maximum TEU: 14,000. Another classification of vessels was the so-called Panamax with a length of 294 m, beam of 32m, and 12 m., draft with a maximum capacity of 5000 TEU. These are suitable for passage through the old locks of the Panama Canal whose dimensions are 320m. long, 32 m. wide and 12 m. draft ([PortalPortuario, 2023](#)).

The diversity of tramp vessel marine service configurations is a general cargo market dealing with smaller shipments. Fractional loads can be sent. "Weekly services on fixed days" do not have a route, itinerary, or fixed schedule, allowing this system to be available to ship any cargo from any port.

Typology Dynamar services specific frequency operated with exclusive ships for that work, services that offer departures, implementing charter trips, operated under incentive, within the "Parcelization" commercial route, in which a ship is chartered.

The general cargo market includes specialized ships. Heavy cargo ships do not operate on fixed routes but are attracted to those areas where large investments are made in the oil and gas industry. The reefer ships high-value food products that require end-to-end refrigeration and atmosphere control service. Refrigerated transportation is a one-way business.

Global trade problems

90% of global trade is carried out through a port supply chain with management of critical routes that can supply the service with quality parameters, low cost and delivery time. The exports carried out by the triad require port infrastructure for their supply. However, this has been surpassed and the port necks represent a serious problem for current trade, and this will become more acute in the coming years ([Wu, X. et. al., 2024](#)).

An imbalance between exports and imports is what currently occurs in the multipoint and point-to-point port supply chain.

Eurasian trade to America requires a business plan capable of satisfying the critical routes of port trade. The American continent needs to promote critical trade routes. A proposal made to all Latin American countries that have transpacific crossing conditions is to carry out dry port projects, also called; dry channels, internal ports, interoceanic land bridges or trunks, which operate as complementary to the Panama Canal for the passage of TEUs ([Bogataj et. al. 2022](#)).

The competition to present projects for interoceanic dry crossings from the Atlantic to the Pacific by the developing countries of Latin America with commercial alliances to the Triad countries and independently has not been long in coming. The participating countries due to their geopolitical conditions that make them suitable are Mexico, Guatemala, Honduras, El Salvador, Nicaragua, Costa Rica, Venezuela and Colombia. The country of Costa Rica is the only one that proclaims itself out of the competition, because it prefers to bet on the conservation of its ecosystems as a means of sustainable development. However, you could become interested in the projects and change your mind ([Anbleyth-Evans, 2023](#) and [Chou et. Al. 2021](#)).

Previous evaluations place them as the most suitable countries due to their geopolitical conditions and previous infrastructure already built in their territories, leaving Nicaragua, Mexico and Colombia as participants with interest in carrying out the three projects to compete simultaneously. But this does not exclude the other participating countries.

The draft conditions of ports in Latin America range between 10 and 15 m. at most. The port infrastructure in the Air draft parameter in unloading gantries ranges around 35m.

Nicaragua, together with a Chinese businessman, planned to build the Nicaragua Canal that would measure 278 kilometers long, between 230 to 520 meters wide, and up to 30 meters deep. However, in 2021 it was canceled, and the dreams of the canal fell apart, leaving only a dry port. It currently has the advantage of road infrastructure with expansion projects.

Mexico will rehabilitate a 200 km railway system in the Isthmus of Tehuantepec, with connection to the ports of Coatzacoalcos and Salina Cruz Oaxaca, which could be an alternative to alleviate the high demand in the passage of containers. With the advantage that this step already exists and is only being adapted.

Colombia's project is the so-called dry canal, which would be 220 kilometers long and would go from the Pacific to a city that would be built near Cartagena de Indias. Having the advantage of its port network of great global impact with proximity to the Panama Canal.

It is worth mentioning that Latin American countries compete to host either a wet canal or a dry canal in their territory and this will depend largely on foreign investors from the Triad and G7 countries. On the other hand, it is clear that the construction of a wet canal in Latin America similar to the Suez Canal could leave the dry canals disabled and out of competition. However, if they are not built, the dry canals will be trunks supporting the Panama Canal in the coming decades. A revaluation of built projects will emerge and place their impact on international trade on a higher scale (Li et al., 2024 and Wu et al., 2024).

The melting of ice in the Arctic ice cap caused by global climate change has made new transpolar routes possible, shortening the distances between Asia and Europe and between Asia and North America. Some studies have illustrated the logistics cost advantages of these new routes, comparing them with the dominant Panama Canal and Suez Canal routes (Mechai et. al. 2024).

Transportation cost strategies and risks in shipping companies

Mixed containerization is a strategy of shipping companies to prorate transportation costs, because the charges for perishable products yield greater profits that balance the costs of non-perishable products. However, refrigerated products also face higher charges in every sense such as tariffs, port handling, customs, tracking, storage insurance, etc. The client will have to pay all of these to the shipping company that, together with its logistics manager services, will carry out total or partial monitoring depending on the client's requirement from point to point or in multipoint trunk services (Bogataj et al., 2022).

Port terminals require infrastructure for loading and unloading, because a container ship can hold 1 to 5% of its total cargo of refrigerated containers and these require manual connection and disconnection conditions by port terminal operators, and a refrigerated contact transfer infrastructure through electric power generating plants that supply the chassis of trucks or trains that will carry out the transfer. In addition to special care, the fact that the containers are not airtight, generating condensation during their transfer, requires logistics accompanied by a very complete and expensive infrastructure to be able to supply the timely transfer of the containers. Most container ships carry mixed loads of standard and refrigerated container ships, so thinking about only supplying standard container ships greatly reduces the possibility of supplying the port central, being competitive with port customs at an international level in a network of supply criticizes that under the concept of logistics, quality and delivery time it will always look for port areas that offer lower costs, times and port tariffs, with logistics that ensure protection at all times in the event of any situation that puts the integrity of the container at risk. (De Santa Marta, 2020 and Fazi et al., 2020).

The security factor having a very important value in the supply chain (De Santa Marta, 2020 and Fazi et al., 2020).

Commercial agriculture must be competitive and depends on crop specialization to achieve economies of global scale, it implies greater dependence on technology. About 37% of the world's land area is devoted to agriculture, of which 68% is devoted to pasture and 32% to cropland. About 10% of the value of world trade refers to agricultural products food distribution.

As an economy becomes increasingly urbanized, it must rely on food distribution systems beyond its region to meet demand. Long-distance food distribution systems make it possible to establish a constant supply between regions of the world at different stages of their harvest cycles. The term food mile factor of weight-distance relationship in food distribution. The higher it is, the more energy needs to be expended to maintain the food supply. Many food products, cereals, are massively transported by grain elevators and bulk vessels such as railways and ships bulk foods main markets, are processed into primary foods. Therefore, agricultural production levels, regulates and maintains port systems in their different scales and classifications in a competitive state. However, limited production of these products in developing countries that lack technological exports can mark competitiveness in the balance of imports and exports.

Cold chains handle about 70% of all food consumed in the United States. In China, less than 25% of meat and about 5% of fruits and vegetables. The United States imports about 30% of all its fruits and vegetables, and 20% of its food exports, about 25% of all Food products transported in the cold chain are wasted every year between 50 and 60% of all production, due to integrity violations, resulting in temperature fluctuations and product degradation.

The efficiency and reliability of temperature-controlled transportation has reached a point that allows the food industry to take advantage of global seasonal variations. Emerging vulnerabilities in global food systems cause international organizations to generate market mechanisms that create incentives to distribute food.

Port systems are affected in the supply chain network by technological risks, sociopolitical risks; conflicts, corruption, theft, commercial restrictions, lack of reliability in the government, operation of criminal groups, social instability, marginalization, areas of poverty, lack of energy, urban infrastructure, services, customs fraud, floor collection and geopolitics among others, since these mechanisms generate instability in the attraction of investment that has an impact on economic volatility and price supply and demand shocks that generate unrest and demonstrations by social groups. The influence of these risks on the supply chain means that market prices could be lower than the cost of production and distribution. A simple integration measure relates to customs delays, a major trade impediment, adding uncertainty to supply chain management. For regulators, trade facilitation improves their effectiveness and reduces the risk of customs duty evasion.

The geography of ports takes shape at different scales, from the port and its terminals at the local level to the global maritime transport system. Sites can be modified by adding infrastructure such as docks, docks, breakwaters, forming a port, geography is the core of the added value that maritime transport provides, and ports are the places that generate this value.

Ports depend on geographical limitations, changes in commercial and technical aspects of maritime transport, changes in logistics, geography of ports, development of transport terminals, supply of infrastructure, anticipated transport demand. On the other hand, the presence of infrastructure does not guarantee traffic, because shipping lines can reassign the sequence of the ports they serve as business opportunities change. The growth of port traffic implies improvements in spaces, maritime profiles, increased stowage, and an increase in the number and length of docks. As maritime traffic grows, port terminals and activities tend to expand in a valorization process from their original sites to locations with better maritime and land access in an unsustainable race with a sequential perspective to satisfy the demand of supply chains.

The creation of dry canals with internal port infrastructure must be extensive and focused on serving shipping interests, otherwise no advantageous ocean location will overcome the peripheral land disadvantage.

Competitiveness, peripheral ports must be more proactive than ports centrally close to maritime networks or large internal markets, proximity to a circular route and have good facilities and connections.

Advantages can be found in a better-performing inland transportation network, personalized customer focus, flexible business environment, and increased reliability that comes from certain asset availability.

Connectivity to maritime transport networks makes it possible to identify critical routes that involve less port navigation time. The availability of storage in the terminal's stacking yard functions as a buffer and temporary storage area between offshore operations and land transportation.

The space consumed by container terminals increases space requirements, changing the geography of ports and has promoted the migration of terminals to new peripheral sites. It is recommended that in the layout of internal ports, large spaces be considered for the yards that will support TEU mobility and port revenue. The interior of the port is a strategic market area to interact and compete in the creation of interior freight corridors and centers.

The development of intermodal corridors and inland terminals allowed deep penetration into the country's interior via shuttle trains and barges. The rise of intermodalism and transportation corridors influenced the inland reach of seaports. Intermodalism has not only given ports incentives to expand their reach inland, but has also become more discontinuous, especially beyond the port's immediate hinterland. Such a process may even lead to the formation of "islands" in the distant hinterland for which the cargo hub achieves a comparative advantage in costs and services over rival seaports. Conventional market perspectives based on the decline of distance are not adequate to address this new reality. High-volume intermodal corridors typically offer a more favorable relationship between transportation price, delivery time and distance than conventional, continuous inland transportation coverage (Chou et al., 2021).

The hinterland of a port consists of overlapping service areas of individual hinterland terminals and available modal options and the size of each area depends on the service frequency and rates. The foreland is a maritime space over which a port has commercial relations; maritime transport networks are a common representation of the foreland concept. For successful integration, ports seek balance in import services; however, when it decreases, they turn inward to promote exports. This balancing logistics achieves a successful balance.

Inward movements generate low-paid activities such as repositioning of empty units, fixed delivery schedules, waiting for an available docking bay at a distribution center, network control and tracking.

Terminalization encourages the establishment of a hierarchy of flows along a transport chain where terminals act as important regulators, either as bottlenecks or as buffers. Transshipment hubs tend to be deeper to accommodate container ship drafts, which puts them at a technical advantage and encourages feeder hub services and interline relay configurations between mainline vessels.

Railway dry ports are found throughout Europe, often linked to the development of logistics zones. Depending on the European country considered, these logistics zones receive different names, such as "plateformes logistiques" in France, "GVZ" in Germany, "Interporti" in Italy, "Freight Villages" in the United Kingdom, "Transport Centers" in Denmark, and "ZAL" in Spain. The largest railway facilities have packages of up to 10 tracks with a maximum length of 800 meters per track. Rail hubs are typically equipped to allow simultaneous lot exchanges (direct transshipment) using rail-mounted gantry cranes (Bartulović et al., 2023).

Kansas City can be considered the most advanced inland port initiative in North America. There are four railway lines with private capital that compete to provide better service to the intermodal system. All nations in the world are thinking about the generation of multi-member projects and foreign investments.

In North America they take advantage of the planning and establishment of a new intermodal rail terminal carried out at the same time as a logistics zone project. Compared to Europe, North American dry ports tend to be larger and cover a much more substantial market area. Although the main disadvantage is the seasonal snowfall (Bu et. al., 2023) and (Cidell, 2024).

In Asia, indoor terminals are much more recent. Satellite facilities near port terminals accommodate activities that decongest port operations. Metropolitan inland facilities to provide better connectivity to port terminals along the coast, as well as to support the logistics of a growing domestic consumer market. Major dry port development is underway on the Yangtze River, up to the upper reaches near Chongqing, about 2,400 km upstream from Shanghai. Intermodal rail development addresses the importance of the existing rail network for passengers and dry bulk goods. Intermodal rail and barge traffic is increasing, as is the use of inland ports (Bernacki et. al., 2024).

Methodology

This research had a mixed approach, applying both quantitative and qualitative technologies, using systematic processes, as well as records and estimated data. The objective of this research was to analyze the feasibility of dry canals in the American continent as sustainable development projects for the relief of the Panama Canal. For this, the application of the quantitative method was relevant in the identification of control variables involved in previous studies such as; statistics, decision making, geopolitics and modernization. The characterization of data obtained from requirements so that a dry port can act as a detonator of sustainable and sustainable development in a cutting-edge environment.

Records of results obtained by different port companies, governments of different countries and previous studies of dry ports that iterate in the global port supply chain network, were considered as the application of the qualitative method that allowed the possibility of obtaining results from the estimation of variables, which played an important role in decision making to understand the evolution and trends of a global port culture.

The operational data resulting from this research determined special adjacent requirements such as an uncertainty in the way dry port conditions adapt depending on their geopolitics, infrastructure, quality of service in a continuous reduction of costs and delivery times, among other. Finally, using the mixed method, an analysis of the control variables that allow involvement in the evolution of maritime trade routes places all port systems that provide supply chain services in a committed competition to cover the parameters required by the port infrastructure trends of sustainable development, in an avant-garde environment, but How to achieve the success of a dry port? This depends on the preference for use as a port route over its competitors. The global port chain is migrating from a government sector to a private company sector, which makes it a transnational private capital company that is governed to a certain extent by the laws of the country of settlement and international laws, but business strategies and company laws are governed by the private company, as well as the profits among its shareholders. The feasibility of a dry port for any Latin American country must take into consideration that the top of the profit pyramid is occupied by the transnational, not the government of the country or the region of settlement.

Results

The excessive number of dry ports as transport infrastructure generates the possibility of overinvestment, duplication since many inland places would like to claim a participation in global value chains. Case in Western Europe, abundance of inland terminals, Rhine-Scheldt delta, underlines the excessively competitive environment and waste of resources. North America, different ownership and governance structure, the establishment of an inland port, the intermodal terminal component is mainly in the hands of railway operators. Furthermore, local governments can devise the development of inland ports with the expectation of dry port development an emerging functional relationship between port terminals and their hinterland. Dry ports assume various functions with collocation with logistics zones, a dominant development paradigm based on their regional configuration.

The size of each inland port area depends on the frequency and rates of intermodal transport services by rail or barge, which acts efficiently presenting an environmental benefit with CO₂ emissions approximately 25% lower than they would normally be (Chou et al., 2021).

When using dry ports, there are some challenges is the increase in the volume of cargo transported by rail. The current railway and road infrastructure is not sufficiently developed to be able to withstand the increasing loads. Some countries have insufficient railways to quickly transport the goods that arrive at them. Localized seaports sometimes offer strong competition that undermines the ability to be the most economical option (Centurião et al., 2024 and Wu et al., 2024).

Dry canals can be sustainable, sustainable development and circular economy projects in the optimization of export and import routes. One of the largest inland ports in the world is in Duisburg, Germany. More than three million maritime containers and 130 million tons of goods arrive at this dry port every year. The location makes it one of the main crossings of the Silk Road. One of the most advanced and developed dry ports in all of Asia is in Lat Krabang, Thailand. On the outskirts of Bangkok, capacity to process half a million shipping containers, but has a record of having handled 1.7 million in 2008 (Irawan et al., 2024).

Discussion of results

A dry port in areas of extreme poverty and with a lack of infrastructure can detonate as an area of sustainable development, but to do so it will have to go through several stages of adaptation such as the creation of promising infrastructure that invites businessmen to invest in the purchase of large areas of land that have previously been changed from agricultural, mining, agricultural, tourism or settlements of demographics adhered to a culture to industrial type use with port activity. The placement of railway and port infrastructure requires large investments, which are obtained by revaluing the land that was initially dedicated to primary activities and by changing its land use to industrial, the value of the surrounding land will increase, which governments use to reinvest in technologies, port, railway and road transport infrastructure.

This predisposition of an initial infrastructure will trigger progress in the region with demographic, cultural, social displacements and the arrival of industrial and port infrastructure. However, this does not ensure the feasibility and sustainability of the industrial and port development project, since this system will become a new member of the competition in the port routes but its impact and development depend on the competition and continuous adaptation of its development plan. Business and its global competitiveness to attract port clients due to the transfer advantages it offers based on continuous reinvestment in infrastructure and technologies to be competitive in the hierarchy of dry ports (Asadi Dalivand et al., 2024 and Centurião et al., 2024).

In China's strategy to evade the Panama Canal, and to reduce customs costs for its products to be a more competitive power, there is the possibility of building a wet canal (that has similarities to the Suez Canal) by agreement with one of the countries. Latin Americans, where they can have control of passage at least for the next century. And to generate a business strategy where Latin American countries that have interoceanic crossings from the Atlantic to the Pacific Ocean generate dry channels that serve as trunks to the Panama Canal for the passage of goods (Anbleyth-Evans, 2023).

After evaluating various possibilities of dry canals in all cases and due to the existing conditions in countries with these characteristics, a project to build a wet canal breaks with the budgets of any nation, in addition to the fact that the construction of the canal would be in alliance with another nation, for this reason the construction of dry canals, although requiring less investment, represents codependency of several nations that, in the end, together with the negotiations, can represent a proximity in the long run to customs tariffs similar to those paid to the United States. And in any case, the transport of a large quantity of products must face trunk channels with the risks they represent. China proposes a new, easier, more economical, viable and less ecological impact possibility to bring its industrial products to the United States. This strategy is to build companies in the border area with Mexico and, through trains, transport products to the countries of the United States and Canada (Zhou, 2023).

In a business strategy, China could prefer to build island-type ports in the northeastern area of the Gulf of Mexico and enable the port of Tamaulipas as an internal port to manufacture products in the border area with Mexico. In addition to having the proximity to the Ports; New York, New Jersey, Virginia, Georgia, Houston, South Carolina, Miami that communicate directly to the Atlantic Ocean. And although this does not resolve the customs taxes with the United States for the entry into its territory of products of Asian origin, it does represent an alternative in transportation time, in situations of saturation of the Panama Canal and in a balance in the lissing process of gray containers (Bu et al., 2023).

The ideology of sustainable and sustainable development of power countries such as China, fight in a commitment that goes hand in hand with green technologies in their productive development chains. For this reason, the development of dry canals in any of the Latin American countries for the passage of electric cars and other goods by port fleets seeking decarbonization is not an alternative that they can charge in exchange for exports through the passage of a canal," NO" for China its culture, ideologies and its technologies. Powerful manufacturing countries are developing technological and development strategies in conjunction with other nations and even offshore manufacturing so that these leading countries in the world can indicate that their manufacturing is green with measurable indices between powers that make the difference between these to be classified as one of the most powerful in the leadership of sustainable development technologies (Zhou, 2023).

Therefore, they could make channel development agreements through third parties, but never through governments, that is, development agreements that impact the environment are developed through private entrepreneurs of different nationalities, but not directly linked to governments or companies that seek to develop products with green chains through technologies. Environmentally responsible companies cannot be generated when in the chain of design, logistics, production, marketing, circular economy and sustainability of the technological development chain that commit in any of these processes to a direct or indirect attack on sustainable development (Asadi Dalivand et al., 2024).

Conclusions

The existence of dry channels in Europe, Asia and North America are the basis of their feasibility as part of the network structure of the global port supply chain. These have specific characteristics that support mobility, making it more efficient and reducing the pollution of polluting gases emitted into the atmosphere. Dry ports have limitations in infrastructure such as draft and loading and unloading height. However, they serve as perfect trunks for island-type ports, being able to receive the largest ships in the world today. Dry ports have their scale and competition within the port supply chain, being feasible at this level, but it is not possible that they can compete with deep-draft ports or interoceanic canals. These may be in a regionalization of internal ports to supply a nearby major port, making them compete for services, quality, price and time, which will reduce their profit margin, making some unprofitable because they are not the optimal option for the company route logistics of the shipping companies, but they balance the lack of import services with exports of agro-industrial products from the region. The dry canals in Latin America as trunk projects to the Panama Canal are feasible as development projects for what they are designed and the purposes they pursue such as buffering of loading-unloading and relocation of containers, being key in the coming years in the network of the international port supply chain. However, all will be continually re-evaluated to remain competitive in the global port supply network in an evolutionary process of continuous reinvestment. On the other hand, there are factors that can collapse any dry port project and they are insecurity, ecological impact, discontent due to social displacement when they realize that they are not at the top of the pyramid in the profits generated by the dry canal, because this This position is occupied by shipping companies and, most importantly, the limited service and lack of export products from the region makes them an easy target for crime, further losing confidence in the route.

Declarations

Conflict of interest

The authors declare no interest conflict. They have no known competing financial interests or personal relationships that could have appeared to influence the article reported in this article.

Author contribution

Castillo-Aguirre, Alfredo Humberto: Contributed to the project idea, research method and technique, about to develop all the project.

Cruz-Gomez, Marco Antonio: Apported the studies, and bases in the área of railway systems, and also engeneering port.

Mejia-Perez, José Alfredo: Apported with traffic logistics, and ambiental engeneering.

Espinosa-Carrasco, María Del Rosario: Contributed withe the economic factor, and situation with the relation China/Latam, and economic factor in ports of Europe.

Availability of data and materials

The data obtained, it´s about the capacity of each port in America, showing that if it´s factible for a dry canal, or another project:

Box 2
Table 1
Ranking 2023. Americas Top 33 ports

Núm.	Port/terminal	Country	Throughput, in millions of TEU's
1	Port of Los Angeles, California	USA	9.9
2	Port of New York and New Jersey	USA	9.4
3	Port of Long Beach, California	USA	9.1
4	Port of Savannah, Georgia	USA	5.8
5	Panama Caribbean (Colon area)	Panama	4.8
6	Santos	Brazil	4.2
7	Port of Houston, Texas	USA	3.9
8	Manzanillo	México	3.6
9	Port of Virginia	USA	3.6
10	Port of Vancouver, British Columbia	Canada	3.6
11	Port of Seattle and Tacoma, Washington	USA	3.3
12	Panama Pacific	Panama	3.3
13	Cartagena Bay	Colombia	3.2
14	Port of Charleston, South Carolina	USA	2.8
15	El Callao (all terminals)	Peru	2.7

16	Port of Oakland, California	USA	2.3
17	Guayaquil (all terminals)	Ecuador	2.2
18	Port of Halifax, Nova Scotia	Canada	2.1
19	Lázaro Cárdenas	Mexico	1.8
20	San Antonio	Chile	1.5
21	Moin/Limon complex	Costa Rica	1.3
22	Buenos Aires, Metropolitan area	Argentina	1.2
23	Itajaí-Navegantes	Brazil	1.2
24	Port of Miami, Florida	USA	1.1
25	Paranaguá	Brazil	1.1
26	Veracruz	Mexico Gulf	1.1
27	Montevideo	Uruguay	1.1
28	São Francisco do Sul, Itapoá	Brazil	1.0
29	Port of Montreal, Quebec	Canada	1.0
30	Buenaventura (all terminals)	Colombia	1.0
31	Altamira, Tampico	Mexico	0.8
32	Valparaiso	Chile	0.7
33	Puerto Cortés	Honduras	0.7

Funding

This research was support by the Tribology and Transport Group by Marco Antonio Cruz Gómez S-3098-2018 0000-0003-1091-8133, 349626.

Acknowledgements

To the Benemérita Universidad Autónoma de Puebla; Engineering Faculty for the support in the use of its infrastructure., To the Tribology and Transport Group, BUAP, for their support in the analysis and development of the work, and 189 Disaster Prevention, Sustainable Development and Tribology Academic body, BUAP.

Abbreviations

ASEAN	Association of Southeast Asian Nations
ECOWAS	Economic Community of West African States
EU	The European Union
GVZ	Güterverkehrszentren
MERCOSUR	Mercado Común del Sur
MSC	Mediterranean Shipping Company

Article

NAFTA	North American Free Trade Agreement
Ro-Ro	Roll on Roll Off
TEU	Twenty-foot equivalent unit
UNCTAD	United Nations Conference on Trade and Development
WTO	The World Trade Organization
ZAL	Logistics Activities Zones

References

Basics

Anbleyth-Evans, J. (2023). [Port developments and marine democracy in Latin America](#). *Marine Policy*, 157(105767), 105767.

Centurião, D., Abrita, M. B., Neto, A. R., Camilo, A. P., Vignandi, R. S., Junior, G. E., Weber, V., Marques, N., & Maciel, R. F. (2024). [Impacts of road transport infrastructure investments on the Latin American Integration Route](#). *Regional Science Policy & Practice*, 16(8), 100061.

De Santa Marta, C. P. (2020, julio 18). [10 Mayores y Principales Compañías Navieras del Mundo](#). Noticias Puerto de Santa Marta.

Supports

Asadi Dalivand, A., & Torabi, S. A. (2024). [Sustainable-resilient seaport-dry port network design considering inter-modal transportation](#). *Journal of Cleaner Production*, 452(141944), 141944.

Bartosiewicz, A., Kucharski, A., & Miszczyński, P. (2024). [Efficiency of maritime container terminals in the Baltic Sea region using data envelopment analysis slack-based model](#). *Research in Transportation Business & Management*, 56(101166), 101166.

Cidell, J. (2024). [Canals, containers, and corridors: Bringing river geomorphology to North America’s largest inland port](#). *Journal of Transport Geography*, 115(103819), 103819.

Fazi, S., Fransoo, J. C., Van Woensel, T., & Dong, J.-X. (2020). [A variant of the split vehicle routing problem with simultaneous deliveries and pickups for inland container shipping in dry-port based systems](#). *Transportation Research Part E: Logistics and Transportation Review*, 142(102057), 102057.

Irawan, C. A., Salhi, S., Jones, D., Dai, J., & Liu, M. J. (2024). [A dry port hub-and-spoke network design: An optimization model, solution method, and application](#). *Computers & Operations Research*, 167(106646), 106646.

Li, L., Liu, J., Yang, J., Ma, X., & Yuan, H. (2024). [Investigating the efficiency of container terminals through a network DEA cross efficiency approach](#). *Research in Transportation Business & Management*, 53(101107), 101107.

Discussions

Bartosiewicz, A., Kucharski, A., & Miszczyński, P. (2024). [Efficiency of maritime container terminals in the Baltic Sea region using data envelopment analysis slack-based model](#). *Research in Transportation Business & Management*, 56(101166), 101166.

Bernacki, D., & Lis, C. (2024). [Sustainable gains from inland waterway investments at port-city interface](#). *Renewable and Sustainable Energy Reviews*, 200(114584), 114584.

Bogataj, D., Bogataj, M., Campuzano-Bolarin, F., & Nicolás, J. A. M. (2022). [Location advantages of the container port for perishable goods in the Murcia region](#). *IFAC-PapersOnLine*, 55(10), 2701–2706.

Bu, F., Liu, J., Liao, H., & Nachtmann, H. (2023). [An alternative solution to congestion relief of U.S. seaports by container-on-barge: A simulation study](#). *Simulation Modelling Practice and Theory*, 129(102836), 102836.

Chou, C.-C., Hsu, H.-P., Wang, C.-N., & Yang, T.-L. (2021). [Analysis of energy efficiencies of in-port ferries and island passenger-ships and improvement policies to reduce CO₂ emissions](#). *Marine Pollution Bulletin*, 172(112826), 112826.

Mechai, N., & Wicaksono, H. (2024). [Causal inference in supply chain management: How does ever given accident at the Suez canal affect the prices of shipping containers?](#). *Procedia Computer Science*, 232, 3173–3182.

PortalPortuario (2023, diciembre 17). [Naves tipo panamax son el 8,2% de la flota mundial a siete años de la ampliación del Canal de Panamá](#).

Wu, X., Wang, K., Fu, X., Jiang, C., & Zheng, S. (2024). [How would co-opetition with dry ports affect seaports' adaptation to disasters?](#). Transportation Research. Part D, Transport and Environment, 130(104194), 104194.

Zhou, J. (2023) [A double-edged sword: Chinese direct investment in Latin America](#). Structural Change and Economic Dynamics, 67, 234–249.

Dynamic evaluation of composite roofs: thermal optimization with PCM under extreme climate conditions

Evaluación dinámica de techos compuestos: optimización térmica mediante PCM en condiciones climáticas extremas

López Salazar, Samanta ^{*a}, Simá, E. ^b, Chagolla-Aranda, M. A. ^c and Chávez-Chena, Y. ^d

^a TecNM/CENIDET • LBH-6330-2024 • 0009-0004-9880-5145 • 918135
^b TecNM/CENIDET • JZS-9886-2024 • 0000-0001-7601-1273 • 83891
^c TecNM/CENIDET • LBI-3033-2024 • 0000-0002-7649-7389 • 368646
^d TecNM/CENIDET • LBH-6345-2024 • 0000-0003-3348-397X • 37563

CONAHCYT classification:

Area: Engineering
Field: Engineering
Discipline: Mechanical Engineering
Subdiscipline: Thermal Engineering

<https://doi.org/10.35429/JCE.2024.8.19.1.14>

Article History:

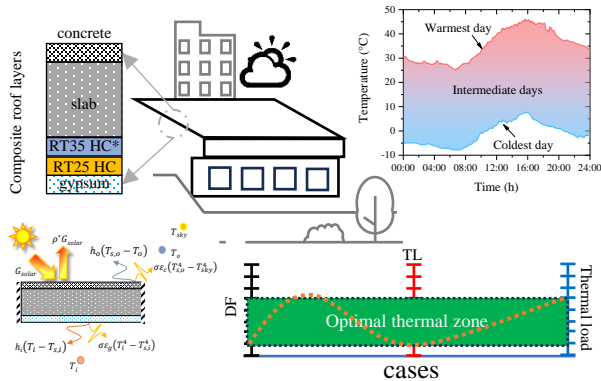
Received: January 25, 2024
Accepted: December 31, 2024



* [\[d18ce057@cenidet.tecnm.mx\]](mailto:d18ce057@cenidet.tecnm.mx)

Abstract

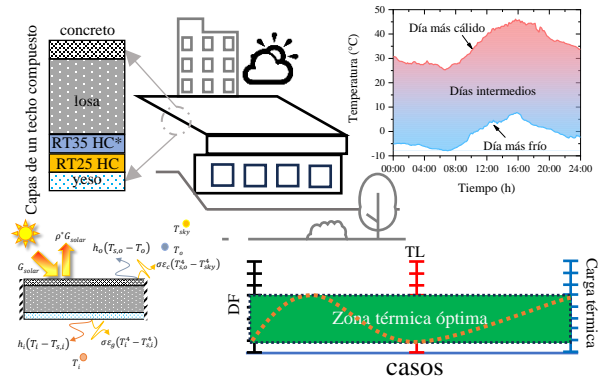
The thermal performance of different roof configurations was analyzed, comparing the integration of phase change materials (PCM) with polystyrene insulation under extreme climatic conditions. The decrement factor (DF), time lag (TL), and thermal load were examined. The results indicated that configuration with PCM, either in double layers or with increased thickness, showed the best thermal performance. The optimal configuration, C45, which includes a double layer of PCM with RT25 HC on the bottom layer and RT35 HC* at the top layer, achieved a DF of less than 0.2, a TL between 2 and 10 hours, and a thermal load of 2.5 kWhm⁻². This study confirms that adding a PCM layer is the most effective strategy, followed by the increase of the thickness, as well as the addition of insulation, and finally, an additional layer.



Composite roofs, Thermal insulation, Beat management

Resumen

Se analizó el rendimiento térmico de diferentes configuraciones de techos, comparando la integración de materiales de cambio de fase (PCM) con el aislamiento de poliestireno en condiciones climáticas extremas. Se analizó el factor de decremento (DF), el tiempo de retardo (TL) y la carga térmica. Los resultados indicaron que las configuraciones con PCM, ya sea en doble capa o con mayor espesor, presentaron el mejor rendimiento térmico. La configuración óptima, C45, que incluye una doble capa de PCM con RT25 HC en la capa inferior y RT35 HC* en la capa superior, logró un DF inferior a 0.2, un TL entre 2 y 10 h, y una carga térmica 2.5 kWhm⁻². Este estudio confirma que añadir una capa de PCM es la estrategia más efectiva, seguida por el incremento del espesor, agregar aislamiento y, por último, una capa adicional.

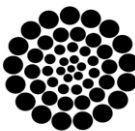


Techo compuesto, Aislamiento térmico, Gestión de calor

Citation: López Salazar, Samanta, Simá, E., Chagolla-Aranda, M. A. and Chávez-Chena, Y. [2024]. Dynamic evaluation of composite roofs: thermal optimization with PCM under extreme climate conditions. Journal Civil Engineering. 8[19]-1-14: e30819114.



ISSN 2523-2428/© 2009 The Author[s]. Published by ECONFAN-Mexico, S.C. for its Holding Republic of Peru on behalf of Journal Civil Engineering. This is an open access article under the CC BY-NC-ND license [<http://creativecommons.org/licenses/by-nc-nd/4.0/>]
Peer Review under the responsibility of the Scientific Committee MARVID® - in contribution to the scientific, technological and innovation Peer Review Process by training Human Resources for the continuity in the Critical Analysis of International Research.



RENIECYT
Registro Nacional de Instituciones y
Empresas Científicas y Tecnológicas
1702902 CONAHCYT

Introduction

As global temperatures rise due to climate change, the residential sector faces increasing demand for electricity, particularly to maintain thermal comfort. Worldwide, buildings are responsible for about 40.0 % of total energy consumption and contribute roughly 33.0 % of global greenhouse gas emissions. Heating and cooling systems, which are important for maintaining indoor climate control, account for 50.0 % to 70.0 % of a building's total energy use, depending on the climate and the efficiency of the building envelope (Somu et al., 2021). The increased use of these systems, driven by higher temperatures, has intensified this demand, putting additional strain on energy resources (Mejía et al., 2020).

Thermal gain in a building, defined as the amount of unwanted heat entering through the building envelope, is a significant factor contributing to increased energy consumption. It is estimated that around 25.0 % of this thermal gain comes from windows, 35.0 % from walls, and approximately 30.0 % from roofs (Shove et al., 2014). These statistics emphasize the importance of thoughtful design and material selection to maximize energy efficiency, with a particular focus on roofs. Roofs play a crucial role in a building's thermal load due to their direct exposure to solar radiation and their larger surface area compared to other elements of the building envelope.

To mitigate these effects and reduce thermal gain in roofs, various construction solutions have been developed, such as ventilated roofs (Wang et al., 2024), reflective materials (Parikh et al., 2023), and thermal insulators (Shrimali & Agrawal, 2024). Among these, expanded polystyrene (EPS) is one of the most commonly used materials in construction due to the effectiveness in reducing heat transfer and the low cost. However, while EPS is effective at minimizing heat loss, the ability to dynamically manage thermal flow is limited compared to more advanced materials like phase change materials, PCM, (Arumugam et al., 2024).

In this context, PCM has emerged as an innovative solution for enhancing thermal management in construction, due to their capacity to absorb, store, and release large amounts of energy as latent heat during phase changes. This ability to more efficiently moderate indoor temperatures is particularly valuable in roofs, where direct exposure to solar radiation and temperature fluctuations can cause significant thermal variations inside the building.

Several studies have demonstrated the effectiveness of integrating PCM into roofs to reduce indoor thermal fluctuations and decrease the building's overall thermal load. Piselli et al. (2019) evaluated membranes with integrated PCM for roofs, finding that the inclusion of PCM lowered the roof's surface temperature and heat flow. Following this, Bhamare et al. (2020) developed a 3D model showing that a 2° inclination in the PCM layer provides optimal daily heat gain reduction and improves the melting and solidification cycle. Similarly, Arumugam & Shaik (2021) analyzed the thermo-economic performance of hollow roofs with PCM, finding that combining PCM in walls and roofs reduces air conditioning costs and CO₂ emissions. Moreover, Qu et al. (2021) evaluated four key parameters in building envelopes with PCM, concluding that the thickness and arrangement of PCM significantly influence energy efficiency, achieving energy savings of up to 34.8 %.

Following the findings of Bhamare et al. (2023), which demonstrated the effectiveness of PCM with a 2 cm air layer, Dardouri et al. (2023) conducted several studies evaluating the energy performance of buildings with PCM in Mediterranean climates. Using EnergyPlus, they discovered energy savings of up to 41.6 %, particularly with PCMs that have different melting temperatures. In another study, the same authors found that the optimal thickness of PCM and insulation layers can reduce energy demand by up to 76.5 % in double walls and 73.8 % in single walls (Dardouri et al., 2023). Additionally, further analysis of roofs and walls with PCM in various locations revealed that PCMs with melting temperatures of 21 °C are more effective for heating, while those with 29 °C optimize cooling savings (Dardouri et al., 2023).

In a separate study, [Yu et al. \(2023\)](#) conducted simulations to assess the effectiveness of PCM in reducing overheating in buildings during summer. The results showed a decrease in overheating hours between 10.9 % and 19.7 %, and a reduction in cooling energy consumption by between 14.6 % and 25.7 %.

[Zahir et al. \(2023\)](#) analyzed the use of thermal energy storage (TES) systems with PCM to enhance the thermal performance of buildings in extremely hot climates, identifying challenges in the selection and encapsulation of PCM due to small daytime temperature variations.

Meanwhile, [Anter et al. \(2023\)](#) evaluated the long-term thermal behavior of different PCM in walls, finding that RT-35HC, placed 1.5 cm from the interior and exterior of the wall, reduces the average internal temperature to 27.7°C and decreases energy gain by 66.0 % during summer.

[Refahi et al. \(2024\)](#) assessed the impact of a double layer of PCM boards with different melting points, achieving energy savings of 6.6 % in heating and 2.8 % in cooling. Moreover, [Zhang et al. \(2024\)](#) proposes an electric heating terminal with PCM thermal storage that improves thermal efficiency in Tibet and reduces melting time by 2.7 hours.

Finally, [Khaleghi & Karatas \(2024\)](#) assessed a prefabricated wall panel with PCM, which showed a decrement factor of 0.007 and a time lag of 8 hours under extreme weather. The panel showed superior thermal performance, enhancing energy efficiency and indoor comfort.

However, most of these studies have been conducted in regions where PCM use is regulated and widely accepted, unlike in Mexico, where conventional methods like expanded polystyrene are still the norm. While research has explored the integration of more complex PCM configurations, such as double layers with different melting points and strategic positioning within roof structures, these analyses have not yet been carried out in the Mexican context.

This study innovatively applies phase change materials (PCM) in composite roof configurations, exploring strategic combinations of different PCM types to optimize thermal efficiency in both extreme cold and hot weather conditions.

By incorporating double layers of PCM, the study not only improves thermal regulation across a wide temperature range but also maximizes heat storage capacity and thermal inertia. Furthermore, a detailed comparison with traditional extruded polystyrene highlights the superior performance of PCM in cold desert climates.

Focusing on a specific climate, such as that of Ciudad Juárez, adds regional relevance and practical value, demonstrating the model's applicability to areas with significant temperature fluctuations and underscoring the potential impact of these findings on sustainable construction practices.

Physical and mathematical model

Figure 1 shows the cross section of a 1.0 m long composite roof made out of several layers of materials. The reference configuration includes a 0.005 m thick external concrete layer, a 0.1 m thick of a reinforced concrete slab and a 0.005 m thick inside gypsum plaster layer.

This type of configuration is widely used in the residential and commercial construction sector, in particular in areas where a combination of structural durability together with an appropriate thermal efficiency is looked up.

This type of concrete slab is commonly found in family housing, office buildings and industrial warehouses, where the reinforced concrete slab provides the resistance needed to support loads, whereas the concrete and gypsum plaster layers act as added barriers helping to moderate the heat transfer.

The described roof configuration provides an equilibrium between construction costs and thermal performance, what make it a popular option for temperate and cold climates.

To optimize the thermal performance of this basic structure, this study incorporates additional layers on the inside surface as well as on the outside. These include a 0.025 m thick insulating polystyrene and phase change materials (PCM's) with different fusion temperatures and varying thickness (10 mm, 20 mm and 30 mm).

Besides, configurations with two layers of 10 mm thick PCM placed in different positions are evaluated. Figure 2 shows these configurations, and in total, the study covers 52 different variants, by alternating the locations of the single and double layers of the PCM as well as the thickness.

These configurations are submitted to a detailed analysis of the heat transfer process in order to evaluate the thermal performance under different environmental conditions.

Figure 3 shows the heat transfer processes experienced by the roof, which are exposed to environmental conditions (ambient temperature, solar radiation and wind velocity) through the upper boundary.

Due to the temperature difference, heat transfer by convection and radiation occurs on this surface, a similar phenomenon happens in the lower boundary that is kept at constant temperature.

One portion of the solar radiation hitting on the outside surface of the roof is absorbed by the concrete slab, provoking the temperature to increase, whereas other portion is reflected in the exterior environment.

The heat absorbed by the concrete slab increases the temperature, starting thus the heat transfer process by conduction throughout all the layers of the roof. This complex process of heat transfer is mathematically modeled in order to predict the behavior and efficiency.

Box 1

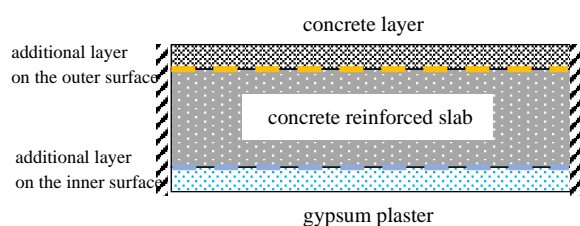
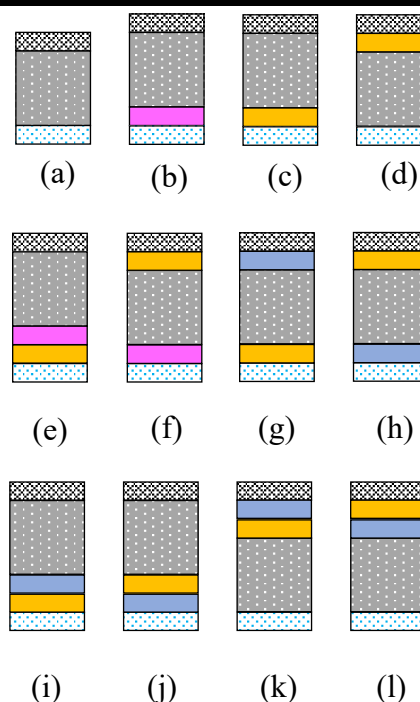


Figure 1

Cross section of a composite roof: reinforced concrete slab with concrete and gypsum plaster coats

Source: Own elaboration

Box 2



- concrete layer
- reinforced concrete slab
- gypsum plaster
- polystyrene insulation
- PCM layer (top or bottom)
- additional PCM layer (top or bottom)

Figure 2

Configurations of the composite roof: layers material and location

Source: Own elaboration.

Box 3

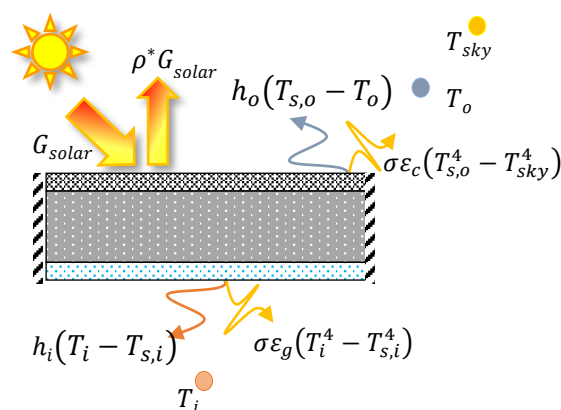


Figure 3

Heat transfer process on a composite roof subject to outside environmental conditions and at constant temperature on the inside surface

Source: Own elaboration.

The mathematical model describing the two-dimensional conduction heat transfer process is shown in Eq. (1). This equation applies to all the layers of the system (concrete, gypsum plaster, reinforced concrete and insulation), as well as the PCM, with the necessary adjustments to take into account the phase change. In order to perform such adjustments, the specific heat capacity method is used, and it introduces the term $C_{P_{eff}}$, including the enthalpy term h_{ls} that occurs during the transition phase. This way, the effective heat capacity encompasses the energy storage as well as the latent heat associated with the phase change, as detailed in Eq. (2). In order to apply this model to a multilayer composite roof, it is important to take into account the way in which the different layer interact in the interfaces.

$$\frac{\partial(\rho C_P T)}{\partial t} = \frac{\partial}{\partial x} \left(\lambda \frac{\partial T}{\partial x} \right) + \frac{\partial}{\partial y} \left(\lambda \frac{\partial T}{\partial y} \right) \tag{1}$$

$$\frac{\partial(\rho_{PCM} C_{P_{eff}} T_{PCM})}{\partial t} = \frac{\partial}{\partial x} \left(\lambda_{PCM} \frac{\partial T_{PCM}}{\partial x} \right) + \frac{\partial}{\partial y} \left(\lambda_{PCM} \frac{\partial T_{PCM}}{\partial y} \right) \tag{2}$$

$$C_{P_{eff}} = \begin{cases} C_{PS} & \text{for } T < (T_m - \Delta T) \\ \frac{C_{PS} + C_{PL}}{2} + \frac{h_{ls}}{2\Delta T} & \text{for } (T_m - \Delta T) < T < (T_m + \Delta T) \\ C_{PL} & \text{for } T > (T_m + \Delta T) \end{cases}$$

An energy balance was performed at each interface to ensure accurate heat transfer across the roof, which is composed of layers of different materials. This approach guarantees continuity between layers, preventing unwanted heat storage that could distort temperature predictions and affect the evaluation of the roof's thermal performance.

This balance is based on Fourier's Law and is implemented in numerical simulations to model heat transfer accurately through the layers. For these simulations, it is important to have precise and accessible data on the thermal physical properties of the materials involved. Table 1 presents the corresponding properties for each material comprising the roof.

Box 4

Table 1

Thermophysical properties of each layer on the composite roof

Material	λ , $\text{Wm}^{-1}\text{ }^{\circ}\text{C}^{-1}$	ρ , kgm^{-3}	C_P , $\text{Jkg}^{-1}\text{ }^{\circ}\text{C}^{-1}$	h_{ls} , Jkg^{-1}
Concrete	1.28	2200	850	-
Reinforced concrete	1.74	2300	920	-
Gypsum plaster	0.40	1200	837	-
Polystyrene insulation	0.03	28	1800	-
RT25 HC 22°C – 26 °C	0.20	880 770	2000	230 000
RT35 HC* 29°C – 36 °C		860 770		158 000
RT44 HC* 41°C – 44 °C		800 700		248 000

Source: Own elaboration

The selection of RT25 HC, RT35 HC*, and RT44 HC PCM is based on the ability to optimize the thermal process in accordance with the characteristic temperatures of the local region. The RT25 HC is chosen due to the melting temperature of 25 °C, which matches the desired indoor temperature, allowing it to stabilize this temperature by absorbing excess heat. The RT35 HC*, with a melting temperature close to 35 °C, is selected because it is similar to the sol-air temperature of the region, helping to mitigate daytime heat peaks. Finally, RT44 HC is selected to manage the maximum outdoor temperature, which is close to 44 °C, by absorbing the extreme heat and preventing it from penetrating into the building, thus improving energy efficiency and thermal comfort.

On the other hand, the boundary conditions to solve the mathematical model are expressed by Eq. (3) and (4). Where Eq. (4) takes into account the solar radiation absorbed by the material, the heat transfer by convection with a convective coefficient as a function of the wind velocity, $h_o=2.8+3.0V_{wind}$ (ASHRAE, 2009) and the solar heat transfer towards the sky vault (Swinbank, 1963).

On the lower boundary, similar effects are considered, in this case the convective coefficient varies as a function of the inside surface temperature of the roof, according to Duffie & Beckman (2013), where $h_i=9.26 \text{ Wm}^{-2}\text{K}^{-1}$ if $T_{s,i} < T_i$ and $h_i=6.13 \text{ Wm}^{-2}\text{K}^{-1}$ if $T_{s,i} > T_i$.

$$-\frac{\partial T}{\partial y} = \alpha^* G_{\text{solar}} + h_o(T_{s,o} - T_o) + \varepsilon\sigma(T_{s,o}^4 - T_{\text{sky}}^4) \quad (3)$$

$$-\frac{\partial T}{\partial y} = h_i(T_i - T_{s,i}) + \varepsilon\sigma(T_i^4 - T_{s,i}^4) \quad (4)$$

The model described earlier is two-dimensional, considering that the heat flow occurs mainly in the horizontal and vertical directions, while the lateral surfaces are treated as adiabatic. This assumption allows for a simplified model that maintains the accuracy of the results, as the lateral heat flow is minimal compared to the main flow through the roof. Moreover, even though the correlations for the convection heat transfer coefficients used in this model were developed several decades ago, they remain widely accepted by the scientific community due to their proven effectiveness and reliability in similar applications. These correlations, such as those reported by Duffie and Beckman, have demonstrated reliability across a wide range of weather conditions and continue to serve as a standard reference in heat transfer studies.

To evaluate the thermal performance of the proposed configurations, three key parameters were used: the decrement factor, the time lag, and the thermal load. The decrement factor (DF) measures the roof's capacity to attenuate outside temperature oscillations before they reach the inside, with a low value indicating good thermal attenuation. The time lag (TL) indicates the time taken by the thermal wave to travel through the roof from the outside to the inside surface; for hot climates, a longer time indicates better performance, as it delays the entry of heat into the building. Finally, the thermal load (CT) represents the total amount of heat that must be removed or added to the building to maintain indoor thermal comfort, with a low value indicating good energy efficiency. The thermal load is calculated as the area under the curve that represents both heat gains and losses over time, as shown in Eq. (5).

This calculation reflects the total amount of energy required to maintain a constant indoor temperature within a space, compensating for both heat entering and leaving the system.

$$CT = \int_{00:00}^{24:00} q(t)dt \quad (5)$$

Weather data

For this study, the BWk climate from the Köppen classification was selected, as it is characterized by a cold desert climate with dry winters. This selection is justified by the need to analyze the thermal performance of composite roofs under both high and low extreme temperature conditions typical of regions with this type of climate. In Mexico, this climate is common in cities like Ciudad Juárez, located in the State of Chihuahua, where ambient temperature varies significantly throughout the year.

Ciudad Juárez was selected as the source for the weather data, as it adequately represents the climate spectrum in Mexico, with extreme high and low temperatures typical of the BWk climate. The weather data were obtained from the National Weather System, which provides reliable and accessible information throughout the year. However, due to the high computational resources required for each simulation of every single and double-layer PCM configuration, a decision was made to focus on the most critical days of the year—those with the highest and lowest recorded temperatures. This selection allows for an efficient evaluation of the roof's thermal performance under the most extreme conditions, ensuring that the analyzed configurations can manage both maximum heating and cooling demands.

On the selected days, the outside ambient temperature varied between -7.9°C as the lowest value, and 46.1°C as the highest value (see Figure 4). Throughout the coldest day, the wind velocity varied between 0.0 ms^{-1} and 2.4 ms^{-1} , while on the warmest day, the wind velocity varied between 0.0 ms^{-1} and 4.5 ms^{-1} . For the coldest day, the highest solar irradiance on the horizontal plane was 789 Wm^{-2} , whereas the south-facing vertical plane received the highest solar radiation compared to other orientations.

On the warmest day, the highest solar irradiance was 1028 Wm^{-2} on the horizontal plane, while the west-facing vertical orientation recorded the highest value after midday. Other cities in Mexico with a climate spectrum similar to Ciudad Juarez include Mexicali in Baja California and Hermosillo in Sonora, where ambient temperatures also vary widely, with similar extreme values. These cities, like Ciudad Juarez, experience extremely hot summers and cold winters, making them relevant to this type of study.

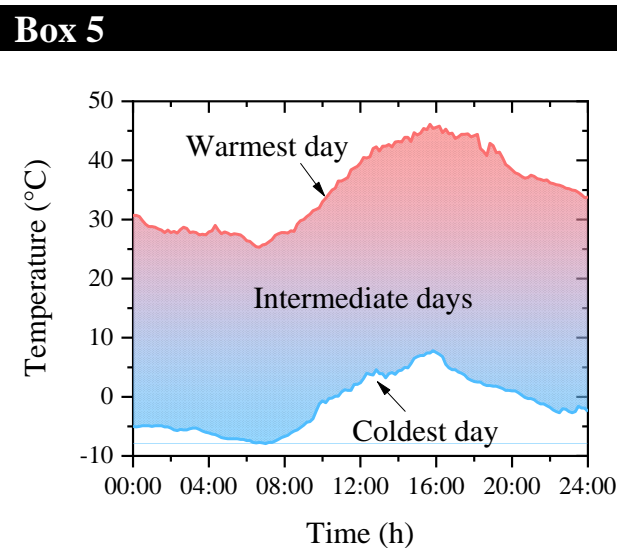


Figure 4
Recorded temperature interval: comparison respect to the climate spectrum of the region
Source: Own elaboration.

Methodology

This study implemented the Finite Volume Method to solve the governing equations for two-dimensional heat conduction in transient states, applicable to both solid materials and phase change materials (PCM). Time discretization employed a fully implicit scheme, and the diffusive term was discretized using a centered scheme. The algebraic equations were solved using the Alternate Directions Gauss-Seidel method (LGS-ADI), with a residual tolerance set at 10^{-8} to ensure accuracy.

The code used in this study is recognized by the scientific community, with some configurations previously published by the authors (López Salazar et al., 2023). To further validate the reliability of the results, the code was additionally tested against experimental data reported by Chagolla-Aranda et al. (2017).

This validation, detailed in Figure 5, demonstrates the code's ability to accurately replicate experimental results, highlighting the robustness and reliability of the implemented numerical code.

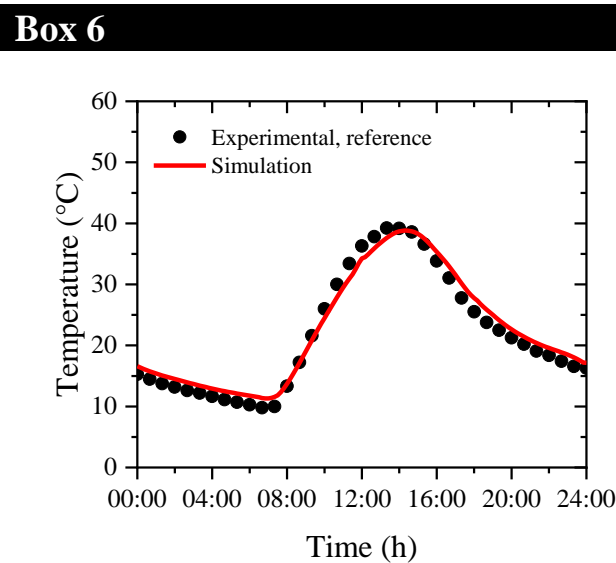


Figure 5
Surface temperature validation of a referenced roof compared to experimental data
Source: Own elaboration

Results

In this section, the results obtained for the different configurations of composite roofs evaluated in this study are presented and analyzed. The configurations include a reference model without additional materials, models with thermal insulation, and those incorporating PCM layers on both the inside and outside surfaces of the reinforced concrete slab. These configurations were designed to assess the thermal performance under extreme weather conditions. The study was divided into three phases to evaluate the impact of different PCM layer thicknesses and combinations:

Phase 1. This phase includes the reference roof, roofs with additional insulation, and roofs with a 10 mm PCM layer on both the outside and inside surfaces. These configurations evaluate how a thinner PCM layer affects thermal attenuation compared to the basic setup.

Phase 2. In this phase, roofs with thicker PCM layers (20 mm and 30 mm) were analyzed to assess how PCM thickness influences thermal storage capacity and indoor temperature regulation.

Phase 3. This phase explored combinations of double PCM layers on both the inside and outside surfaces to determine if combining different types of PCM and their strategic positioning can further optimize heat transfer through the roof.

Table 2 shows the nomenclature used for each case analyzed, to facilitate their identification and allow comparison among the different configurations. The configurations range from the single roof without any additional material to those with thermal insulation and layers of PCM.

Box 7

Table 2
Configuration overview: phases, material composition, and PCM thickness

Phase 1
C1. (a) Ref
C2. (b) Ref+Ins
C3. (c) Ref+e10mmPCMi RT25 HC
C4. (c) Ref+e10mmPCMi RT35 HC*
C5. (c) Ref+e10mmPCMi RT44 HC
C6. (d) Ref+e10mmPCMo RT25 HC
C7. (d) Ref+e10mmPCMo RT35 HC*
C8. (d) Ref+e10mmPCMo RT44 HC
C9. (e) Ref+Ins+e10mmPCMi RT25 HC
C10. (e) Ref+Ins+e10mmPCMi RT35 HC*
C11. (e) Ref+Ins+e10mmPCMi RT44 HC
C12. (f) Ref+Ins+e10mmPCMo RT25 HC
C13. (f) Ref+Ins+e10mmPCMo RT35 HC*
C14. (f) Ref+Ins+e10mmPCMo RT44 HC
Phase 2, 20mm
C14-C16, e20 mmPCM
Phase 2, 30mm
C27 – C38, e30mmPCM
Phase 3
C39. (g) Ref+PCMi RT25 HC+PCMo RT25 HC
C40. (g) Ref+PCMi RT25 HC+PCMo RT35 HC*
C41. (g) Ref+PCMi RT25 HC+PCMo RT44 HC
C42. (h) Ref+PCMi RT25 HC+PCMo RT25 HC
C43. (h) Ref+PCMi RT35 HC*+PCMo RT25 HC
C44. (h) Ref+PCMi RT44 HC+PCMo RT25 HC
C45. (i) Ref+DoublePCMi bRT25 HC + tRT35 HC*
C46. (i) Ref+DoublePCMi bRT25 HC + tRT44 HC
C47. (j) Ref+DoublePCMi bRT35 HC* +tRT25 HC
C48. (j) Ref+Double PCMi bRT44 HC + tRT25 HC
C40. (i) Ref+DoublePCMo bRT25 HC + tRT35 HC*
C50. (i) Ref+DoublePCMo bRT25 HC + tRT44 HC
C51. (j) Ref+DoublePCMo bRT35 HC* + tRT25 HC
C52. (j) Ref+Double PCMo bRT44 HC + tRT25 HC

Source: Own elaboration.

Figure 6 shows the comparison of the thermal performance of the different roof configurations evaluated in this study under the extreme weather conditions recorded on the selected days.

This figure illustrates how each configuration manages heat transfer by comparing the decrement factor (DF), time lag (TL), and thermal load, to identify the configurations that are the most efficient for thermal regulation.

Figure 6a, which corresponds to the coldest day, illustrates how each configuration responds to low outside temperatures. Configurations with PCM on the inside surface, such as C3 and C9, show a lower DF and a longer TL compared to the reference (C1). Notably, configuration C9, which combines insulation with an inside PCM layer, demonstrates a low thermal load, making it an efficient option under cold weather conditions. However, the PCM does not reach the melting point, so no significant phase change is observed.

This indicates that, under these circumstances, the PCM does not actively contribute to heat storage or release, limiting the effectiveness. On the other hand, in configurations belonging to Phase 2, where the PCM thickness was increased to 20 mm and 30 mm (C15 and C38), an additional improvement in thermal attenuation is observed. Configurations with greater PCM thickness are beneficial for reducing heat losses.

Finally, Phase 3 configurations, which evaluate the double PCM layer (C39-C52), exhibit superior thermal performance. Configurations like C39 and C45, which combine different types of PCM on both interior and exterior surfaces, show an extended TL and a low thermal load, proving to be the most effective for maintaining a stable indoor temperature under extremely cold weather.

In contrast, Figure 6b, which corresponds to the warmest day, shows that the PCM undergoes a phase change by absorbing heat when the outside temperatures rise. This demonstrates PCM's ability to regulate heat gain, providing more effective thermal protection. In this high-temperature scenario, configurations C7 and C13, which include PCM on the outside surface, effectively limit heat gain, as seen in the reduced thermal load. In Phase 2, increasing PCM thickness to 20 mm and 30 mm enhances performance under high-temperature conditions.

Configurations such as C28 and C34 show a significant reduction in thermal load, indicating that greater PCM thickness not only reduces heat losses but also limits heat gains on warm days. Phase 3 configurations, which include a double PCM layer, offer the best results. Configurations like C40 and C47 stand out for their ability to extend the time lag and reduce the thermal load, demonstrating their effectiveness in maintaining a comfortable indoor temperature under high-temperature conditions.

Based on the results shown in Figure 6, configuration C45, which incorporates a double layer of PCM with different types of PCM strategically placed on the inside and outside, stands out as the most efficient option for both cold and warm extreme weather conditions. The PCM selection was based on the melting temperature, with materials like RT25 HC for the interior and RT35 HC* for the exterior, allowing phase change across the relevant temperature range for the studied climate. This configuration shows a high capacity to retain indoor heat during the coldest day, due to the low decrement factor and long time lag, while also efficiently limiting heat gains during the warmest daytime and controlling the thermal load. The phase change in the PCM plays a crucial role, as it stores energy as latent heat during warm days and releases it when temperatures drop, something that polystyrene insulation cannot achieve. Due to the versatility and superior performance in both scenarios, configuration C45 emerges as the best option for maintaining thermal comfort and energy efficiency in the building.

Configuration C39, which also has a double layer of PCM, is ranked as the second-best option and offers a good balance between heat conservation and reduction of thermal gains. The third-best option is configuration C9, which combines thermal insulation with a single layer of PCM on the lower surface, standing out primarily for heat conservation during cold days. While the polystyrene acts as a constant barrier against heat transfer, PCM dynamically adapts to varying conditions during phase change, providing greater thermal inertia and improving energy efficiency under extremely fluctuating temperatures.

Configurations in Phase 2, such as C28 and C34, which include thicker layers of PCM (20 mm and 30 mm, respectively), also demonstrate good performance, particularly in reducing thermal loads on warm days. Finally, configurations in Phase 1 like C3 and C7, which use a 10 mm thick PCM, show acceptable performance but are less effective compared to the previously described configurations in attenuating heat loss and limiting thermal gain.

Configuration C2, which incorporates polystyrene insulation, shows moderate performance in thermal attenuation and thermal load management on both the coldest and warmest days. However, configurations that include PCM, such as C45 (double layer of PCM) and C39 (a layer of PCM on the inside and outside surfaces), show better performance under both extreme climate conditions.

On the coldest day, configurations with PCM not only provide better insulation to reduce indoor heat loss but also exhibit a longer time lag and lower thermal load compared to polystyrene. This occurs because, although the PCM does not undergo a phase change during the coldest day, the high thermal storage capacity still contributes to heat conservation. On the warmest day, the PCM also proves to be more efficient at limiting heat gain, offering more effective thermal regulation than polystyrene.

While polystyrene is a widely used and cost-effective insulation material, the results suggest that incorporating PCM instead can significantly enhance the roof's thermal performance, especially in climates with high temperature fluctuations. To optimize energy efficiency and thermal comfort, it is advisable to consider PCM inclusion rather than polystyrene in composite roof applications.

The appropriate hierarchical order to improve the thermal efficiency of the roof begins with adding a PCM layer. Configurations with a PCM layer have shown superior thermal regulation by retaining heat during cold days and effectively limiting heat gain during warm days. The next step is to increase the PCM layer's thickness, providing additional benefits such as increased thermal storage capacity, improved time lag, and further reduced thermal load.

Following this, adding insulation—while having a lesser impact than the PCM layer—remains an effective strategy for enhancing overall thermal efficiency. Finally, adding an extra PCM layer is the most advanced strategy, maximizing thermal efficiency by offering higher storage capacity, though this approach is more complex and expensive to implement. This procedure represents the most effective configuration for optimizing the roof's thermal performance under varying weather conditions.

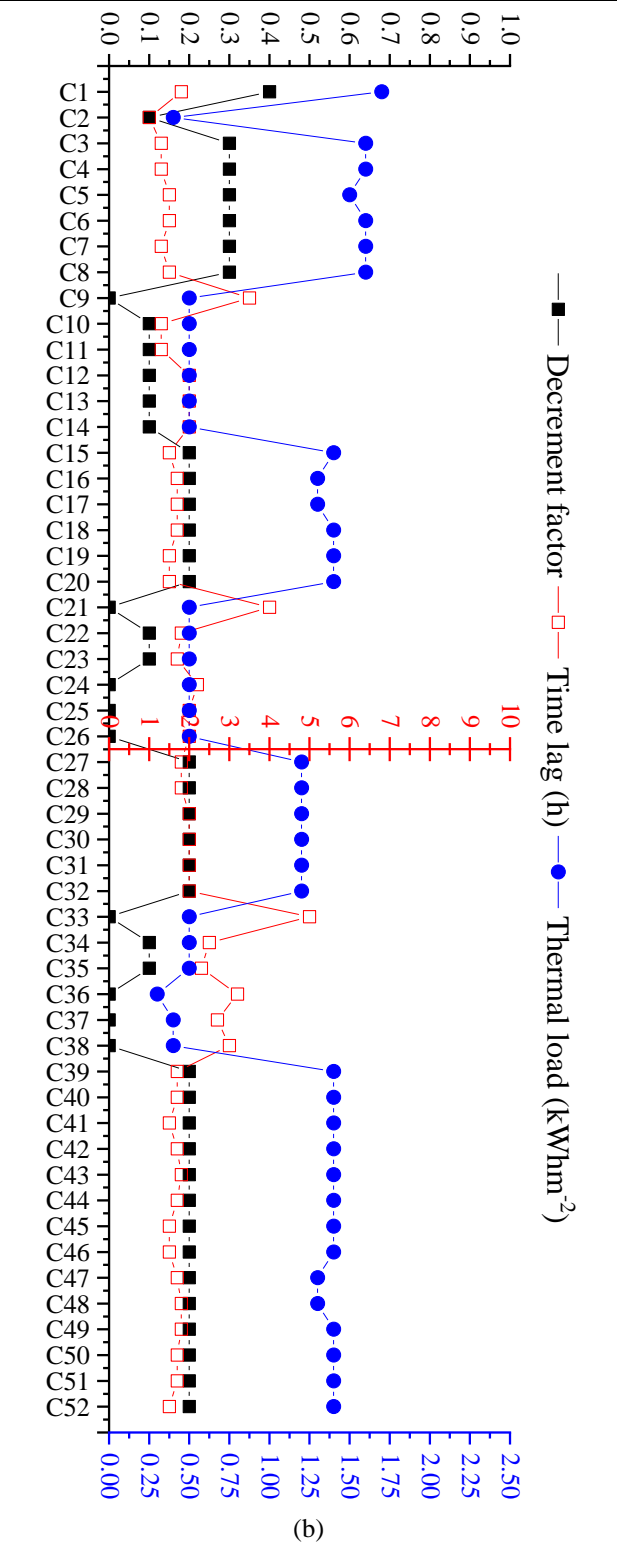
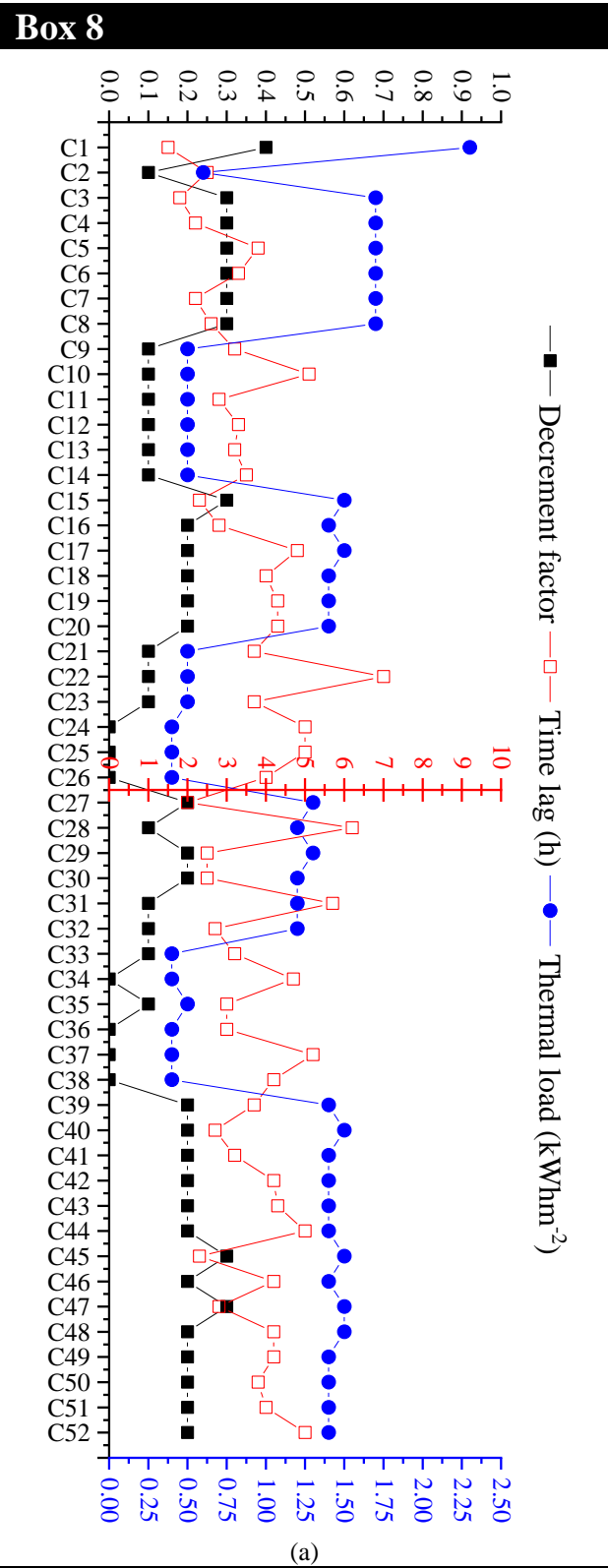


Figure 6
Comparison of the thermal performance on different roofs configurations under extreme weather conditions: (a) coldest day, (b) warmest day

Source: Own elaboration

Therefore, an optimal configuration is one that has a low DF, ideally below 0.2, which indicates an excellent capacity for attenuating outside thermal fluctuations and reducing heat transfer to the interior.

The TL should be appropriate for the weather conditions: a large TL, close to 10 hours, is desirable for warm climates to delay incoming heat, whereas a short TL, around 2-4 hours, is more beneficial for cold climates to allow incoming heat when outside temperatures are low. For thermal load, an efficient configuration should remain below 2.5 kWhm^{-2} , which reflects low energy consumption and a good capacity to maintain a comfortable indoor temperature.

Conclusions

In this study, the thermal performance of different roof configurations was evaluated, focusing on the integration of phase change materials (PCM) compared to traditional thermal insulation methods such as expanded polystyrene. Through numerical analysis, key parameters such as the decrement factor (DF), time lag (TL), and thermal load were analyzed under extreme weather conditions.

The results showed that configurations including a PCM, particularly those with a double layer or thicker PCM, demonstrated significantly better performance. Specifically, the optimal configurations achieved a DF below 0.2, a TL appropriate to the climate (between 2 and 10 hours), and a thermal load lower than 2.5 kWhm^{-2} . Configuration C45, which includes a double layer of PCM with melting temperatures of 25°C and 35°C , located on the inside and outside surfaces respectively, stood out as the most efficient for both the coldest and warmest days, even surpassing configurations with polystyrene insulation.

The comparative and hierarchical analysis of all configurations reveals that the addition of a PCM is the most effective strategy to optimize the thermal performance of roofs, followed by increasing the thickness of the PCM layer, the inclusion of insulation, and finally, the addition of an extra layer of PCM. These strategies progressively improve energy efficiency and indoor thermal comfort.

The comparison with extruded polystyrene showed that, although this material is still an effective and viable option in terms of costs, it does not offer the same level of thermal performance as a PCM, especially under extreme weather conditions.

The phase change capability of a PCM, which enables the material to absorb and release latent heat, is key to the superiority under these conditions, as it significantly improves the thermal inertia of the roof—a behavior that cannot be replicated by polystyrene. Therefore, for applications where thermal efficiency and comfort are to be maximized, the use of a PCM is recommended as an alternative or complement to traditional insulation options.

Finally, this study contributes to the energy efficiency field in construction by providing quantitative data and analysis to guide further investigations and practical applications. The inclusion of PCM in composite roofs not only improves thermal performance but also offers a sustainable solution to reduce energy demand in buildings. Future studies could explore the use of PCM in combination with other advanced materials, as well as extending their application to other types of constructions and weather conditions, thereby widening the possibilities for thermal optimization and energy savings.

Annexes

Declarations

The authors declare that no funds were received to support this research.

Conflict of interest

The authors declare no interest conflict. They have no known competing financial interests or personal relationships that could have appeared to influence the article reported in this article.

Author contribution

López Salazar, Samanta; Conceptualization, Methodology, Software, Writing – original draft preparation.

Simá, E.; Project administration, supervision.

Chagolla-Aranda, M.A.; Formal Analysis, Visualization.

Chávez-Chena, Y.; Writing – review & editing, Formal Analysis.

Availability of data and materials

The data supporting the findings of this study are available from the corresponding author upon reasonable request.

Funding

No funding was received to support this research.

Acknowledgements

López Salazar, Samanta acknowledges the National Council of Humanities, Sciences and Technologies (CONAHCYT) for the financial support given through her doctorate scholarship program (CVU: 918135 and GRANT NUMBER: 789202) as well as the Technological National Institute of Mexico (TecNM-CENIDET).

To Professor J. Xamán †.

Abbreviations

A	area, m^2
C_p	specific heat, $Jkg^{-1}K^{-1}$
CT	thermal load, $kWhm^{-2}$
DF	decrement factor
G	solar radiation, Wm^{-2}
q	heat flux per unit area, Wm^{-2}
t	time, s
T	temperature, $^{\circ}C$
TL	time lag, h
α^*	absortance
Δt	time step, s
ε	emittance
λ	thermal conductivity, $Wm^{-1}K^{-1}$
ρ	density, kgm^{-3}
ρ^*	reflectance
i	indoor environment/inside
s, i	inner surface
s, o	outdoor surface
o	outdoor environment/outside

References

Antecedents

López Salazar, S., Lima-Téllez, T., Yang, R., Simá, E., Hernandez-López, I., & Dong, L. (2023). [Comparative assessment of roofing strategies for thermal load reduction, energy efficiency, and CO₂ emission mitigation in a tropical climate](#). In P. Moreno-Bernal, P. Escamilla-Ambrosio, L. Hernandez-Callejo, S. Nesmachnow, D. Rossit, & C. Torres-Aguilar (Eds.), VI Ibero-American Congress of Smart Cities (pp. 208-222).

Basics

Somu, N., R, G. R. M., & Ramamritham, K. (2021). [A deep learning framework for building energy consumption forecast](#). *Renewable And Sustainable Energy Reviews*, 137, 110591.

Shove, E., Walker, G., & Brown, S. (2014). [Material culture, room temperature and the social organization of thermal energy](#). *Journal Of Material Culture*, 19(2), 113-124.

Bhamare, D. K., Rathod, M. K., Banerjee, J., & Arıcı, M. (2023). [Investigation of the Effect of Air Layer Thickness on the Thermal Performance of the PCM Integrated Roof](#). *Buildings*, 13(2), 488.

American Society of Heating and Refrigerating and Air-Conditioning Engineers, 680 ASHRAE Handbook of Fundamentals, American Society of Heating and Refrigerating and Air-Conditioning Engineers, Inc., 2009.

Swinbank, W. C. (1963). [Long-wave radiation from clear skies](#). *Quarterly Journal of the Royal Meteorological Society*, 89(381), 339-348.

Duffie, J. A., & Beckman, W. (2013). [Solar engineering of thermal processes](#). En John Wiley & Sons, Inc. eBooks.

Supports

Mejía, K. J., Del Mar Barbero-Barrera, M., & Pérez, M. R. (2020). [Evaluation of the Impact of the Envelope System on Thermal Energy Demand in Hospital Buildings](#). *Buildings*, 10(12), 250.

Wang, H., Chen, Y., Guo, C., Zhou, H., & Yang, L. (2024). [Study on optimal layout and design parameters of ventilated roof for improving building roof thermal performances](#). *Energy and Buildings*, 320, 114576.

Parikh, K., Mehta, S., Gajjar, C., Patel, H., & Patel, G. (2023). [Improving Roof Surface Temperature Control Using Heat-Reflective Inorganic Composition for Paint and Coating Application](#). *Journal Of Testing And Evaluation*, 52(2), 20230377.

Shrimali, R., & Agrawal, N. K. (2024). [Climate responsive insulation strategies: a comparative analysis for enhanced energy conservation and reduced environmental footprint in Indian urban contexts](#). *Environment Development And Sustainability*.

Piselli, C., Castaldo, V. L., & Pisello, A. L. (2019). [How to enhance thermal energy storage effect of PCM in roofs with varying solar reflectance: Experimental and numerical assessment of a new roof system for passive cooling in different climate conditions](#). *Solar Energy*, 192, 106-119.

Bhamare, D. K., Rathod, M. K., & Banerjee, J. (2020). [Numerical model for evaluating thermal performance of residential building roof integrated with inclined phase change material \(PCM\) layer](#). *Journal Of Building Engineering*, 28, 101018.

Arumugam, C., & Shaik, S. (2021). [Air-conditioning cost saving and CO2 emission reduction prospective of buildings designed with PCM integrated blocks and roofs](#). *Sustainable Energy Technologies And Assessments*, 48, 101657.

Qu, Y., Zhou, D., Xue, F., & Cui, L. (2021). [Multi-factor analysis on thermal comfort and energy saving potential for PCM-integrated buildings in summer](#). *Energy And Buildings*, 241, 110966.

Dardouri, S., Tunçbilek, E., Khaldi, O., Arıcı, M., & Sghaier, J. (2023). [Optimizing PCM Integrated Wall and Roof for Energy Saving in Building under Various Climatic Conditions of Mediterranean Region](#). *Buildings*, 13(3), 806.

Dardouri, S., Mankai, S., Almoneef, M. M., Mbarek, M., & Sghaier, J. (2023). [Energy performance based optimization of building envelope containing PCM combined with insulation considering various configurations](#). *Energy Reports*, 10, 895-909.

Dardouri, S., Tunçbilek, E., Khaldi, O., Arıcı, M., & Sghaier, J. (2023). [Optimizing PCM Integrated Wall and Roof for Energy Saving in Building under Various Climatic Conditions of Mediterranean Region](#). *Buildings*, 13(3), 806.

Yu, J., Dong, Y., Zhao, Y., Yu, Y., Chen, Y., & Guo, H. (2023). [Using phase change materials to alleviate overheating phenomenon of residential buildings in severe cold and cold regions of China](#). *Case Studies In Thermal Engineering*, 49, 103207.

Anter, A. G., Sultan, A. A., Hegazi, A., & Bouz, M. E. (2023). [Thermal performance and energy saving using phase change materials \(PCM\) integrated in building walls](#). *Journal Of Energy Storage*, 67, 107568.

Refahi, A., Rostami, A., & Amani, M. (2024). [Implementation of a double layer of PCM integrated into the building exterior walls for reducing annual energy consumption: Effect of PCM wallboards position](#). *Journal Of Energy Storage*, 82, 110556.

Zhang, M., Zheng, Y., He, Y., Jin, Z., Zhang, Y., & Shi, L. (2024). [Novel modular PCM wall board for building heating energy efficiency: Material preparation, manufacture and dynamic thermal testing](#). *Applied Thermal Engineering*, 124168.

Khaleghi, H., & Karatas, A. (2024). [Assessing the dynamic thermal performance of prefabricated wall panels in extreme hot weather conditions](#). *Journal Of Building Engineering*, 82, 108351.

Differences

Arumugam, C., Shaik, S., Roy, A., Kontoleon, K. J., Cuce, E., Shaik, A. H., Chakraborty, S., Alwetaishi, M., Cuce, P. M., & Gupta, M. (2024). [Analysis of the benefits of adopting roof sandwich panels integrated with PCM versus PUR to mitigate energy costs and carbon dioxide emissions](#). *Journal Of Energy Storage*, 77, 109947.


Zahir, M. H., Irshad, K., Shafiullah, M., Ibrahim, N. I., Islam, A. K., Mohaisen, K. O., & Sulaiman, F. A. (2023). [Challenges of the application of PCMs to achieve zero energy buildings under hot weather conditions: A review](#). Journal Of Energy Storage, 64, 107156.

Chagolla-Aranda, M., Simá, E., Xamán, J., Álvarez, G., Hernández-Pérez, I., & Téllez-Velázquez, E. (2017). [Effect of irrigation on the experimental thermal performance of a green roof in a semi-warm climate in Mexico](#). Energy And Buildings, 154, 232-243.

Analysis of the behavior of the seafloor of the mouth of the Grijalva river, Tabasco in the years 2012, 2017 and 2021

Análisis del comportamiento del fondo marino de la desembocadura del río Grijalva, Tabasco en los años 2012, 2017 y 2021

Aguilar-Ramírez, Ana María^a, Domínguez-González, Agustín^b, Utrera-Zárate, Alberto^c and Molina-Navarro, Antonio^d

^a Instituto Oceanográfico del Golfo y Mar Caribe •  LKK-4649-2024 •  0000-0003-2867-8254 •  811392
^b Instituto Oceanográfico del Golfo y Mar Caribe •  LJN-2742-2024 •  0000-0002-3199-5771 •  811473
^c Instituto Oceanográfico del Golfo y Mar Caribe •  LJR-4336-2024 •  0000-0002-6282-4449 •  365626
^d Instituto Oceanográfico del Golfo y Mar Caribe •  LLK-6696-2024 •  0000-0001-7949-8371 •  811437

CONAHCYT classification:

Area: Physics-Mathematics and Earth Sciences
Field: Earth and space sciences
Discipline: Hydrology
Subdiscipline: Hydrography

 <https://doi.org/10.35429/JCE.2024.8.19.1.10>

Article History:


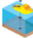

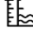







Received: January 24, 2024
Accepted: December 31, 2024

*  [\[marianaram1305@hotmail.com\]](mailto:marianaram1305@hotmail.com)



Abstract

Bathymetric surfaces created from bathymetric data obtained by Hydrographic Survey Brigades allow the representation of the relief of the seabed of a specific area and thus perform the analysis of its behavior. Therefore, the main objective is to characterize the seabed of the mouth of the Grijalva Tabasco River, by means of the difference surfaces and the TIN Model, and thus make a comparison between them, defining their variability as a result of sedimentation. The bathymetries of the hydrographic surveys that were considered for the study were those carried out in 2012 with the R2Sonic multi-beam echosounder, in 2021 with the Hydrotrac II ODOM single-beam echosounder and in 2021 with the Geoswathplus Compact multibeam echosounder, processing the data obtained with the hydrographic programs Caris Base Editor 5.5 and Hypack Software version 17.0 2021, obtaining the bathymetric surfaces of each year mentioned. The results obtained are that there are areas in the lateral parts of the mouth with a higher concentration of sediment, forming a coastal bar 2,500 m long by 612 m wide that reduces the depth to 1.8 m. In addition, it was determined that the period of greatest presence of rain and drag of material was the month of May to November. The above allows the implementation of actions to guarantee the safety of navigation of those larger vessels that sail towards the port of Frontera Tabasco.

GOALS	METHODOLOGY	CONTRIBUTIONS
 Investigating the Seabed by Means of Bathymetry	 Carrying out Bathymetry using echo sounders	 Provide a port for any type of Navigation
 Identification of Channel Depths	 Hydrographic data storage and purification	 Schedule Port Dredging Tasks
 Comparing different Measuring Equipments	 Comparison of data from surveys carried out in other years	 Provide Navigation Security
	 Determination of difference indicators by means of Software	 Contribute to Nautical Cartography

Bathymetric surfaces, Depth, Sedimentation

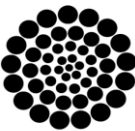
Resumen

Las superficies batimétricas creadas a partir de datos batimétricos obtenidos por las Brigadas de levantamientos Hidrográficos permiten representar el relieve del fondo marino de un área específica y así realizar el análisis del comportamiento de este. Por ello el objetivo principal es caracterizar el fondo marino de la desembocadura del río Grijalva Tabasco, por medio de las superficies de diferencias y Modelo TIN, y así realizar una comparación entre ellas, definiendo su variabilidad por consecuencia de la sedimentación. Las batimetrías de los levantamientos hidrográficos que se consideraron para el estudio fueron las efectuadas en el año 2012 con el ecosonda multihaz R2Sonic, del 2021 con ecosonda monohaz Hydrotrac II ODOM y del año 2021 con la ecosonda Multihaz Geoswathplus Compact, procesándose los datos obtenidos con los programas hidrográficos Caris Base Editor 5.5 y Software Hypack versión 17.0 2021, obteniéndose las superficies batimétricas de cada año mencionado. Los resultados obtenidos es que existen áreas en las partes laterales de la desembocadura con una concentración mayor de sedimento, formando una barra litoral de 2500 m de largo por 612 m de ancho que reduce la profundidad hasta 1.8 m. Además, se determinó que el período de mayor presencia de lluvia y arrastre de material fue el mes de mayo a noviembre. Lo anterior permite la implementación de acciones para garantizar la seguridad de la navegación de aquellas embarcaciones de mayor porte que navegan hacia el puerto de Frontera Tabasco.

OBJETIVOS	METODOLOGÍA	CONTRIBUCIONES
 Investigar el fondo marino por Medio de Batimetrías	 Realización de Batimetrías por medio de Ecosondas	 Prover un puerto para cualquier tipo de Navegación
 Identificación de la profundidades del canal	 Depuración Almacenamiento de datos y hidrográficos	 Programar las tareas de dragado del puerto
 Comparar los Diferentes equipo de Medición	 Comparación de Datos de levantamientos realizados otros años	 Proporcionar seguridad a la navegación
	 Determinación de indicadores de diferencia por medio de software	 Contribuir a la Cartografía Náutica

Superficies batimétricas, Profundidad, Sedimentación

Citation: Aguilar-Ramírez, Ana María, Domínguez-González, Agustín, Utrera-Zárate, Alberto and Molina-Navarro, Antonio. [2024]. Analysis of the behavior of the seafloor of the mouth of the Grijalva river, Tabasco in the years 2012, 2017 and 2021. Journal Civil Engineering. 8[19]-1-10: e40819110.



Introduction

Bathymetry is limited to the study of ocean depth. In the topographic-hydrographic field it relates to surveys of underwater surfaces. In the field, the surveyor focuses on obtaining heights; in the bathymetric survey, depths are acquired. The purpose of bathymetry is to obtain the XYZ coordinates of points on the seabed. Depth identification is called sounding and consists of calculating the vertical distance between the bottom surface and the specified water level (Ballestero and García, 2010).

A river is defined as a watercourse that is fed from various sources, such as rainfall, land runoff or snowmelt, and flows from its source to its mouth in the sea, lake or other body of water. It is worth mentioning that it is in its final part where the river sediments the materials dragged in the basin (Valdivielso, 2022).

Basile (2018) in his book 'Sediment transport and morphodynamics of alluvial rivers' defines this concept as the granular solid material found in the bed of a river, basin, lake or coast which has been transported and deposited by the action of marine currents or other transport methods throughout its morphological evolution.

Silt is a deposit of sediment, which is carried by water and accumulated in riverbeds, dams, underground reservoirs, wetlands, lagoons, estuaries, navigation channels, harbours, etc., is called silt. The cause of siltation is a decrease in the velocity of the current and a corresponding decrease in the amount and size of solid material that can be carried in suspension. Thus, siltation is the phenomenon in which sediment accumulates and results in the transformation of the environment (Carbajal, 2014).

Among the equipment used for the hydrographic surveys were: the R2Sonic Multibeam echo sounder, Hydrotrac II single-beam echo sounder and the Geoswathplus Compact 250 KHz interferometric Multibeam echo sounder.

The data acquired by means of this equipment provides a bathymetric surface with a resolution of even less than one metre, resulting in a high-resolution configuration of the seabed.

The single beam echo sounder, this type of electronic instrument has a transducer that generates a single acoustic pulse (all the acoustic energy transmitted is confined to a single beam that has a shape similar to a cone) that reaches the seafloor, so it is not possible to obtain 100% coverage of the bottom, being necessary to make lines at a certain distance without being able to know what is between them (sectors without information) (Ballestero, 2010).

The use of multibeam echo sounders for bathymetry has become the most developed and accurate technology available today. This system, which complies with the International Hydrographic Organisation (IHO) standards, provides accurate and complete knowledge of the depth and morphology of the seabed. This Multibeam system consists of a set of sounders that emit several narrow beams of sound in different directions, arranged in a fan-shaped pattern that sweep transversely in the direction in which the vessel is moving (Basile, 2018).

The data acquired by means of this equipment provides a bathymetric surface with a resolution of even less than one metre, resulting in a high-resolution configuration of the seabed. Speaking specifically of ports that are located on the banks of a river, one of their greatest obstacles is fluvial sedimentation, a process that originates from erosion and sediment movement, which produces the deposition of particles, their compaction and consolidation (Arreguín, Preciado, Val and Arganis, 2021).

One of the elements that enable the functionality of ports is the access or navigation channel, the path that safely guides vessels on their arrival, for which it must have sufficient depth and width to guarantee manoeuvres (Rosas, 2012).

Among its characteristics as a fiscal dock for the arrival and protection of vessels, it has a length of 300 m long, 15 m wide, 2.4 m high and an average depth of 6 m (Secretaría de Marina, 2022).

Figure 1 shows the facilities of the port of Frontera in the state of Tabasco, one of the main ports on the banks of the Grijalva River, which has the potential to increase national maritime development and become the hub of support services for oil platforms on the coast of the state of Tabasco, as well as the promoter of coastal and riverine development. Its focus is the oil and fishing industry, managing diverse activities such as the embarkation of passengers and materials to the platforms in the Gulf of Mexico, berthing of vessels and sale of services (Gobierno del estado de Tabasco, 2022).

Box 1



Figure 1
Inner dock of the port of Frontera Tabasco

Source: <https://www.apitab.com.mx>

In accordance with the above, the case of the Grijalva river basin is mentioned, located in the Mexican Southeast (SE) with a large coverage in the states of Chiapas and Tabasco, one of its main ports being the city of Frontera, located on its banks, approximately 10 kilometres (km) from its mouth. As a relevant fact, the depth at the mouth and the navigation channel of the Grijalva River is maintained by dredging, due to the silt generated by the combination of sediment input from the river and coastal dragging, leading to the formation of a bar (plug) with average depths that vary from 2.5 m to 3 m (Comisión de Planeación para el Desarrollo del Estado de Tabasco, 2019).

The Grijalva basin (Figure 2) has a surface area of about 58,025 km²; it comprises in Guatemala a little less than a tenth of its surface area and the rest continues in Mexico (Plascencia *et al*, 2014).

Its extreme geographical coordinates are between 89.6° to 94.5° W, and 15.3° to 18.7° N. It mainly encompasses the Mexican states of Chiapas and Tabasco (World Meteorological Organization, 2006).

This basin can be described in its simplest form as a high mountainous area (Guatemala and Chiapas) where water runoff begins and concentrates in a well-defined channel, which crosses the Northern Chiapas Mountains, receiving water from other tributaries and flows out towards the lower parts of the Tabasco plain, frequently flooding it, and finally flows into the Gulf of Mexico (Plascencia *et al*, 2014).

Box 2

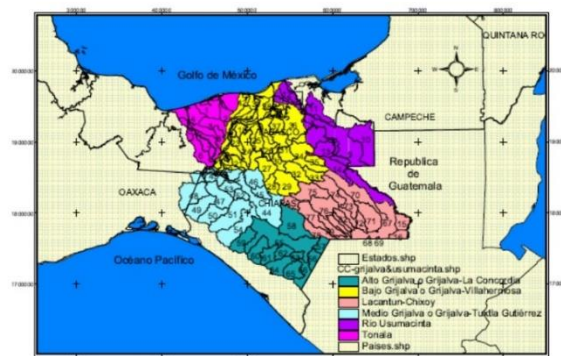


Figure 2
Division of the Grijalva basin

Source: Official Journal of the Federation (2010)

Methodology

This research was carried out by means of bathymetric data, acquired in accordance with the established bottom coverage standards (IHO, 2020) at the mouth of the Grijalva River, Tabasco in the years 2012, 2017 and 2021, with the R2Sonic, Hydrotrac II ODOM) and GeoSwath Plus Compact multibeam echo sounder where their technical specifications are detailed in Table 1.

Box 3

Table 1
Specification System for the Konigsberg R2Sonic, Hydrotrac II ODOM and GeoSwath Plus Compact echo sounders

Features	Echo sounders		
	Hydrotrac II ODOM	R2Sonic	GeoSwath Plus Compact
Type	Monohaz	Multihaz	Multihaz
Frequency	Operator selectable via menu 24, 28, 33, 40, 100, 120, 200, 210 and 340 kHz	170 kHz-450 kHz & 700 kHz (optional)	250 kHz
Maximum depth below transducer		400m±**	100 m
Maximum sweep width	600 m o 1800ft.	100 m	390 m
Maximum coverage	-	-	Up to 12 times the depth
Resolution	ft/.01 m	-	3 mm
Width of the two beams (Horizontal)	-	10° to 160°	0.75 °
Pulse length	Positioning accuracy: 0.63 metres, CEP 50%. - 1.31 metres, 95%. - Typical dynamic accuracy 3 to 5 metres	15 µs-1115 µs	64 us a 448 uS
Maximum refresh rate	-	-	30 times per second (range dependent)
Transducer dimensions	368 mm x 419 mm x 203 mm	280 x 170 x 60 mm	360 x 352 x 150mm
Transducer weight	10.2 kg	2.4 kg	20 kg
Dimensions of the cover unit	-	480 x 109 x 190 mm	135 x 400 x 342 mm

Source: Konigsberg R2Sonic , Hydrotrac II ODOM and GeoSwath Plus Compact operating manuals

Initially, the Hypack 2021 programme in its version 1.21 was used to generate bathymetric surfaces for each epoch, consecutively and through one of the software tools called "TIN model" (Triangle Irregular Network), data processing was carried out to determine the volume of sediments.

The "TIN model" generates a type of vector-based digital geographic data that is constructed by triangulating a set of vertices (points). The vertices are connected with a series of edges to form a network of triangles. In other words, they connect three soundings to make a triangular "face" (Figure 3). The faces can then be used to represent a bathymetric surface detailing volumes created from these triangles.

Box 4

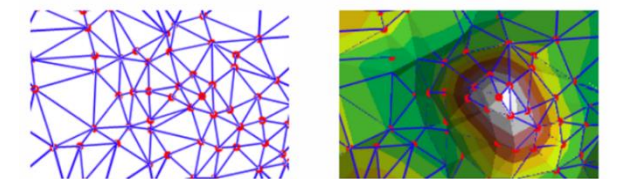


Figure 3
Creation of TIN models

Source: Hypack (2021)

The result after the creation of the TIN model (Figure 4), is the comparison between two bathymetric surfaces that overlap exactly, generating a report which, from the triangle network, determines the volume of sedimentation added and removed, in this case at the mouth of the Grijalva river at the manoeuvring dock of the port of Frontera, Tabasco.

Box 5

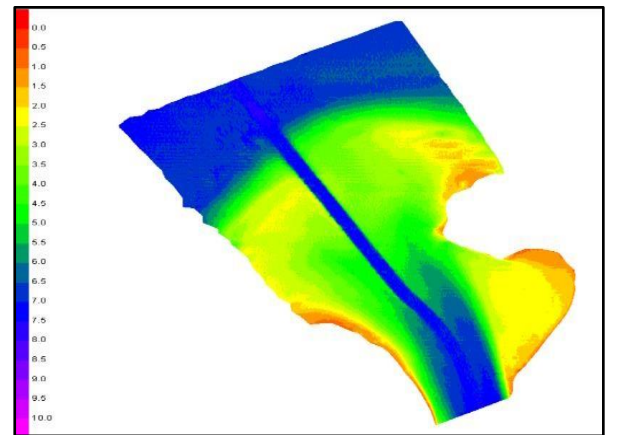


Figure 4
TIN model of the bathymetric data for the year 2021

Source: Hypack (2021)

On the other hand, with the CARIS Base Editor program, the bathymetric surfaces were generated from the same sounding data with which the TIN models were made in Hypack, with the intention of maintaining the same information used and to serve as a point of comparison. The bathymetric surfaces were generated through ‘XYZ’ files (Figure 5), which contain the information on coordinates and depths, using the WGS84 reference datum.

Box 6

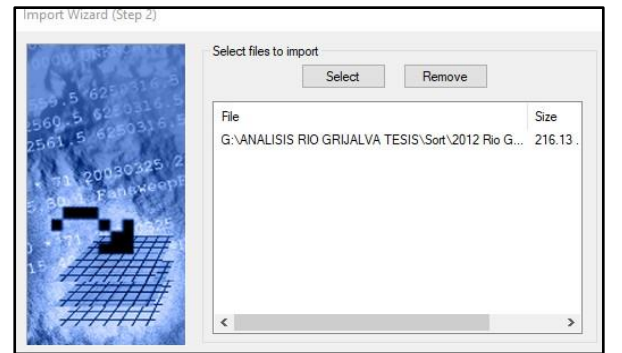


Figure 5
Data in XYZ format, loaded in the ImportWizard

Source: Own elaboration with Caris software Base Editor 5.5 module (2022)

The subsequent result was a three-dimensional bathymetric surface (Figure 6) for each year (2010, 2018 and 2021), where details of the seabed can be seen, distributed uniformly and by colour, in order to obtain a clear idea of the configuration of the area in question.

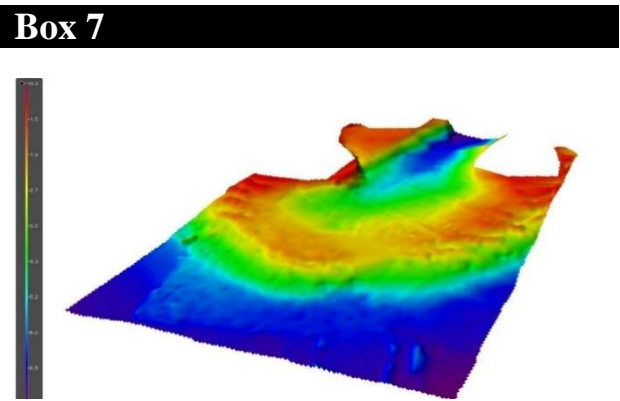


Figure 6
Grid-type base surface of the Grijalva river mouth in 2012

Source: Own elaboration with Caris software
Base Editor 5.5 module (2022)

Once the bathymetric surfaces have been generated for each year, the CARIS Base Editor program has a tool called "coverage difference" which, by interpolating two surfaces, generates a third one, which is the result of the difference between the two surfaces.

Results

Caris module Base Editor 5.5

Difference surfaces

With the base surfaces described above, the Caris Base Editor 5.5 software module allows the creation of a difference surface, which is a tool for recognising variations in the seabed related to the depth of a given space. A 200 m x 200 m grid was superimposed for the establishment of reference points for the analysis of the difference surfaces, allowing a better comparison between the two established periods. In addition, the "Rainbow Map" colour palette was maintained, with negative values (red) indicating sediment accumulation and positive values (blue) highlighting areas of erosion. Finally, the study area was divided into three sections: the offshore part of the mouth, the central part and the upstream end.

In the case of the difference surface of the year 2012-2017 (Figure 7), 30 reference points were taken as a sample, selecting 15 points representative of the aforementioned sections, indicating the depth and the difference between them.

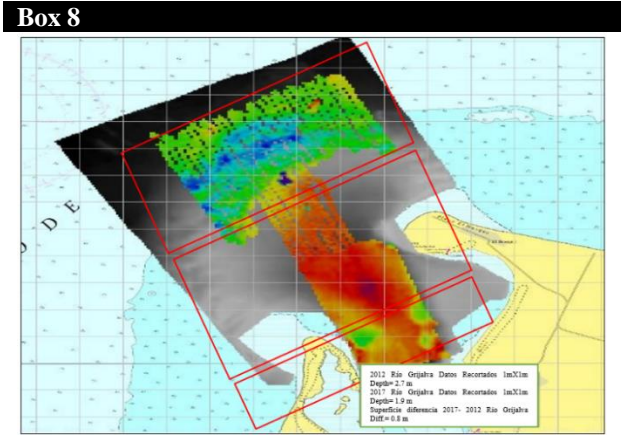


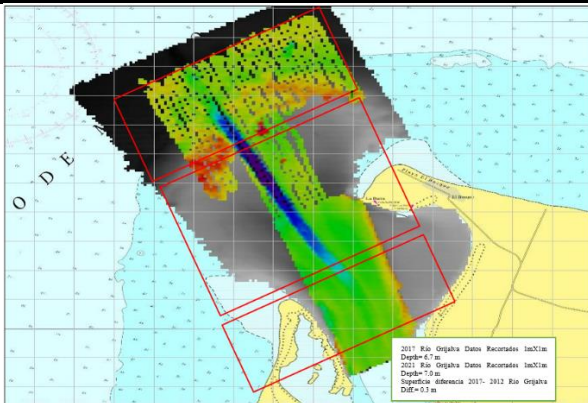
Figure 7
Area difference between the years 2012-2017

Source: Own elaboration with Caris software Base
Editor 5.5 module (2022)

Analysing Figure 7, from the offshore part, we can see in blue and green a maximum increase in depth varying from 3.4 to 6.6 m (3.2 m difference) and a minimum increase from 2.4 to 3.8 m (1.4 m difference), i.e. the phenomenon of seabed erosion occurred in that area. As one moves towards the central part, a decrease in depth is observed, going from 4.2 to 3.8 m (0.4 m difference) as a minimum and from 5.8 to 4.8 m (1 m difference) as a maximum, this being due to the siltation present in the area. This phenomenon becomes constant towards the upstream part of the mouth, especially in the navigation channel, with a greater range in the decrease in depth from 2.7 to 1.9 m (0.8 m difference) as a minimum and from 4.3 to 3.3 m (1 m difference).

For the analysis of the difference surface of the year 2017-2021 (figure 8), 15 representative points were selected from 29 reference points, together with the depth data in the years 2017, 2021 and the difference between them.

Box 9

**Figure 8**

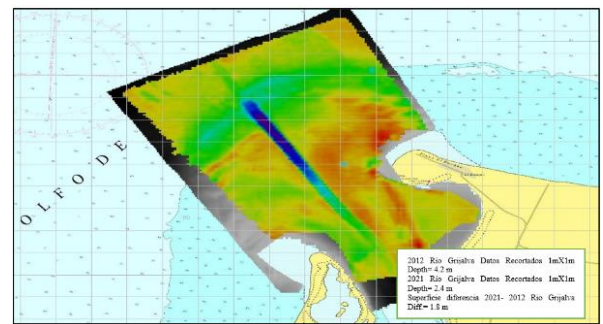
Difference area between the years 2017-2021

Source: Own elaboration with Caris software Base Editor 5.5 module (2022)

Analysing the previous figure and comparing it with Figure 9, a greater uniformity in the colour scale is observed, highlighting the green colour, indicating that the depth of the seabed remained constant; however, some orange areas stand out, revealing accumulation of sediment. Speaking of depths in the outer part, they varied from 6.4 to 7.4 m (1 m difference) as a maximum and from 5.9 to 6 m (0.1 difference) as a minimum; in other words, the seabed showed erosion in that part. However, if we move towards the central part of the mouth, we can clearly see the coastal bar that is beginning to form as a result of sedimentation, changing from 4.0 to 2.3 m (1.7 m difference) as a maximum and from 3.2 to 3.0 m (0.2 m difference) as a minimum. It should be noted that the bathymetry of the year 2021 is after the dredging of the Dutch company Van Oord in this area, therefore, it is not surprising that the part of the mouth upstream presents an increase in depth, going from 4.9 to 6.0 m (1.1 m difference) as a maximum and from 7.2 to 7.3 m (0.1 m difference) as a minimum. This difference surface shows the benefits of applying proper maintenance based dredging works.

Finally, a difference surface (Figure 9) was created between the years 2012 and 2021, showing a predominance of yellow and orange, i.e. the phenomenon of sedimentation prevailed in the study area, forming a kind of barrier with a tendency towards the eastern side of the mouth. In terms of depths, there was a decrease in average depth of 0.3 m in the area of the river, which was caused by the phenomenon of sedimentation.

Box 10

**Figure 9**

Area difference between the years 2012-2021

Source: Own elaboration with Caris software Base Editor 5.5 module (2022)

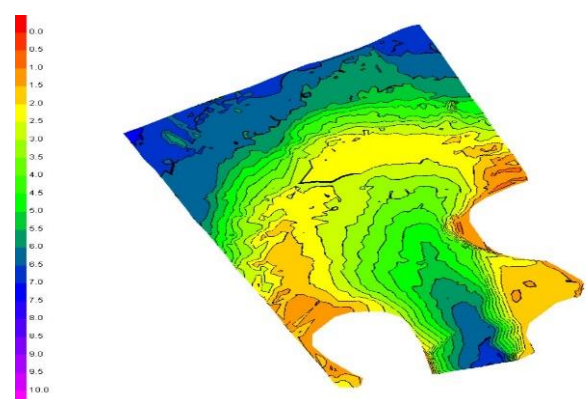
Hypack Version 2021

TIN models

Below are the TIN Models for the years 2012, 2017 and 2021, elaborated with the aforementioned programme, based on the information obtained by the Hydrographic Survey Brigades, using the bathymetric and positioning equipment described in the previous chapter. As a preamble, it should be mentioned that the input files were in XYZ format, as required by the system.

Figure 10 shows the TIN Model that was created using the 2012 bathymetric data in XYZ format as base files. For this model a colour scale was attached to reference the depths in a range of 0.0 to 10.0 m with a spacing of 0.5 m; the option to observe the isobaths was also selected.

Box 11

**Figure 10**

TIN model of bathymetric data for the year 2012

Source: Own elaboration in the Hypack Version 2021 (2022)

Similarly, Figure 11 shows the TIN Model that was created using the bathymetric data of the year 2017 in XYZ format as base files. For this model, the same colour scale of the previous model in a range of 0.0 to 10.0 m was attached, in order to have the same reference in terms of depths.

Box 12

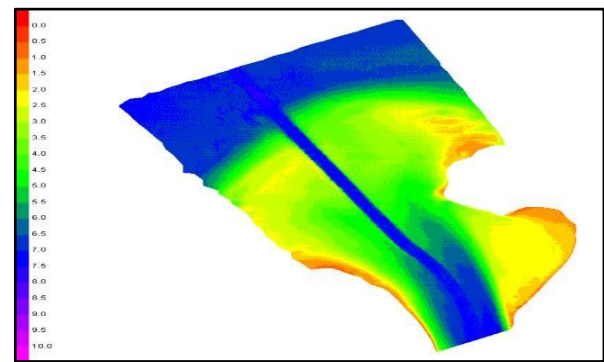


Figure 11
TIN model of bathymetric data for the year 2017

Source: Own elaboration in the Hypack Version 2021 (2022)

Finally, Figure 12 shows the TIN Model considering the bathymetry of the year 2021. The same characteristics annexed to the previous models were taken into account. It is worth mentioning that this model is defined by being elaborated with multibeam data, i.e. it has a large amount of bathymetric information that allows visualising how the seabed of the study area is constituted.

Box 13

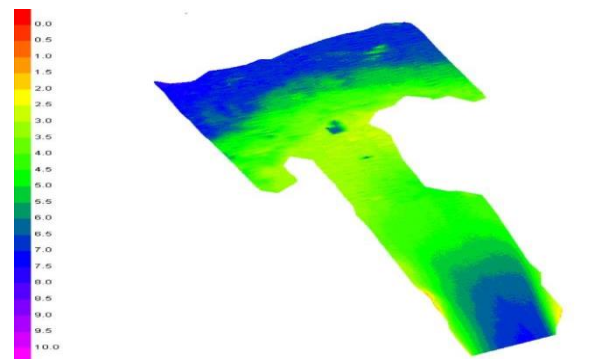


Figure 12
TIN model of bathymetric data for the year 2021

Source: Own elaboration in the Hypack Version 2021 (2022)

Calculation of TIN-to-Level volumes

According to the Hypack Version 2021 manual, for the volume calculation it is indicated that the Main File to be entered is the oldest or pre-dredging file and the Additional File should be the most recent or Post-dredging file.

Figure 13 shows the results obtained after the calculation of the TIN- a- LEVEL volume of the XYZ difference file for the years 2012 and 2017. Analysing the above Figure, we can state that the maximum difference detected was 5.13 m and the minimum was 1.61 m, with an average difference of 0.82 m. The number of triangles created for the TIN Model was 7,100,188. A sedimented area of 2,521,400.7 m² and a gained volume of 3,320,165.6 m³ was determined; the eroded area was 1,051,637.3 m² and a lost volume of 388,276.2 m³; the calculation of the net sedimented volume yielded a result of 2,931,889.4 m³. Considering that the sea surface area surveyed is 10,433,028.3 m², this indicates an average of 0.28 m³ of sediment per m².

Furthermore, if we take into account the seasonality of the bathymetric data, we can deduce that in the study area an amount of 586,337.88 m³ of sediment was deposited per year.

Box 14

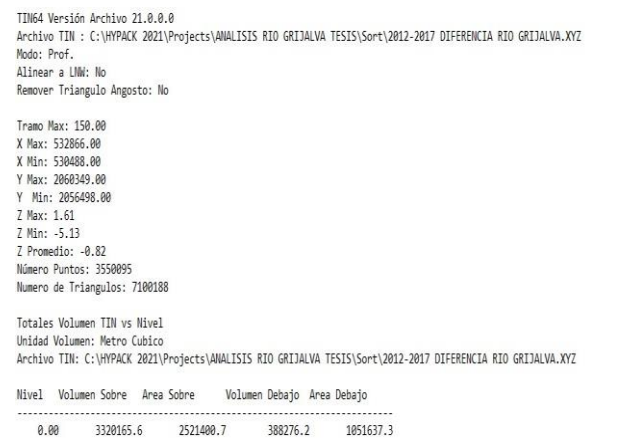


Figure 13
Results of the TIN-to-Level volume calculation between 2012 and 2017

Source: Own elaboration in Hypack Version 2021 (2022)

Figure 14 shows the results obtained after the calculation of the TIN-at-LEVEL volume from the XYZ difference file for the years 2017 and 2021. With the information shown, it is concluded that the maximum difference detected was 3.77 m and the minimum was 4.90, with a mean of 0.31 m.

The number of triangles created for the TIN Model was 7,590,058. A sedimented area of 2,416,914.2 m² and a gained volume of 1,889,308.5 m³ was determined; the eroded area was 1,401,269.3 m² and a lost volume of 734,675.2 m³; the calculation of the net sedimented volume yielded a result of 1,154,633.3 m³.

With a study area of 10,433,028.3 m², an average of 0.11 m³ of sediment per m² is obtained, which is much lower compared to the previous period; this can be related to the mm of accumulated rainfall and runoff in the basin, as well as other external factors such as marine currents, tides and wind, etc. Considering the temporality between the bathymetric data, it is deduced that in the study area an amount of 288,658.325 m³ of sediment was accumulated per year.

Box 15

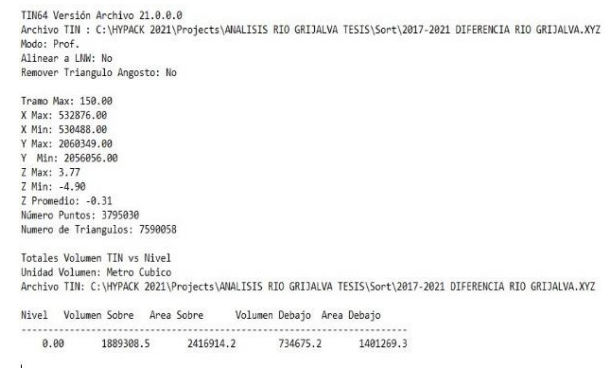


Figure 14
Results of the TIN-to-Level volume calculation between 2017 and 2021

Source: Own elaboration in Hypack Version 2021 (2022)

Conclusions

Through the analysis and processing of the bathymetric information obtained in the hydrographic surveys of 2012, 2017 and 2021, it can be concluded that there is a variation in depth as a result of sedimentation and precipitation in the basin.

However, it is important to mention that there are other external factors that intervene in the decrease in depth and that should be taken into account in future research, such as marine currents and periodic tidal movements. This was established by processing the bathymetric information in the hydrographic software Caris and Hypack, and the following was determined.

Firstly, using the hydrographic programme Caris Base Editor 5.5 module and the corresponding bathymetries, difference surfaces were created that allowed an adequate comparison of depths. For a more detailed analysis, control points were set up in both programmes to ensure a controlled and organised measurement. It was found that between 2012 and 2021 the study area showed constant sedimentation in the central part and upstream of the mouth, with the formation of a littoral barrier 2,500 m long by 600 m wide and a drastic decrease of the operational draught in certain areas of the access channel of up to one and a half metres. This dynamic of the seabed does not guarantee the safety of larger vessels that would allow for port development in Frontera.

Secondly, it was determined that the longest period in which there was the greatest volume of sediment was between 2012 and 2017, when it was calculated at 2,931,889.4 m³; this is related to the variable rainfall that was greater in the same period due to the large presence of meteorological phenomena.

Among the benefits of the Hypack programme is the creation of the TIN models of the XYZ difference files, which, based on a reference, made it possible to visually analyse the areas of the navigation channel where sedimentation forms sandbanks that represent a danger to ships. It was noted that, due to the geomorphology of the river delta and the marine currents, the material tends to be deposited on the left bank of the study area.

One of the problems encountered was the type of bathymetric data being compared. When using bathymetric data from 2012 and 2017, the data is considered to have gaps or blanks between the surveyed lines, therefore, maximum confidence in the results obtained was not guaranteed.

Recommendations

In view of the above conclusions, a series of recommendations are described with which one of the specific objectives of the present investigation is fulfilled in view of the problem of siltation and change of depth at the mouth of the Grijalva river.

To ensure the use of Multibeam echo sounders in the subsequent hydrographic survey in the study area, which would guarantee more bathymetric information and a better analysis of the dynamics of the seabed. In addition, consideration should be given to the implementation of an Annual Hydrographic Survey Plan and Programme for the river delta in question, as this would allow to determine how the loss of depth is carried out and thus communicate the operational draft of the access channel to vessels.

Implementation of structures known as breakwaters on the sides of the mouth, which would prevent the participation of sea currents in the phenomenon of siltation, which is one of the variables that should be included when analysing the behaviour of the seabed in subsequent studies. This reinforcement at the entrance of the river would reduce the constant application of maintenance works and a saving for the port administrations at the moment of guaranteeing the operational draught of the area.

It is recommended to implement an adequate long-term dredging plan and programme prior to the construction of the breakwaters, which together with the Multibeam bathymetry, will guarantee that the depth in the access channel is adequate for navigation of larger vessels and therefore a notable increase in the activities registered by the port of Frontera, Tabasco.

That the three levels of government, private companies and academic institutions coordinate to carry out similar studies not only of the mouth, but of the entire Grijalva-Usumacinta river basin, since the process of the present investigation was halted on several occasions due to lack of information. This would allow for better quality in future research and, consequently, a more solid basis for finding the most viable and adequate solutions to the problem of siltation.

Conflict of interest

The authors declare that they have no conflicts of interest. There are no known competing economic interests or personal relationships that could have influenced the article reported in this paper.

Authors' contribution

The contribution of each researcher in each of the points developed in this research was defined based on:

Aguilar Ramírez, Ana María: Contributed to the project idea, method and research technique. She carried out the data analysis and wrote the article.

Domínguez González, Agustín: Systematised the background to the article. He supported the data cleaning and processing. He also contributed to the drafting of the article.

Utrera Zarate, Alberto: Contributed to the research design, the type of research and the approach.

Molina Navarro, Antonio: Worked on the determination of statistical data differences and systematisation of results. He also collaborated on the writing of the paper.

Availability of data and materials

The bathymetric survey data for the years 2012, 2017 and 2021 were provided by the Dirección General Adjunta de Oceanografía, Hidrografía y Meteorología (DIGAOHM) through the Dirección de Hidrografía belonging to the Secretaría de Marina, which together with the Instituto Oceanográfico del Golfo y Mar Caribe allowed the processing of this information.

Funding

The research did not receive any funding.

Acknowledgements

The Secretary of the Navy for providing the necessary data for this study, their willingness and support were fundamental to the development and quality of this research.

Casimiro Aguilar Ramírez of the Interamericano Centro Lingüístico A.C. for his invaluable support in the translation of this work into English.

References

Basics

Gobierno del Estado de Tabasco. (2022). Administración Portuaria Integral de Tabasco. Obtenido de <https://www.tabasco.gob.mx>

Comité de Planeación para el Desarrollo del estado de Tabasco. (2019). Programa Institucional de la Administración Portuaria Integral Tabasco.

M. González Espinosa, & M. C. Brunel Manse, Montañas, pueblos y agua. Dimensiones y realidades de la cuenca Grijalva (págs. 29-79). Ciudad de México, México: Juan Pablos Editor.

Valdivielso, A. (2022). [IAGUA](#).

[Apitab](#) (2024) obtenido de <https://www.apitab.com.mx/>

Soporte

[Hypack](#). 2021. [Hypack](#). Obtenido de <https://www.Manual de software Hypack y Hysweep> (Acceso el 17 de junio de OHI. 2020. “Normas de la OHI para los Levantamientos Hidrográficos publicación S-44”. Mónaco Bureau Hidrográfico Internacional.

Secretaría de Marina. (2022). [Frontera, Tabasco](#). DIGAOHM, Hidrografía.

Ballester Mora, L., & García Sala, D. (2010). Estudio batimétrico con ecosonda multihaz y clasificación de fondos. Universidad Politécnica de Catalunya. Escola Politécnica Superior d' Edificació de Barcelona, Barcelona, España.

Differences

Organización Meteorológica Mundial. (2006). [Gestión Integrada de Crecientes-Caso de estudio- México: Rio Grijalva](#). Programa Asociado de Gestión de Crecientes.

Rosas Carrillo, E. G. (2012). [Dragado en puertos mexicanos](#). [Dragado en puertos mexicanos](#).

Discussions

Basile, P. A. (2018). [Transporte de sedimentos y morfodinámica de ríos aluviales](#). Rosario: UNR Editora. Editorial de la Universidad Nacional de Rosario

Plascencia Vargas, H., González Espinosa, M., Ramírez Marcial, N., Álvarez Solís, D., & Musálem Castillejos, K. (2014). [Características físico-bióticas de la cuenca del Río Grijalva](#).

Carbajal Evaristo. 2014. “Evaluación del impacto del azolvamiento en La Laguna Cerritos a partir de la canalización del Río Cintalapa Vol. 1 P. 8-116.

Influence of particle size on soil consolidation processes

Influencia del tamaño de partículas en los procesos de consolidación de los suelos

Rojas, Eduardo^a, Reynoso, Eva Guadalupe^b and Arroyo, Hiram^{*c}

^a Universidad Autónoma de Querétaro • JLX-6216-2023 • 0000-0001-6042-505X • 3312
^b Universidad de Guanajuato • 0009-0008-5359-6238
^c Universidad de Guanajuato • DVZ-5627-2022 • 0000-0002-8343-698X • 349586

CONAHCYT classification:

Area: Engineering
Field: Engineering
Discipline: Civil Engineering
Subdiscipline: Transport

<https://doi.org/10.35429/JCE.2024.8.19.4.7>

Article History:

Received: January 20, 2024
Accepted: December 31, 2024

* [\[h.arroyo@ugto.mx\]](mailto:h.arroyo@ugto.mx)



Abstract

Settlements in infrastructure works such as roads, bridges and highways are often underestimated due to a lack of understanding of the phenomena associated with volumetric deformations of soils. This can lead to significant damage to the structures built on them and in some cases it will be necessary to demolish them or render them useless. This study shows the difference in long-term deformations that occur between two types of soil depending on their particle sizes. The study shows the results of two soil samples subject to consolidation, with identical initial moisture content, but with a different particle size distribution. It also shows how the consolidation process occurs and the direct influence of particle size on the long-term volumetric reduction process of soils.

Objectives	Methodology	Contribution
<ul style="list-style-type: none">Subject soil samples to secondary consolidation processes.Produce samples of different particle sizes to undergo consolidation processes.Qualitatively and quantitatively analyze secondary consolidation in samples with different particle sizes.	Soil samples were obtained from a T2 industrial kaolin sufficiently fine to exhibit volumetric deformations by primary and secondary consolidation. This soil was mixed with inert material to make samples with a different granulometry and to analyze the differences that occur in volumetric deformations with different granulometries.	The experimental results derived from the analysis of soil mixtures show the difference in response, both in consolidation times and in their magnitude. In this sense, it is observed that a different soil structure generates a consequent structure of pore sizes, and it is considered possible to study and quantify this process from the distribution of pore sizes.

Resumen

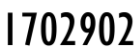
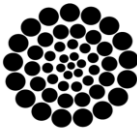
Los asentamientos en obras de infraestructura como vialidades, puentes y carreteras frecuentemente suelen subestimarse debido a la falta de comprensión de los fenómenos asociados a las deformaciones volumétricas de los suelos. Esto puede conducir a daños importantes en las estructuras desplantadas sobre ellos y en algunos casos será necesario demolerlas o inutilizarlas. Este estudio muestra la diferencia en las deformaciones de largo plazo que ocurren entre dos tipos de suelo en función de sus tamaños de partículas. En el estudio, se muestran los resultados de dos muestras de suelo sujetas a consolidación, con humedades iniciales idénticas, pero con una distribución granulométrica distinta. También se muestra la manera en que ocurre el proceso de consolidación y la influencia directa del tamaño de partícula sobre el proceso de reducción volumétrica de largo plazo de los suelos.

Objetivos	Metodología	Contribución
<ul style="list-style-type: none">Someter muestras de suelo a procesos de consolidación secundaria.Producir muestras de diferentes granulometrias para someterlas a procesos de consolidación.Analizar cualitativamente y cuantitativamente la consolidación secundaria en muestras con diferentes granulometrias.	Se obtuvieron muestras de suelo de un caolín industrial T2 suficientemente fino para exhibir deformaciones volumétricas por consolidación primaria y secundaria. Este suelo se mezcló con material inerte tipo inerte para fabricar muestras con una granulometría distinta y analizar las diferencias que ocurren en las deformaciones volumétricas con diferentes granulometrias.	Los resultados experimentales derivados del análisis de las mezclas de suelo evidencian la diferencia en respuesta, tanto en los tiempos de consolidación, como en la magnitud de estos. En este sentido, se observa que una estructura diferente de suelos, genera una estructura consecuente de tamaños de poro y se considera posible estudiar y cuantificar este proceso a partir de la distribución de tamaños de poro.

Soil consolidation, saturated soils, mechanical behaviour

Consolidación, suelos saturados, comportamiento mecánico

Citation: Rojas, Eduardo, Reynoso, Eva Guadalupe and Arroyo, Hiram. [2024]. Influence of particle size on soil consolidation processes. Journal Civil Engineering. 8[19]-1-7: e50819107.



Introduction

Soils as construction material and as support elements for the infrastructure of nations represent the first barrier for the civil engineer before creating a successful structure that serves the purposes intended for it (Lambe & Whitman, 1969; Juárez-Badillo, 1975).

Settlements produced in structures are often exceeded in the planned calculations. As an example of this, there is the attempt to build the New Mexico City Airport on highly compressible soils which shows a settlement of 15 centimeters per year due to the extraction of water in nearby areas. The Kansai International Airport in Japan placed on a seabed (Furdoi, 2010) is 4 km long and 1 kilometer wide. It was designed to support long-term settlements, however two years later it had sunk 8 meters more than expected. Another clear example is the Tower of Pisa which took approximately 200 years to complete and currently suffers from a 5.3-degree inclination (Barnes, 2010, Mimura & Jeon, 2011).

The consolidation effects caused by settlements are estimated for infrastructure projects exclusively focusing on primary consolidation, which can be much smaller than long-term deferred consolidation (Lewis & Schrefler, 1987). On the other hand, the type of soil has a fundamental importance in the consolidation process both in the time in which these settlements occur, as well as in their magnitude (Lloret & Alonso, 1980; Cai, Chen, Cao, & Ren, 2018; Pandey et al., 2024; Zaini et al., 2024).

Terzaghi established the methodology to study the consolidation phenomenon. In the consolidation phenomenon, since the soil is saturated, the volumetric deformations of the soil depend on the quantity of water that flows through the soil pores. In addition, the water flow depends on the dissipation of the pore pressure that is generated when an increase in load is applied to the soil. Thus, it is possible to make a coupling between the deformation equations and the water flow equation.

Soil consolidation is a phenomenon that is analyzed from the point of view of the volumetric deformation produced by loads and external agents in the soil.

These volumetric deformations are commonly quantified based on the volume of water expelled in a consolidation test (Rojas & Chávez, 2013). The volume of water expelled, as well as the deformations, are used to extrapolate the laboratory results towards the calculation of settlements in structures and roads using the void ratio as a parameter for this. The information required to carry out and conduct this analysis are a) the initial conditions of the site, that is, the thickness of the compressible layer (Xie et al., 2024), b) the compressibility properties, that is, the slopes of the normally consolidated and preconsolidated sections, c) the load levels to which the soil will be subjected. The latter are obtained from an analysis of the pressures to which the soil layer will be subjected.

To obtain these parameters, it is necessary to know the geometry and the way in which the superstructure will subject the compressible soil layer to stress. That is, an embankment or a foundation slab transmit stresses in a different way to the compressible soil layer because their geometries are different (Berre, 1982; Bowles, 1979; Braja, 2008).

On the other hand, once they are known, it is desirable that the loads remain for the necessary time. The necessary time will be sufficient to reproduce the characteristics that will occur in the field. For this, the theory of soil mechanics uses the concept of consolidation curve, which is analyzed, and the consolidation times are extrapolated to field conditions to identify the times that will be required for the soil to settle or deform due to consolidation under the imposed loads.

Two types of consolidation are identified by soil mechanics theory. The first infers that soil is deformed exclusively by water migration from its particles, without plastic flow or additional deformations (Coduto, 1994). Conventional consolidation equipment can usually transmit these stresses and produce these deformations in relatively short times. That is, a soil sample, representative of a compressible soil stratum, can achieve its final stage of primary consolidation in 24 hours since soil samples are small compared to their represented strata.

Using a graphical method, these results can be extrapolated, and various soil parameters can be easily determined, such as the hydraulic conductivity of the material, which is a property that varies as the soil consolidates because it is an indicator of the dimensions of the pores in the material sample.

However, the most important result is to quantify the settlements produced by the imposed loads (Wood, 1990).

For this, it will be totally relevant that the pressure that is being transmitted to the soil sample is the same as that suffered by the soil deposit in the field.

In this sense, it is natural that soil never stops suffering volumetric deformations since the migration of water outside its borders slows down but never stops (Chen et al., 2024). In practical cases, this is the reason why it is assumed that primary consolidation is the one that will be used since, on the one hand, it is assumed that it has the largest dimensions, and on the other hand, the waiting times must be practical to develop a geotechnical design that serves the necessary purposes in the field (Thanayamwatté et al., 2024).

On the other hand, if sufficient time is allowed, it will be seen that this slowing down of the deformations does not stop and evolves in its dimensions. This additional process is called "secondary consolidation" and is typical of highly compressible clayey and silty soils.

All these problems are related to the phenomenon of long-term soil consolidation and, although this phenomenon has been studied for a long time, there is no single criterion on the causes that generate it. Various explanations have been given and a large amount of analysis has been carried out to obtain an equation that can explain this phenomenon. Among the main explanations for this phenomenon are: the effect of water viscosity and the various pore sizes (Cotecchia & Chandler, 2000; Futai, Almeida, & Lacerda, 2004).

There are different parameters that can influence the conditions and processes of consolidation, such as the initial humidity of the site, its density, the viscosity of the liquid contained in its pores, and the mineralogical composition.

These phenomena are well described by sophisticated numerical analysis, for example, using the finite element method, or more advanced methods. All of them, however, see the success of their numerical predictions in the reliability with which the parameters are obtained.

Constitutive models for soils have undergone modifications as knowledge of soils and their elemental characteristics has advanced; however, the authors consider that success is based on the adequate recovery of the parameters that feed these constitutive equations (Arroyo & Rojas, 2019).

This research proposes to experimentally exhibit the differences that exist in the consolidation processes of soils in soil mixtures that have comparable initial properties, however, they have a different particle size distribution.

The first section describes the characteristics of the soils and their manufacturing processes. Then, the experimental study process and the equipment used are described.

Manufacturing of the samples

Two samples were manufactured with different particle sizes, but with identical initial humidity using T2 type kaolin clay as the main material. T2 type kaolin is a finely ground material. According to the soil properties, this material is a silicate, it is found within the group of clays and its main component is kaolinite. Chemically, kaolin is known as hydrated aluminosilicate, according to a typical analysis it is composed of 48.56% Silicon Oxide (SiO_2), 37.03% Aluminum Oxide (Al_2O_3), 4.22% Iron Oxide (Fe_2O_3) and 1.09% Sodium (Na_2O).

Regarding the typical physical properties of kaolin, it is characterized by having a low percentage of non-mesh rejection. 325 (less than 7 percent), has a humidity of less than 3.86%, a pH of 7, its specific density is 2.4 gr./cc and apparent density 1.09 gr./cc, the percentage of injection losses at 950° C is 11.80 and, visually, it has a beige color.

The sand used for the mixture of test 1 is composed of 96.90% Silicon Oxide (SiO_2) and has an actual density of 2.65 g/cm^3 , based on its behavior under granulometric analysis we know that 3.15% was retained under mesh no. 20, 45.11% by mesh no. 30 and 41.33% by mesh no. 40.

The mixture for test 1 was prepared with 70% kaolin and 30% sand, adding a total humidity of 40%. That is, it was prepared using 70 g of kaolin mixed with 30 g of sand and moistened with 40 g of water, which gives a weight of 140 g for the mixture. Once the material was prepared and properly homogenized and at rest, the sample was manufactured. The filter paper and the consolidation ring were placed on the consolidometer tray; with the help of a spatula, the mixture was added inside the ring in small quantities without compacting until reaching a height of 2.03 cm and a diameter of 6.2 cm, which gave a volume of 61.29 cm^3 . The total wet weight of the sample was 117.2 g and a specific weight of 1.9 g/cm^3 .

Different proportions of the material were considered for the preparation of the mixture used in test 2. 100% kaolin with a humidity of 40% was used. Following the same procedure for homogenization and manufacturing and considering the same dimensions, this sample had a total wet weight of 113.6 g and a specific weight of 1.85 g/cm^3 .

The mixture used for test 1 that contained sand visually had a more liquid appearance, unlike the mixture prepared for test 2 that had a more plastic consistency and was easy to mold.

Consolidation equipment used

Experimental tests indicate that secondary consolidation only occurs in fine soils. When the results of a consolidation test are plotted on the axes of log time versus volumetric strain, a curve is obtained showing a predominant slope where large volumetric changes are observed. As time increases, this slope rapidly decreases to give way to a smaller slope that shows long-term volumetric changes (secondary consolidation). Volumetric changes related to the predominant slope have been termed “primary consolidation,” while long-term volumetric strains have been termed secondary consolidation.

The consolidometers used in each of the tests are identical, both are mainly composed of a metal tray, a lever arm and a micrometer with which the deformations are measured (Figure 1).

Box 1

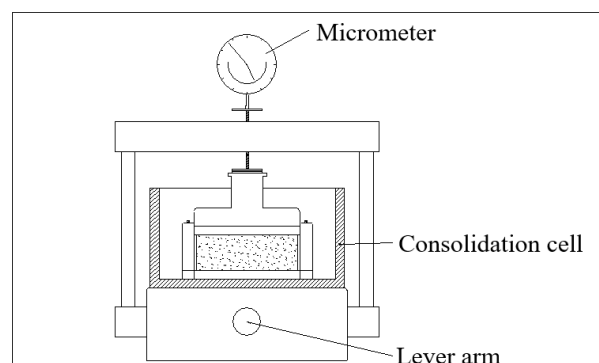


Figure 1

Schematic of the consolidometer used in the study

Source: Own elaboration

As shown in Figure 2, the metal tray has a porous stone embedded inside with a fixed ring, as well as a ring where the sample is placed, a second porous stone that is placed on top, a clamping ring and a loading disk with a uniform base that goes on the porous stone that has the function of applying the load in a uniform manner and at the same time measuring the deformation with the help of a micrometer.

Box 2

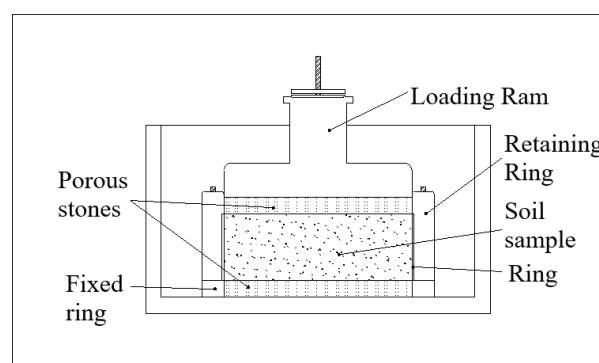


Figure 2

Detail of the soil sample mounting in the consolidometer

Source: Own elaboration

The micrometer can measure up to 12 mm of deformation.

The lever arm has a load plate where, by placing the weights, the corresponding load with the required scale is applied to the sample with the loading disk.

Sample placement process in the consolidometer

Since the consolidation tray has a fixed porous stone, only the filter paper with the sample and the ring were placed. Another filter paper, a second porous stone and the loading disk were placed on the sample. The retaining ring was inserted and secured with screws. This retaining ring prevents water from draining the sample.

Before placing the tray, we must check that the lever arm of the consolidometer moves easily and that the scale is correct (1:10).

For both tests, once the tray was ready, it was assembled on the fixed base of the consolidometer. The micrometer was placed with the necessary care so as not to move or alter the sample and it was verified that the reading had no modifications to corroborate that it was working correctly.

Next, we continued with the sample saturation stage. Water was added to the tray little by little using a trowel until it covered the lower part of the loading disk and the recording of the readings for each micrometer began every 5 seconds, increasing the time range of the readings as the saturation time passed, that is, starting from 1 min, the readings were recorded every 60 seconds until reaching 5 min. The readings were graphed until the consolidation stage was concluded when the first load was applied.

Results

From the moment the first load was applied, the recording of the readings began by graphing the logarithmic time and the deformation in millimeters in a consolidation curve.

The 1 kg load was added to the consolidometer of test 1, which contained 70% kaolin and 30% sand, that is, a stress of 0.3 ton/m2 was applied, taking into account that the area of the sample is 30.19 cm².

In Figure 3, we can see that after 45 seconds the end of the consolidation stage was reached, with the sample deforming approximately 0.04 millimeters.

So far, the sample has deformed 0.58 mm and continues with secondary consolidation.

Box 3

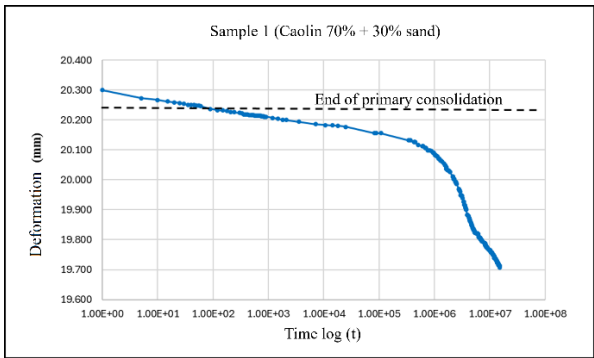


Figure 3 Consolidation curve of test 1 with 70% kaolin and 30% sand Source: Own elaboration

Box 4

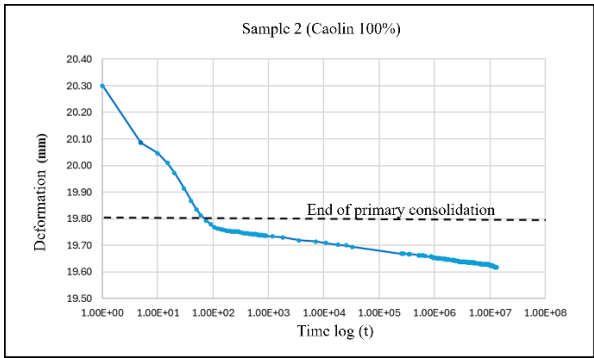


Figure 4 Consolidation curve of test 2 with 100% kaolin Source: Own elaboration

In test 2, a stress of 5 ton/m2 was added, that is, a load of 1.5 kg was applied to the lever arm of the consolidometer.

Based on Figure 4, we can see that the primary consolidation stage ended after 60 seconds and had a deformation of 0.5 mm. In addition, we can see that it has deformed about 0.68 mm so far.

Conclusions

The experimental results derived from the analysis of the soil mixtures show the difference in response, both in the consolidation times and in their magnitude. This is mainly due to the microstructure generated within the mixtures (Arroyo, Rojas, Pérez-Rea, Horta, & Arroyo, 2015), which must also be due to the manufacturing of the same in terms of their initial humidity and the applied pressures (Della Vecchia, Dieudonné, Jommi, & Charlier, 2014).

In this sense, a different soil structure would generate a consequent structure of pore sizes and it is considered possible to study and quantify this process from the distribution of pore sizes (Rojas, Pérez-Rea, Gallegos, & Leal, 2012).

The influence of these last two parameters remains to be reviewed to recognize how they influence the compaction processes and establish operating conditions for the compacted materials as a function of their construction processes and the time they last (Tsutsumi & Tanaka, 2012).

Declarations

Conflict of interest

The authors declare no interest conflict. They have no known competing financial interests or personal relationships that could have appeared to influence the article reported in this article.

Author's contribution

Rojas, Eduardo: Contributed to the project idea, research method, technique and manuscript revision.

Reynoso, Eva Guadalupe: Contributed performing the consolidation tests.

Arroyo, Hiram: Contributed to data analysis and interpretation, manuscript writing and revision.

Availability of data and materials

The datasets used or analyzed during the current study are available from the corresponding author upon reasonable request.

Funding

The funding received by the University of Guanajuato, for this project derived from the grant 110/2024 of the Institutional Scientific Research Call is appreciated and acknowledged.

Acknowledgements

Support from the University of Guanajuato in providing the facilities to undergo the referred tests is greatly appreciated.

Abbreviations

No abbreviations are contained within the paper.

References

Antecedents

Cai, Y., Chen, Y., Cao, Z., & Ren, C. (2018). A combined method to predict long-term settlements of roads on soft soil under cyclic traffic loadings. *Geotechnical Act.*

Furdoi, T. (2010). The second phase construction of Kansai international airport considering the large and long-term settlement of the clay deposits. *Soils and Foundations*, 50(6), 805-816.

Mimura, M., & Jeon, B. (2011). Numerical Assessment for the Behavior of the Pleistocene Marine Foundations due to Construction of the 1st Phase Island of Kansai International Airport. *Soils and Foundations*, 51(6), 1115 - 1128.

Basics

Barnes, G. (2010). *Soil Mechanics: Principles and Practice*.

Bowles, J. E. (1979). *Physical and Geotechnical Properties of Soils*.

Braja, M. D. (2008). *Advanced Soil Mechanics*. London, United Kingdom: Taylor & Francis Ltd.

Coduto, D. P. (1994). *Foundation Design, Principles and Practices*. New Jersey: Prentice Hall.

Juárez-Badillo, E. (1975). Constitutive relationships for soils. Paper presented at the Symp. on Recent Developments in the Analysis of Soil Behavior and Their Application to Geotechnical Structures, University of New South Wales, NSW, Australia.

R. W., & Schrefler, B. A. (1987). The finite element method in the deformation and consolidation of porous media. Chichester.

Lambe, T. W., & Whitman, R. V. (1969). *Soil Mechanics*. New York: Wiley.

Wood, D. M. (1990). *Soil Behaviour and Critical State Soil Mechanics*: Cambridge University Press.

Supports

Arroyo, H., Rojas, E., Pérez-Rea, M. L., Horta, J., & Arroyo, J. (2015). [A porous model to simulate the evolution of the soil–water characteristic curve with volumetric strains](#). *Comptes Rendus Mecanique*, 343(4), 264-274.

Arroyo, H., & Rojas, E. (2019). [Fully coupled hydromechanical model for compacted soils](#). *Comptes Rendus Mecanique*, 347(1), 1-18.

Chen, Y. Z., Fan, C., Dong, Q., & Wei, J. (2024). Permeability improvement of contaminated soil treated by nano Zero-Valent Iron (nZVI) through a modified slurry-consolidation procedure. Wan-Huan Zhou, Zheng Guan and Xue Li, editors, 93.

Futai, M. M., Almeida, M. S. S., & Lacerda, W. A. (2004). [Yield, Strength, and Critical State Behavior of a Tropical Saturated Soil](#). *Journal of Geotechnical and Geoenvironmental Engineering*, 130(11), 1169-1179.

Rojas, E., & Chávez, O. (2013). [Volumetric behavior of unsaturated soils](#). *Canadian Geotechnical Journal*, 50, 209-222.

E., Pérez-Rea, M. L., Gallegos, G., & Leal, J. (2012). [A porous model for the interpretation of mercury porosimetry tests](#). *Journal of porous media*, 15(6), 517-530.

Thom, R., Sivakumar, R., Sivakumar, V. Murray, E. J., & Mackinnon, P. (2007). Pore size distribution of unsaturated compacted kaolin: the initial states and final states following saturation. *Géotechnique*, 57(5), 469-474.

Tsutsumi, A., & Tanaka, H. (2012). [Combined effects of strain rate and temperature on consolidation behavior of clayey soils](#). *Soils and Foundations*, 52(2), 207-215.

Zaini, M. S. I., Hasan, M., & Almuaythir, S. (2024). Experimental study on the use of polyoxymethylene plastic waste as a granular column to improve the strength of soft clay soil. *Scientific Reports*, 14(1), 22558.

Discussions

Cotecchia, F., & Chandler, R. J. (2000). [A general framework for the mechanical behavior of clays](#). *Géotechnique*, 50(4), 431-447.

Della Vecchia, G., Dieudonné, A.-C., Jommi, C., & Charlier, R. (2014). Accounting for evolving pore size distribution in water retention models for compacted clays. *International Journal for Numerical and Analytical Methods in Geomechanics*, 39(7), 702-723.

Lloret, A., & Alonso, E. E. (1980). Consolidation of unsaturated soils including swelling and collapse behavior. *Géotechnique*, 30(4), 449-447.

Pandey, B. K., Rajesh, S., & Chandra, S. (2024). Engineering and physicochemical response of soft clay with electrokinetic consolidation process. *Acta Geotechnica*, 1-17.

Thanayamwatté, P., Sivakugan, N., & To, P. (2024). Hydraulic Backfill Consolidation in Underground Mine Stopes. *International Journal of Geosynthetics and Ground Engineering*, 10(3), 1-11.

Xie, J., Wen, M., Tu, Y., Wu, D., Liu, K., & Tang, K. (2024). Thermal consolidation of layered saturated soil under time-dependent loadings and heating considering interfacial flow contact resistance effect. *International Journal for Numerical and Analytical Methods in Geomechanics*, 48(5), 1123-1159.

Strength analysis of structural concrete blocks with five mixture materials

Análisis de resistencia de bloques de concreto estructural con cinco dosificaciones de materiales

Álvarez-Arellano, Juan Antonio^a, Lastra-González, Isabel Christine^b, El-Hamzaoui, Youness^c and Álvarez-Bello Martínez, Rodrigo Daniel^d

- ^a  Universidad Autónoma del Carmen •  JRX-8666-2023 •  0000-0001-6341-417X •  273636
- ^b  Universidad Autónoma del Carmen •  JRX-8666-2023 •  0000-0003-4935-6107 •  255686
- ^c  Universidad Autónoma del Carmen •  G-2865-2019 •  0000-0001-5287-1594 •  292367
- ^d  Universidad Autónoma del Carmen •  LJK-8428-2024 •  0009-0000-9000-255X •  799281

CONAHCYT classification:

Area: Engineering
Field: Engineering
Discipline: Mechanical Engineering
Sub-discipline: Materials mechanics

 <https://doi.org/10.35429/JCE.2024.8.19.6.1.11>

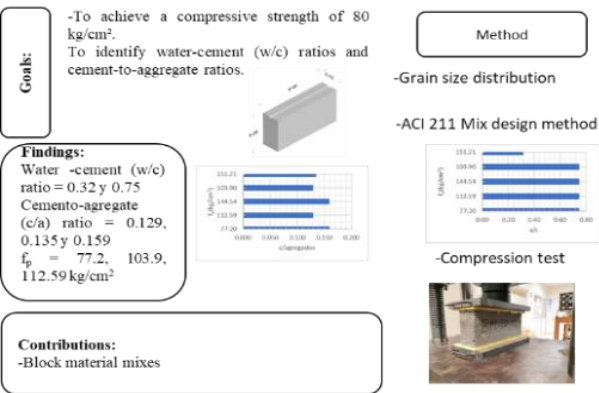
History of the article:
Received: September 05, 2024
Accepted: December 30, 2024



*  jalvarez@pampano.unacar.mx

Abstract

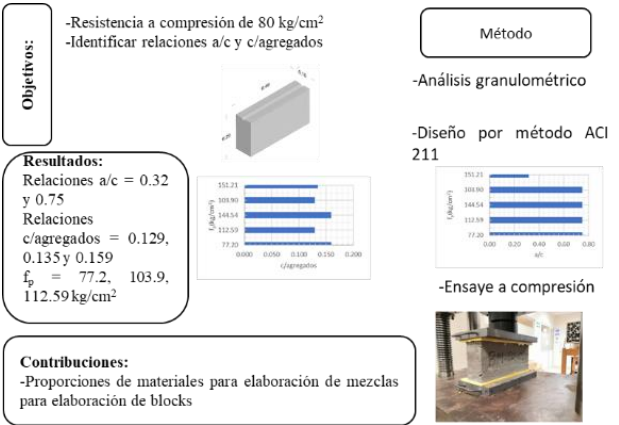
The structural system based on masonry walls is widely used in Mexico. Concrete block, one of its main components, exhibits significant variability in the material properties due to the frequent use of locally available resources for its production. Therefore, analyzing the physical properties of these blocks is essential. In this study, laboratory experiments were conducted considering five proposed mix designs. The water-cement ratios evaluated were 0.32 and 0.75, while the cement-to-aggregate ratios were 0.129, 0.135, and 0.159. The results indicate that both parameters significantly influence the compressive strength of the blocks, with higher strengths observed at lower water-cement ratios. Furthermore, the majority of the measured strengths exceeded the target value of 80 kg/cm².



Block, masonry, mixture materials

Resumen

El sistema estructural a base de muros de mampostería, es de uso frecuente en México. El block, es uno de los elementos que lo conforman y tiene la mayor variación en las propiedades de los materiales que lo componen, debido a que para su elaboración se utilizan generalmente materiales de la región. Por tal motivo, es importante analizar las propiedades físicas de estos. En el presente estudio, se presentan los resultados de experimentos de laboratorio considerando cinco dosificaciones propuestas, en las cuales se estudiaron relaciones agua-cemento de 0.32 y 0.75 y la relaciones cemento/agregados 0.129, 0.135 y 0.159. Los resultados indican, que ambos influyen en la resistencia a compresión de las piezas de blocks, presentándose la mayor resistencia a menores relaciones agua/cemento. La mayoría de las resistencias alcanzadas superan el valor objetivo de 80 kg/cm².



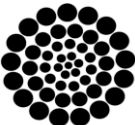
Block, mampostería, dosificaciones de materiales

Citation: Álvarez-Arellano, Juan Antonio, Lastra-González, Isabel Christine, El-Hamzaoui, Youness and Álvarez-Bello Martínez, Rodrigo Daniel. Strength analysis of structural concrete blocks with five mixture materials. Journal Civil Engineering. 8[19]1-11: e60819111.



ISSN: 2523-2428 / © 2009 The Author[s]. Published by ECORFAN-Mexico, S.C. for its Holding Republic of Peru on behalf of Journal Civil Engineering. This is an open access article under the CC BY-NC-ND license <http://creativecommons.org/licenses/by-nc-nd/4.0/>

Peer review under the responsibility of the Scientific Committee MARVID®- in the contribution to the scientific, technological and innovation Peer Review Process through the training of Human Resources for continuity in the Critical Analysis of International Research.



RENIECYT

Registro Nacional de Instituciones y Empresas Científicas y Tecnológicas

1702902

CONAHCYT

Introduction

Structural masonry is a widely used system in Mexico, so in addition to the existence of skilled labour, it is adapted to the different regions of the country. In an effort to standardise both the quality of the construction processes and the materials used, several standards have been established in Mexico, such as NMX-C-038 (2014), NMX-C-073 (2004), NMX-C-077 (1997), among others, as well as technical regulations including the NTC-DM (2023). These technical references include both procedures and minimum requirements for some masonry elements, including concrete blocks. Thus, for example, the NTC-DM (2017) updated the requirements for prismatic pieces made with materials available in the Valley of Mexico.

As an important reference in the update of the Mexican regulations, results of several studies were reported to improve the mixes to produce block pieces using aggregates available in the Valley of Mexico. Researchers analysed the properties of local materials and proposed optimal dosages that comply with current regulations, seeking to increase the compressive strength of the pieces. The studies included evaluation of the physical and mechanical properties of aggregates commonly used in manufacturing in the Valley of Mexico.

In addition, it was identified that aggregate properties can vary significantly even within the same region, which could affect the reproducibility of the proposed mixes in other regions. Important findings include that the implementation of the proposed mixes requires quality control during the manufacturing process, which represents a limitation for producers with limited resources and specifically for artisanal manufacturers (Tena *et al.*, 2017).

Similarly, another study identified the lack of a dosing method in the Ecuadorian industry for the production of hollow concrete blocks, they report that it is done empirically using lightweight aggregates such as pumice stone and fine sand. The study proposes the application of the ACI 211.2 (1998) method for lightweight structural concrete. The results allow improving the strength and quality of handmade products Villacís *et al.* (2020).

In the field of sustainability, results are reported that contribute both to the use of materials from the region and recycled materials, one of them is oriented to the use of recycled steel fibres from discarded tyres as reinforcement in soil-cement blocks. The results indicated that the addition of 1.5% fibre improved the compressive strength of the blocks by 20% compared to the non-fibre equivalent. In contrast, 0.75% showed no significant improvement. The study highlights the technical and environmental feasibility, proposing it as a sustainable alternative for the production of building materials from recycled materials. The researchers contribute with an alternative to improve building materials using recycled waste Oliveira *et al.* (2022).

Other contributions, including that related to the elaboration of a hybrid cement (Martínez-Gutiérrez *et al.*, 2024) alkaline activated with sodium sulphate, indicate that replacing 10% of the fine aggregate with cork decreases compressive strength by 29%, but increases thermal conductivity by 32%, thus improving the thermal comfort of structural blocks. Studies have also been carried out concerning the use of construction waste (Molina *et al.*, 2023) from demolition (CDW), which is a serious global environmental problem due to its high volume and impact.

The study discusses the manufacture of lightweight concrete blocks by incorporating CDW and ashes from thermoelectric power plants as an ecological and economical solution. Other researchers (Hossain *et al.*, 2024) conducted an experimental test programme to measure parameters such as compressive strength and density, comparing blocks produced with different mixes of recycled and conventional aggregates. The results show that certain alternative aggregates allow the production of blocks with acceptable mechanical properties. They highlight that the use of recycled materials has the particularity that the quality and availability may vary according to the region, which could limit the standardisation or traceability of the results in terms of quality. Additionally (Guerra and Ruiz, 2024), other proposals include the incorporation of recycled glass fibres in concrete mixes for structural purposes, designed for an initial strength of 210 kg/cm², obtaining improvements in mechanical properties.

Similar proposals (Soras, 2024) include aggregates of ground glass and expanded polystyrene, where it is observed that the strength decreased as the percentage of the latter material increased, due to its low density and adhesion in the mix.

Also noteworthy is the proposal that analyses the potential of oyster shell as a partial substitute or additive to reduce the exploitation of natural resources and promote recycling for concrete production. This study included percentages of crushed shell (5%, 10%, 15%, 20%) and as an additive (5%, 10%, 20%, 30%), in accordance with Mexican construction standards (De Dios-Suárez *et al.*, 2024). The results of this research are not focused on the use of concrete in the production of blocks, so it would be useful for other cases.

In addition to the use of recycled materials, studies are also reported on precast concrete blocks incorporating cabuya fibres and IP cement, considering five types of concrete blocks that consisted of adding 0.5%, 1.0%, 1.5%, 2.0% cabuya fibre. These studies indicate reduction of the thermal conductivity coefficient of the blocks, improvement of their thermal insulation capacity, as well as maintaining adequate mechanical properties (Laureano and Valladares, 2024).

Recently, the influence of both hollow and solid blocks was studied, considering the bonding mortar for masonry, for which the researchers (Rafi and Khan, 2024), carried out experimental tests of the mechanical properties of masonry prisms subjected to uniaxial compression. The tests considered specimens with solid and hollow prismatic geometry of 100 mm and 150 mm thickness, using five ratios of 1:2, 1:3, 1:4, 1:5 and 1:6 by weight. The results indicate that the failure mode and compressive behaviour is not significantly affected by the type of mortar, although there were differences between the solid and hollow block prisms in the post-peak region of the stress-strain curve of the tested specimen.

As can be seen, the literature review suggests that the use of recycled materials or materials from the region leads to diverse results, so that even though their use cannot be standardised or regulated, specific studies are required for materials from the region if the use of available materials is to be promoted.

In the absence of a database to try to generalise recommendations, the regulations in Mexico encourage further regional or local studies to be carried out in order to have results that broaden the current regulatory scope. Based on the above, the following results of studies of available materials in the Municipality of Carmen, Campeche are presented.

Methodology

The process of elaboration of concrete blocks requires previous steps, which start with the selection of the material based on previous experiences that have led to favourable results. However, the selection requires the availability of economic resources that are generally available at the industrial level. Another scenario to be solved is to propose dosages considering the material in the region.

The first step in the final design of the block pieces consists of selecting the material to be included in the mix, obtaining physical properties and carrying out the granulometric analysis of the fine and coarse aggregates. This analysis provides the general classification of the gradation of the material. In parallel, parameters including loose volumetric weight, loose volumetric weight, moisture percentage, absorption, fineness modulus and others are obtained.

The next step is to make the mixture from the proposed dosages. After the blocks have been produced, they must be cured for subsequent testing to verify the design strength parameters, which are generally considered to be the compressive strength, shear strength and absorption of the pieces. Thus, the values obtained are compared with the limits established in the design standards, in Mexico included in the standard NMX-C-441 (2013) for non-structural use with a minimum design strength of 35 kg/cm² and NMX-C-404 (2012) for structural use 60 kg/cm².

Material selection

In the municipality of Carmen, Campeche, there is no identified material bank that meets the technical requirements needed to produce the blocks. Therefore, the material used for the tests and the elaboration of specimens was purchased from a commercial establishment specialised in construction materials.

These suppliers offer the inputs required for the manufacture of concrete blocks, including cement, sand, gravel, stone dust and granules.

Geometry of the block pieces

According to NTC-DS (2023), solid pieces are considered to be those with a net area of at least 75 % of the gross area in their most unfavourable cross-section, and whose outer walls have a thickness of not less than 20 mm. Hollow parts are those with a net area of at least 50 per cent of the gross area; also, the thickness of their outer walls is not less than 15 mm. For hollow parts with two to four cells, the minimum thickness of the inner walls is at least 13 mm. For multi-perforated parts, whose perforations are of the same dimensions and evenly distributed, the minimum thickness of the inner walls of 10 mm for concrete parts. In addition, the requirements for the thickness of the outer and inner walls indicated in NMX-C-404 (2012) for hollow and multiperforated pieces shall be complied with.

The geometry of the blocks that make up the masonry structural system is a key factor, since their various shapes and configurations directly influence the final strength of the pieces. For this reason, in the present investigation, specimens with rectangular geometry were elaborated, which allowed focusing the analysis on the influence of the proposed mix proportions. Previous studies by Lastra *et al.* (2021), Álvarez-Arellano *et al.* (2023) and Álvarez-Arellano *et al.* (2024) have examined aspects such as geometry, strength values of commercial parts manufactured with materials from different regions of the country, as well as the increase in strength when incorporating a commercial additive.

In the present study, the geometrical data shown in Figure 1 were considered, resulting in the parts shown in Figure 2.

The pieces evaluated are considered solid blocks, since their net area, defined as the effective cross-section of the material, is equal to their gross area, which implies the absence of voids or significant perforations that affect their structural classification. In a subsequent stage, the pieces were classified according to their mechanical strength, following the parameters and specifications defined by the current NMX-C-038 (2014) standard.

Box 1

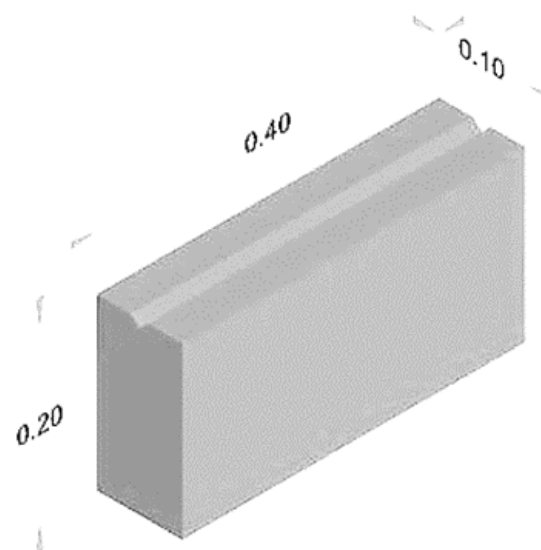


Figure 1

Nomenclature defining the dimensions of the studied concrete block

Box 2



Figure 2

Geometry of manufactured parts.

The compressive strength shall be evaluated in accordance with the current NMX-C-036 (2013) standard. For this purpose, the reference values indicated in Table 1, which establishes the minimum values of the masonry structural system, shall be taken as reference values.

Box 3

Table 1
Minimum Allowable Compressive Strength Values

Type of part and material	f'_p	\bar{f}_p
Handmade solid clay partition walls	6(60)	9(90)
Solid or perforated clay or concrete partition walls	10(100)	15(150)
Clay or concrete hollow partition wall	6(60)	9(90)
Solid or multi-drilled clay or concrete block	10(100)	15(150)
Clay or concrete hollow block	6(60)	9(90)

Source: NTC-DM (2023)

Material particle size

The granulometry of the material is fundamental for the design of the mix, these aspects are included in the NMX-C-073 (2004) standard which refers to the determination of the volumetric mass of fine and coarse aggregates or a combination of both; standard NMX-C-077 (1997) refers to the method for the granulometric analysis of fine and coarse aggregates, in order to determine the distribution of particles of different sizes by means of sieves; standard NMX-C-164 (2014), establishes the test method for the determination of the relative density and absorption of coarse aggregate. In the results reported, the recommendations included in these standards were followed. It should be noted that the mixtures carried out include commercial material available to the general public, which is usually used for the production of block pieces by artisanal means.

The granulometric analysis of the sand for the production of the blocks provided the results shown in Table 2. The analysis considered tare mass (M_t) of 40 gr, tare mass plus sample (M_t+M_{mi}) of 3400 gr and initial sample mass (M_{mi}) of 3000 gr. From the same process, the values indicated in Table 2 for the percentage of gravels of 0.91%, 99.09 of sands and zero percent of fines were calculated.

From Table 2, the values of the effective diameters $D_{10} = 0.42$, $D_{30} = 0.51$, $D_{60} = 0.68$ were calculated using the interpolation expression suggested by Bardet (1997). Subsequently, the uniformity coefficients defined by $C_u = D_{60}/D_{10}$ were estimated with a value of 1.609, $C_c = (D_{30})^2/(D_{60} \times D_{10})$ curvature coefficient equal to 0.91.

According to the results, the material corresponds to the classification of poorly graded material.

Box 4

Table 2
Sand granulometry

Soil Type	Sieve No.	Opening (mm)	Retained weight (gr)	Percentage retained (%)	Percentage passing (%)
Records	4	4.76	27.00	27.00	99.09
Arenas	10	1.68	65.00	65.00	96.90
	10	1.68	65.00	65.00	96.90
	20	0.84	420.00	420.00	82.72
	40	0.42	2160.00	2160.00	9.82
	60	0.25	275.00	275.00	0.54
	100	0.149	15.00	15.00	0.03
	200	0.074	1.00	1.00	0.00
Finos	Fund		0.00	0.00	0.00
		Mmf =	2963.00	2963	

The granulometry of the granules gave the results shown in Table 3. Tare mass (M_t) was 40 gr, Tare mass plus sample (M_t+M_{mi}) was 3400 gr and Initial sample mass (M_{mi}) was 3000 gr. Applying the same procedure as for sand, the values shown in Table 3 were calculated for the percentage of gravels of 0.91%, 99.09 of sands and zero percent of fines.

Box 5

Table 3
Granulometry of granules

Soil Type	Sieve No.	Opening (mm)	Retained weight (gr)	Percentage retained (%)	Percentage passing (%)
Records	1"	25.4	0.00	0.000	100.00
Arenas	3/4"	19.05	0.00	0.000	100.00
	1/2"	12.7	10.00	0.335	99.66
	3/8"	9.52	315.00	10.553	89.11
	4	4.76	1770.00	59.296	29.82
	10	1.68	810.00	27.136	2.68
	1"	25.4	0.00	0.000	100.00
	3/4"	19.05	0.00	0.000	100.00
Finos	Fund		80.00	2.680	0.00
		Mmf =	2985.00	100	

From Table 3, the values of the effective diameters $D_{10} = 2.22$, $D_{30} = 4.77$, $D_{60} = 6.77$ were calculated. Subsequently, the uniformity coefficients defined by $C_u = D_{60}/D_{10}$ were estimated with a value of 3.04, $C_c = (D_{30})^2/(D_{60} \times D_{10})$ curvature coefficient equal to 1.51. According to the results, the material corresponds to the classification of poorly graded material, since $C_u > 4$ and $1 < C_c < 3$. It is observed that the C_u value of 3.04 is close to 4, which represents better uniformity of the material.

From the particle size analysis of the stone dust and gravel provided characteristics of poorly graded materials.

Proportions used in the mix design

The proportions considered for the elaboration of the bocks were estimated from the dimensions of Figure 1 corresponding to 10x20x40 cm, with a volume of 0.10x0.20x0.40 m = 0.008 m³, target strength of 80 kg/cm². With this data, 1 m³ of concrete for blocks was batched according to the ACI 211.2 (2022) method, and the results shown in Table 4 were obtained.

Box 6

Table 4
Proposed dosage for 1 m³ solid block.

Material	Quantity
Cement (kg)	273.33
Coarse aggregate (kg)	696.85
Fine aggregate (kg)	1020.85
Water (lt)	205

The dosage considered water specific gravity of 1000 kg/m³, cement specific gravity of 3150 kg/m³, fine aggregate (stone dust) of 1454 kg/m³, coarse aggregate (gravel) of 1454 kg/m³, MF(fineness modulus) of 3.0, maximum aggregate size of 3/8", slump of 2.5 cm, fine aggregate (stone dust) absorption of 0.75%, coarse aggregate (gravel) absorption of 0.67%, moisture content of fine aggregate (stone dust) 27.66%, moisture content of coarse aggregate (gravel) 4.89%, compact unit weight of fine aggregate (stone dust) 1664 kg/m³, compact unit weight of coarse aggregate (gravel) 1584 kg/m³, loose unit weight of fine aggregate (stone dust) and coarse aggregate (gravel) 1454 kg/m³.

Compression testing of parts

The compression test requires the prior verification that the surface of the specimens to be tested remains flat, therefore, the block pieces were pitched with sulphur, within the tolerance of ± 0.05 in a length of 150 mm taken in two orthogonal directions. Figure 3 shows one of the cases studied. The tests were carried out on the Shimadzu universal machine with a capacity of 100 Ton.

Box 7



Figure 3
Laying of blocks for compression testing

The calculation of the compressive strength (fp, in kg/cm²) was calculated according to NMX-C-036 (2013) where the maximum load P (kg) and substituted into equation (1), considering as A (cm²) the gross cross-sectional area of each 400 cm² block.

$$fp = \frac{P}{A}$$
 (1)

The corresponding values for each proposed dosage are indicated in the Table 5.

Box 8

Table 5
Summary of five proportions for block making

Dosage	Cement (kg)	Fine aggregate (kg)	Coarse aggregate (kg)	Water (lt)	a/c	c/ aggregates	f _o (kg/cm ²)
D1	2.19	8.17	5.57	1.64	0.75	0.159	77.20
D2	1.92	6.28	8.57	1.44	0.75	0.129	112.59
D3	2.19	7.75	5.97	1.64	0.75	0.159	144.54
D4	1.92	5.85	8.98	1.44	0.75	0.129	103.90
D5	2.02	8.99	5.97	0.64	0.32	0.135	151.21

Discussion of results

The present study is focused on the use of material from the region of the Municipality of Carmen, Campeche. The elaboration of mixtures includes the use of materials available in material shops and they are usually considered in the mixture to elaborate handmade blocks. Therefore, they were considered as the basis for the design. Mix D1 consisted of fine aggregate (stone dust), coarse aggregate (granzón); mix D2 consisted of fine aggregate (stone dust), coarse aggregate (gravel); mix D3 consisted of fine aggregate (sand-stone dust), coarse aggregate (granzón); mix D4, was made up of fine aggregate (sand-stone dust), coarse aggregate (gravel).

Mix D5, was made up of fine aggregate (sand), coarse aggregate (gravel); and all with cement and water with the same physical properties and corresponding proportions. Table 5 shows the dosages corresponding to a 10x20x40 cm block, the water/cement ratio designated as a/c and the cement/aggregate ratio designated as $c/aggregate$.

Table 5 shows w/c ratios of 0.32 and 0.75, for the first case the range of calculated compressive strength varies between 77.2 to 144.54 kg/cm^2 corresponding to D1, which was made with fine aggregate (stone dust), coarse aggregate (granzón) and D3 which was made with fine aggregate (sand-stone dust) as well as coarse aggregate (granzón), respectively.

The variables that influenced the differences in compressive strength are attributed to the moisture content of 27.66% for fine aggregate for D1 and 1.35% for D2. D2 and D4, correspond to similar compressive, w/c , and $c/aggregate$ strengths.

It should be noted that the fine aggregate that corresponds to stone dust, in general, does not have a quality control that allows standardising its properties or maintaining a granulometry that complies with the graduation of controlled materials. However, this material is very frequently used, as it provides the mix with a consistency that allows the mixture to be worked and improves the finish.

Design D5, on the other hand, is characterised by having the lowest w/c ratio, but not the lowest $c/aggregate$ ratio. In this case, the w/c ratio is predominant, being the lowest of all the cases, as shown in Table 5 and visualised in Figure 4. Likewise, according to Figure 5, it is verified that the aggregate cement ratio, with the materials used, could be considered in the interval 0.129 to 0.159 with water-cement ratios of 0.75.

Box 9

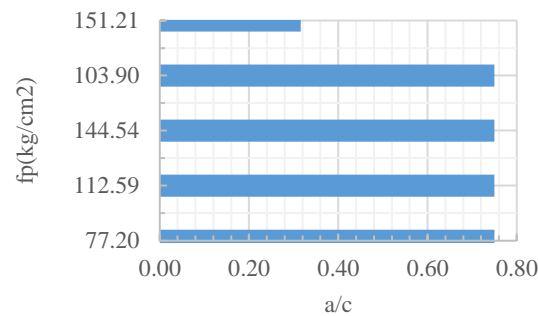


Figure 4

Ratio f_p vs. a/c .

The results obtained indicate that it is possible to obtain resistances that comply with the minimum values of the current standards in Mexico, the reference standard being the NTC-DM (2023). In the absence of local regulations, the designs of masonry structures are based on this technical standard, having the disadvantage that the properties of the materials included in the document to nearby areas of Mexico City, with their own characteristics, as reported by Tena *et al.* (2017), who made a proposal to improve mixtures to produce concrete masonry pieces using materials commonly available in the Valley of Mexico.

Box 10

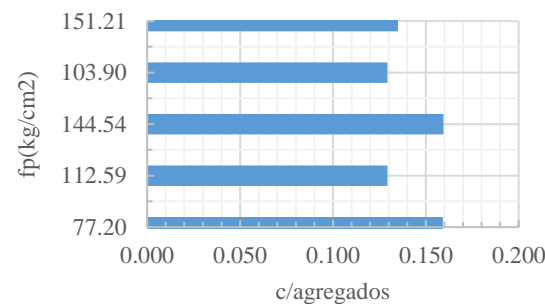


Figure 5

Relation f_p vs. $c/ aggregates$

Conclusions

Five dosages were proposed for concrete mixes considering the properties of the materials available in the Municipality of Carmen, Campeche, highlighting the following:

1. The 5 proposed dosages are formed by the available materials. Dosage D1 consisted of fine aggregate (stone dust), coarse aggregate (granzón); D2, fine aggregate (stone dust) and coarse aggregate (gravel); D3, fine aggregate (sand-stone dust) and coarse aggregate (granzón); D4, fine aggregate (sand-stone dust) and coarse aggregate (gravel); D5, fine aggregate (sand) and coarse aggregate (granzón).
2. The analysis of the cases studied indicates that the w/c ratio is the most influential factor on the strength achieved.
3. The w/c ratio of 0.75 gives higher values than the target strength of this study of 80 kg/cm².
4. The cement/aggregate ratio values of 0.129 and 0.159 generate strengths close to the target strength, however, the water/cement ratio of 0.134 significantly modifies the compressive strength.
5. The materials used in the different dosages are generally classified as poorly graded. This represents the actual conditions under which the block pieces are made by artisanal methods.
6. The five proposed dosages were carried out using the ACI 211 method, which represents an alternative for the mix required for the production of concrete blocks.
7. The dosages studied correspond to materials available in the region, these could be implemented to propose the local technical standard for masonry.

Recapitulating conclusions

In relation to the study carried out, the proposed dosages make it possible to achieve acceptable compressive strengths using material from the region. The authors hope that the results will form part of experimental references for the standardisation of the design and construction practice of masonry structures, especially in the elaboration of pieces through artisanal methods.

Declarations

Conflict of interest

The authors declare that there is no conflict of interest. They have no competing financial interests or personal relationships that could have influenced, or appear to influence, the content presented in this article.

Authors' contribution

The first author conducted experimental studies and drafted the paper, the first co-author contributed to the analysis of results and comparison with existing standards, the second co-author conducted the literature review, and the third co-author conducted the comprehensive review of the full paper.

Availability of data and materials

The data presented in this research are available for consultation if required.

Funding

No internal or external funding was received for this research project; however, it was possible thanks to the postgraduate scholarship of the third co-author (No. CVU 799281) and the economic stimulus of the first author (No. CVU 273636) and second co-author (No. CVU 292367) for belonging to the National System of Researchers (SNII) through the Autonomous University of Carmen (UNACAR).

Acknowledgements

The authors, Juan Antonio Álvarez-Arellano, Isabel Christine Lastra-González, Youness El-Hamzaoui and Rodrigo Daniel Álvarez-Bello Martínez, are grateful for the support of the Consejo Nacional de Humanidades, Ciencias y Tecnologías (CONAHCYT), the Programa para el Desarrollo Profesional Docente (PRODEP) and the Grupo Disciplinar Ingeniería estructural aplicada e ingeniería de la construcción y sus procesos sustentables through the Universidad Autónoma del Carmen (UNACAR).

Abbreviations

NMX	Mexican Standard
NTC	Complementary Technical Standard

Article

NTC-DM	Complementary Technical Standard for masonry design and construction
NTC-DS	Complementary Technical Standard for earthquake design
ACI	American Concrete Institute
RCD	Demolition product material
Cemento	High durability multi-purpose cement
IP	
f'_p	Average compressive strength of block
\bar{f}_p	Design compressive strength of block
f_p	Experimental compressive strength of the block piece
Mt	Tare mass
M _{mi}	Sample mass
C _c	Coefficient of curvature
C _u	Uniformity coefficient
P	Axial load applied
A	Gross cross-sectional area of the block part
D1	Material dosage 1
a/c	Water/cement ratio

References

Background

Álvarez-Arellano, J. A., Lastra-Gonzalez, I. C., Mendoza-Zavala, B., El-Hamzaoui, Y. & Álvarez-Bello Martínez R. D. (2024). [Mejoramiento de Mezclas para Elaboración de Blocks de Concreto Utilizando Aditivo Comercial](#). Congreso Internacional de Investigación Academia Journals. Hidalgo 2024, 16(10).

Álvarez-Arellano, J. A., Lastra-Gonzalez, I. C., Mendoza-Zavala, B., & El-Hamzaoui, Y. (2023). [Analysis of the compressive strength of commercial concrete blocks for structural masonry in Ciudad del Carmen, Campeche](#). Journal of Quantitative and Statistical Analysis, 10(27), 1-8.

Lastra, G. I., Álvarez, A. J., Mendoza, Z. B., & El Hamzaoui, Y. (2021). [Desarrollo de un prototipo de molde para blocks de concreto de tres celdas](#). Congreso Internacional de Investigación Academia Journals. Celaya 2021, 13(10), 1346-1351.

Villacís Troncoso, M., Luna Hermosa, G., Velastegui Zambrano, E., Santacruz, W. A., Zuñiga Morales, P., Nates Pasaje, J. D., & Orbe Pinchao, L. (2020). [Dosificación para elaborar bloques huecos de hormigón que cumplan con la actual NTE INEN 3066](#). Revista Tecnológica - ESPOL, 32(1).

Basics

Bardet J.P. (1997). [Experimental Soil Mechanics](#). Prentice Hall. U.S.

Support

ACI-211.2 (1998). [Standard Practice for Selecting Proportions for Structural Lightweight Concrete](#). ACI Committee 211, American Concrete Institute, Farmington Hills, Michigan, Estados Unidos.

ACI-211.1 (2022). [Selecting Proportions for Normal-Density and High-Density Concrete Guide](#). ACI Committee 211, American Concrete Institute, Farmington Hills, Michigan, Estados Unidos.

NTC-DM (2017). [Normas Técnicas Complementarias para diseño y construcción deestructuras de mampostería 2017](#). Gaceta oficial de la Ciudad de México, recuperado el 26 de diciembre de 2024.

NTC-DM (2023). [Norma Técnica Complementarias para diseño y construcción deestructuras de mampostería 2023](#). Gaceta oficial de la Ciudad de México, recuperado el 06 de noviembre de 2023.

NTC-DS (2023). [Norma Técnica Complementarias para diseño por sismo 2023](#). Gaceta oficial de la Ciudad de México, recuperado el 06 de noviembre de 2023.

NMX-C-038 (2014). [Mampostería–Determinación de las dimensiones de bloques, tabiques o ladrillos y tabicones–método de ensayo](#). Norma NMX-C-038 - ONNCCE-2013. Organismo Nacional de Normalización y Certificación de la Construcción y la Edificación (ONNCCE), México, D.F.

NMX-C-073 (2004). [Industria de la construcción-agregados-masa volumétrica-método de prueba](#). Norma NMX-C-073 - ONNCCE-2004. Organismo Nacional de Normalización y Certificación de la Construcción y la Edificación (ONNCCE), México, Ciudad de México.

NMX-C-077 (1997). [Industria de la construcción - agregados para concreto - análisis granulométrico - método de prueba](#). Norma NMX-C-077 - ONNCCE-1997. Organismo Nacional de Normalización y Certificación de la Construcción y la Edificación (ONNCCE), México, D.F.

NMX-C-164 (2014). [Industria de la construcción - agregados - determinación de la densidad relativa y absorción de agua del agregado grueso](#). Norma NMX-C-0164 - ONNCCE-2014. Organismo Nacional de Normalización y Certificación de la Construcción y la Edificación (ONNCCE), México, Ciudad de México.

NMX-C-441 (2013). [Industria de la construcción - mampostería – bloques, tabiques o ladrillos y tabicones para uso no estructural – especificaciones y métodos de ensayo](#). Norma NMX-C-441 - ONNCCE-2013. Organismo Nacional de Normalización y Certificación de la Construcción y la Edificación (ONNCCE), México, Ciudad de México.

NMX-C-404 (2012). [Industria de la construcción - mampostería – bloques, tabiques o ladrillos y tabicones para uso estructural – especificaciones y métodos de ensayo](#). Norma NMX-C-404 - ONNCCE-2012. Organismo Nacional de Normalización y Certificación de la Construcción y la Edificación (ONNCCE), México, Ciudad de México.

NMX-C-036 (2013). [Mampostería – resistencia a la compresión de bloques, tabiques o ladrillos y tabicones y adoquines–método de ensayo](#). Norma NMX-C-036 - ONNCCE-2013. Organismo Nacional de Normalización y Certificación de la Construcción y la Edificación (ONNCCE), México, Ciudad de México.

Differences

Martínez-Gutiérrez, F., Valencia-Saavedra, W. G., & Mejía-de-Gutiérrez, R. (2024). [Bloque de baja conductividad térmica a partir de un concreto geopolimérico híbrido basado en cenizas volantes y otros residuos industriales](#). *Tecnológicas*, 27(61), e3102.

De Dios-Suárez, J., Pérez-Escobar, B. L., Ramírez-Morales, E., Rojas-Blanco, L., Pérez-Hernández, G., Ramírez-Betancour, R., Pérez Castro, A., & López-Cervantes, A. (2024). [Resistencia a compresión en probetas elaboradas con triturado de concha de ostión](#). *Journal of Energy, Engineering, Optimization and Sustainability*, 8(3), 129-136.

Guerra Atauje, D. A., & Ruiz López, P. A. (2024). [Análisis de la influencia de la fibra de vidrio reciclada en la incorporación de elementos de concreto estructural](#) [Tesis de licenciatura, Universidad Peruana de Ciencias Aplicadas]. Repositorio Académico UPC. <http://hdl.handle.net/10757/683146>

Hossain, M. M., Alam, M. A., Hossain, S., Hossain, I., & Tasnim, S. A. (2024). [Manufacturing environmentally friendly hollow blocks using different aggregates: Effect on mechanical properties](#). *The Dhaka University Journal of Earth and Environmental Sciences*, 12(2), 153–158.

Laureano Toribio, E., & Valladares Vargas, A. D. (2024). [Propuesta de elaboración de bloques prefabricados de concreto con fibras de cabuya y cemento IP, con la finalidad de reducir su conductividad térmica y mejorar su resistencia térmica](#) [Trabajo de suficiencia profesional, Universidad Peruana de Ciencias Aplicadas]. Repositorio Académico UPC.

Oliveira, M. M., Pereira, G. H. A., Filho, A. G. S., Vieira, C. M. F., & Mendes, J. F. (2022). [Compressive strength assessment of soil–cement blocks incorporated with waste tire steel fiber](#). *Materials*, 15(5), 1777.

Molina Salazar, D. L., Lara Córdoba, A. L., & Sánchez Molina, J. (2023). [Desarrollo de bloques de concreto livianos utilizando residuos de construcción y demolición, y cenizas de termoelectrica](#). *Revista Colombiana de Tecnologías de Avanzada (RCTA)*, 2(42), 78–85.

Soras Ortiz, K. Y. (2024). [Análisis de las propiedades físico mecánicas del bloque hueco de concreto con la incorporación de fibras de caucho neumático reciclado](#), Abancay 2023 [Tesis de licenciatura, Universidad Tecnológica de los Andes]. Repositorio Digital Institucional.













Discussions

Tena, A., Liga, A., Pérez, A., & González, F. (2017). [Proposal for improved mixes to produce concrete masonry units with commonly used aggregates available in the Valley of Mexico](#). Revista ALCONPAT, 7(1), 36–56.





Rafi, M. M., & Khan, S. (2024). [Assessing Mechanical Properties of Concrete Block Masonry under Uniaxial Compression for Design Applications](#). Journal of Materials in Civil Engineering, 16(4).

[[Title in TNRoman and Bold No. 14 in English and Spanish]

Surname, Name 1st Author*^a, Surname, Name 1st Co-author^b, Surname, Name 2nd Co-author^c and Surname, Name 3rd Co-author^d [No.12 TNRoman]


- ^a  [Affiliation institution](#),  [Researcher ID](#),  [ORCID ID](#), [SNI-CONAHCYT ID](#) or CVU PNPC [No.10 TNRoman]
- ^b  [Affiliation institution](#),  [Researcher ID](#),  [ORCID ID](#), [SNI-CONAHCYT ID](#) or CVU PNPC [No.10 TNRoman]
- ^c  [Affiliation institution](#),  [Researcher ID](#),  [ORCID ID](#), [SNI-CONAHCYT ID](#) or CVU PNPC [No.10 TNRoman]
- ^d  [Affiliation institution](#),  [Researcher ID](#),  [ORCID ID](#), [SNI-CONAHCYT ID](#) or CVU PNPC [No.10 TNRoman]

All ROR-Clarivate-ORCID and CONAHCYT profiles must be hyperlinked to your website.

Prot-  [University of South Australia](#) •  [7038-2013](#) •  [0000-0001-6442-4409](#) •  416112

CONAHCYT classification:
https://marvid.org/research_areas.php [No.10 TNRoman]

Area:
Field:
Discipline:
Subdiscipline:

DOI: <https://doi.org/>
Article History:
Received: [Use Only ECORFAN]
Accepted: [Use Only ECORFAN]
Contact e-mail address:
*  [example@example.org]



Abstract [In English]
Must contain up to 150 words
Graphical abstract [In English]

Your title goes here		
Objectives	Methodology	Contribution

Authors must provide an original image that clearly represents the article described in the article. Graphical abstracts should be submitted as a separate file. Please note that, as well as each article must be unique. File type: the file types are MS Office files.No additional text, outline or synopsis should be included. Any text or captions must be part of the image file. Do not use unnecessary white space or a "graphic abstract" header within the image file.

Keywords [In English]
Indicate 3 keywords in TNRoman and Bold No. 10

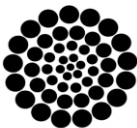
Abstract [In Spanish]
Must contain up to 150 words
Graphical abstract [In Spanish]

Your title goes here		
Objectives	Methodology	Contribution

Authors must provide an original image that clearly represents the article described in the article. Graphical abstracts should be submitted as a separate file. Please note that, as well as each article must be unique. File type: the file types are MS Office files.No additional text, outline or synopsis should be included. Any text or captions must be part of the image file. Do not use unnecessary white space or a "graphic abstract" header within the image file.

Keywords [In Spanish]
Indicate 3 keywords in TNRoman and Bold No. 10

Citation: Surname, Name 1st Author, Surname, Name 1st Co-author, Surname, Name 2nd Co-author and Surname, Name 3rd Co-author. Article Title. Journal Civil Engineering. Year. V-N: Pages [TN Roman No.10].



Introduction

Text in TNRoman No.12, single space.

General explanation of the subject and explain why it is important.

What is your added value with respect to other techniques?

Clearly focus each of its features.

Clearly explain the problem to be solved and the central hypothesis.

Explanation of sections Article.

Development of headings and subheadings of the article with subsequent numbers

[Title No.12 in TNRoman, single spaced and bold]

Products in development No.12 TNRoman, single spaced.

Including figures and tables-Editable

In the article content any table and figure should be editable formats that can change size, type and number of letter, for the purposes of edition, these must be high quality, not pixelated and should be noticeable even reducing image scale.

[Indicating the title at the bottom with No.10 and Times New Roman Bold]

Box

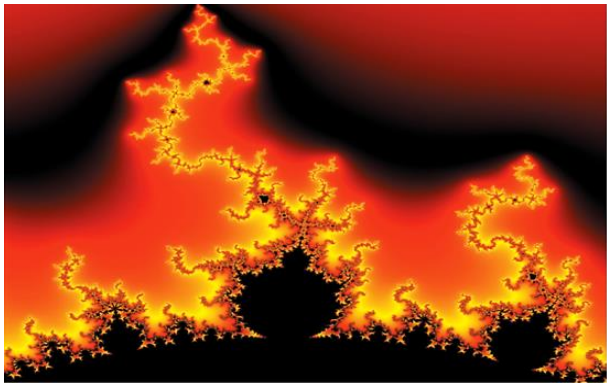


Figure 1

Title [Should not be images-everything must be editable]

Source [in italic]

Box

Table 1

Title [Should not be images-everything must be editable]			

Source [in italic]

The maximum number of Boxes is 10 items

For the use of equations, noted as follows:

$$Y_{ij} = \alpha + \sum_{h=1}^r \beta_h X_{hij} + u_j + e_{ij} \tag{1}$$

Must be editable and number aligned on the right side.

Methodology

Develop give the meaning of the variables in linear writing and important is the comparison of the used criteria.

Results

The results shall be by section of the article.

Conclusions

Clearly explain the results and possibilities of improvement.

Annexes

Tables and adequate sources.

The international standard is 7 pages minimum and 14 pages maximum. Declarations

Conflict of interest

The authors declare no interest conflict. They have no known competing financial interests or personal relationships that could have appeared to influence the article reported in this article.

Author contribution

Specify the contribution of each researcher in each of the points developed in this research.

Prot-
Benoit-Pauleter, Gerard: Contributed to the project idea, research method and technique.

Availability of data and materials

Indicate the availability of the data obtained in this research.

Funding

Indicate if the research received some financing.

Acknowledgements

Indicate if they were financed by any institution, University or company.

Abbreviations

List abbreviations in alphabetical order.

Prot-
ANN Artificial Neural Network

References

Use APA system. Should not be numbered, nor with bullets, however if necessary numbering will be because reference or mention is made somewhere in the Article.

Use the Roman alphabet, all references you have used should be in Roman alphabet, even if you have cited an article, book in any of the official languages of the United Nations [English, French, German, Chinese, Russian, Portuguese, Italian, Spanish, Arabic], you should write the reference in Roman alphabet and not in any of the official languages.

Citations are classified the following categories:

Antecedents. The citation is due to previously published research and orients the citing document within a particular scholarly area.

Basics. The citation is intended to report data sets, methods, concepts and ideas on which the authors of the citing document base their work.

Supports. The citing article reports similar results. It may also refer to similarities in methodology or, in some cases, to the reproduction of results.

Differences. The citing document reports by means of a citation that it has obtained different results to those obtained in the cited document. This may also refer to differences in methodology or differences in sample sizes that affect the results.

Discussions. The citing article cites another study because it is providing a more detailed discussion of the subject matter.

The URL of the resource is activated in the DOI or in the title of the resource.

Prot-
Mandelbrot, B. B. [2020]. [Negative dimensions and Hölders, multifractals and their Hölder spectra, and the role of lateral preasymptotics in science](#). Journal of Fourier Analysis and Applications Special. 409-432.

Intellectual Property Requirements for editing:

- Authentic Signature in Color of [Originality Format](#) Author and Coauthors.
- Authentic Signature in Color of the [Acceptance Format](#) of Author and Coauthors.
- Authentic Signature in blue color of the [Conflict of Interest Format](#) of Author and Co-authors.

Reservation to Editorial Policy

Journal Civil Engineering reserves the right to make editorial changes required to adapt the Articles to the Editorial Policy of the Research Journal. Once the Article is accepted in its final version, the Research Journal will send the author the proofs for review. ECORFAN® will only accept the correction of errata and errors or omissions arising from the editing process of the Research Journal, reserving in full the copyrights and content dissemination. No deletions, substitutions or additions that alter the formation of the Article will be accepted.

Code of Ethics - Good Practices and Declaration of Solution to Editorial Conflicts

Declaration of Originality and unpublished character of the Article, of Authors, on the obtaining of data and interpretation of results, Acknowledgments, Conflict of interests, Assignment of rights and Distribution

The ECORFAN-Mexico, S.C Management claims to Authors of Articles that its content must be original, unpublished and of Scientific, Technological and Innovation content to be submitted for evaluation.

The Authors signing the Article must be the same that have contributed to its conception, realization, and development, as well as obtaining the data, interpreting the results, drafting and reviewing it. The Corresponding Author of the proposed Article will request the form that follows.

Article title:

- The sending of an Article to Journal Civil Engineering emanates the commitment of the author not to submit it simultaneously to the consideration of other series publications for it must complement the Format of Originality for its Article, unless it is rejected by the Arbitration Committee, it may be withdrawn.
- None of the data presented in this article has been plagiarized or invented. The original data are clearly distinguished from those already published. And it is known of the test in PLAGSCAN if a level of plagiarism is detected Positive will not proceed to arbitrate.
- References are cited on which the information contained in the Article is based, as well as theories and data from other previously published Articles.
- The authors sign the Format of Authorization for their Article to be disseminated by means that ECORFAN-Mexico, S.C. In its Holding Republic of Peru considers pertinent for disclosure and diffusion of its Article its Rights of Work.
- Consent has been obtained from those who have contributed unpublished data obtained through verbal or written communication, and such communication and Authorship are adequately identified.
- The Author and Co-Authors who sign this work have participated in its planning, design and execution, as well as in the interpretation of the results. They also critically reviewed the paper, approved its final version and agreed with its publication.
- No signature responsible for the work has been omitted and the criteria of Scientific Authorization are satisfied.
- The results of this Article have been interpreted objectively. Any results contrary to the point of view of those who sign are exposed and discussed in the Article.

Copyright and Access

The publication of this Article supposes the transfer of the copyright to ECORFAN-Mexico, SC in its Holding Republic of Peru for its Journal Civil Engineering, which reserves the right to distribute on the Web the published version of the Article and the making available of the Article in This format supposes for its Authors the fulfilment of what is established in the Law of Science and Technology of the United Mexican States, regarding the obligation to allow access to the results of Scientific Research.

Article Title:

Name and Surnames of the Contact Author and the Co-authors	Signature
1.	
2.	
3.	
4.	

Principles of Ethics and Declaration of Solution to Editorial Conflicts

Editor Responsibilities

The Publisher undertakes to guarantee the confidentiality of the evaluation process, it may not disclose to the Arbitrators the identity of the Authors, nor may it reveal the identity of the Arbitrators at any time.

The Editor assumes the responsibility to properly inform the Author of the stage of the editorial process in which the text is sent, as well as the resolutions of Double-Blind Review.

The Editor should evaluate manuscripts and their intellectual content without distinction of race, gender, sexual orientation, religious beliefs, ethnicity, nationality, or the political philosophy of the Authors.

The Editor and his editing team of ECORFAN® Holdings will not disclose any information about Articles submitted to anyone other than the corresponding Author.

The Editor should make fair and impartial decisions and ensure a fair Double-Blind Review.

Responsibilities of the Editorial Board

The description of the peer review processes is made known by the Editorial Board in order that the Authors know what the evaluation criteria are and will always be willing to justify any controversy in the evaluation process. In case of Plagiarism Detection to the Article the Committee notifies the Authors for Violation to the Right of Scientific, Technological and Innovation Authorization.

Responsibilities of the Arbitration Committee

The Arbitrators undertake to notify about any unethical conduct by the Authors and to indicate all the information that may be reason to reject the publication of the Articles. In addition, they must undertake to keep confidential information related to the Articles they evaluate.

Any manuscript received for your arbitration must be treated as confidential, should not be displayed or discussed with other experts, except with the permission of the Editor.

The Arbitrators must be conducted objectively, any personal criticism of the Author is inappropriate.

The Arbitrators must express their points of view with clarity and with valid arguments that contribute to the Scientific, Technological and Innovation of the Author.

The Arbitrators should not evaluate manuscripts in which they have conflicts of interest and have been notified to the Editor before submitting the Article for Double-Blind Review.

Responsibilities of the Authors

Authors must guarantee that their articles are the product of their original work and that the data has been obtained ethically.

Authors must ensure that they have not been previously published or that they are not considered in another serial publication.

Authors must strictly follow the rules for the publication of Defined Articles by the Editorial Board.

The authors have requested that the text in all its forms be an unethical editorial behavior and is unacceptable, consequently, any manuscript that incurs in plagiarism is eliminated and not considered for publication.

Authors should cite publications that have been influential in the nature of the Article submitted to arbitration.

Information services

Indexation - Bases and Repositories

LATINDEX (Scientific Journals of Latin America, Spain and Portugal)

EBSCO (Research Database - EBSCO Industries)

RESEARCH GATE (Germany)

GOOGLE SCHOLAR (Citation indices-Google)

MENDELEY (Bibliographic References Manager)

HISPANA (Information and Bibliographic Orientation-Spain)

Publishing Services

Citation and Index Identification H

Management of Originality Format and Authorization

Testing Article with PLAGSCAN

Article Evaluation

Certificate of Double-Blind Review

Article Edition

Web layout

Indexing and Repository

Article Translation

Article Publication

Certificate of Article

Service Billing

Editorial Policy and Management

1047 La Raza Avenue -Santa Ana, Cusco-Peru. Phones: +52 1 55 6159 2296, +52 1 55 1260 0355, +52 1 55 6034 9181; Email: contact@ecorfan.org www.ecorfan.org

ECORFAN®

Chief Editor

Jaliri-Castellon, María Carla Konradis. PhD

Executive Director

Ramos-Escamilla, María. PhD

Editorial Director

Peralta-Castro, Enrique. MsC

Web Designer

Escamilla-Bouchan, Imelda. PhD

Web Diagrammer

Luna-Soto, Vladimir. PhD

Editorial Assistant

Trejo-Ramos, Iván. BsC

Philologist

Ramos-Arancibia, Alejandra. BsC

Advertising & Sponsorship

(ECORFAN® Republic of Peru), sponsorships@ecorfan.org

Site Licences

03-2010-032610094200-01-For printed material ,03-2010-031613323600-01-For Electronic material,03-2010-032610105200-01-For Photographic material,03-2010-032610115700-14-For the facts Compilation,04-2010-031613323600-01-For its Web page,19502-For the Iberoamerican and Caribbean Indexation,20-281 HB9-For its indexation in Latin-American in Social Sciences and Humanities,671-For its indexing in Electronic Scientific Journals Spanish and Latin-America,7045008-For its divulgation and edition in the Ministry of Education and Culture-Spain,25409-For its repository in the Biblioteca Universitaria-Madrid,16258-For its indexing in the Dialnet,20589-For its indexing in the edited Journals in the countries of Iberian-America and the Caribbean, 15048-For the international registration of Congress and Colloquiums. financingprograms@ecorfan.org

Management Offices

1047 La Raza Avenue - Santa Ana, Cusco - Peru.

Journal Civil Engineering

“Physicochemical characterization of the material used in the manufacture of brick in an artisanal way”

Salazar-Peralta, Araceli, Bernal-Martínez, Lina Agustina, Pichardo-Salazar, José Alfredo and Pichardo-Salazar, Ulises

Tecnológico Nacional de México. Tecnológico de Estudios Superiores de Jocotitlán

Centro de Bachillerato Tecnológico Industrial y de Servicios No. 161

Centro de Estudios Tecnológicos Industrial y de Servicios No. 23

“Feasibility of dry canals in the Americas”

Castillo-Aguirre, Alfredo Humberto, Cruz-Gómez, Marco Antonio, Mejia-Perez, José Alfredo and Espinosa-Carrasco, María del Rosario

Benemerita Universidad Autónoma de Puebla

“Dynamic evaluation of composite roofs: thermal optimization with PCM under extreme climate conditions”

López Salazar, Samanta, Simá, E., Chagolla-Aranda, M. A. and Chávez-Chena, Y.

TecNM/CENIDET

“Analysis of the behavior of the seafloor of the mouth of the Grijalva river, Tabasco in the years 2012, 2017 and 2021”

Aguilar-Ramírez, Ana María, Domínguez-González, Agustín, Utrera-Zárte, Alberto and Molina-Navarro, Antonio

Instituto Oceanográfico del Golfo y Mar Caribe

“Influence of particle size on soil consolidation processes”

Rojas, Eduardo, Reynoso, Eva Guadalupe and Arroyo, Hiram

Universidad Autónoma de Querétaro

Universidad de Guanajuato

“Strength analysis of structural concrete blocks with five mixture materials

Álvarez-Arellano, Juan Antonio, Lastra-González, Isabel Christine, El-Hamzaoui, Youness and Álvarez-Bello Martínez, Rodrigo Daniel

Universidad Autónoma del Carmen

